University of Alberta

Characterizing the Performance of a Single-layer Fabric System
through a Heat and Mass Transfer Model

by

Dan Ding

A thesis submitted to the Faculty of Graduate Studies and Research
in partial fulfillment of the requirements for the degree of

Master of Science

Department of Mechanical Engineering

©Dan Ding
Spring 2010
Edmonton, Alberta

Examining Committee

Dr. Tian Tang, Mechanical Engineering

Dr. Guowen Song, Human Ecology

Dr. André G. McDonald, Mechanical Engineering

To my parents

and

To you

Abstract

A mathematical model is developed to study the coupled heat and moisture transfer through a fabric system that consists of a single layer of fabric and an air gap. Properties of air and moisture are sensitive to temperature and hence are assumed to be functions of local temperature. Therefore the model is applicable to a broad range of boundary conditions. A numerical scheme is proposed to solve the distributions of temperature and moisture concentration throughout the layers, from which the thermal and evaporative resistances of the fabric system can be evaluated. Experiments are conducted for two particular fabrics using a sweating guarded hotplate, and the data show good agreement with the model predictions. Using this model, the effects of parameters in environmental conditions, air gap and material properties on the thermal and evaporative resistances are studied. This work provides fundamental basis for the optimization of garment fit and material properties to achieve good performance for the clothing system.

Acknowledgements

First and foremost, I would like to thank my supervisor Dr. Tian Tang, for her inspiration and guidance during the course of this program, as well as her endless patience towards me throughout this endeavourer. She made this research an enjoyable academic journey in my life. I also want to thank Dr. Guowen Song, for his guidance, efforts and encouragement that lead me to the end of this work. This work would not have been carried out smoothly without his proactive insights and lots of innovative ideas.

Special thanks to Dr. André G. McDonald, for instilling me the knowledge that enhanced my understanding in this field of study. I would thank Dr. Kajsa Duke, for her time in organizing my defense as the committee chair.

Special thanks are extended to Dr. Peter Schiavone, for his encouragement to me and his sense of humor.

I wish to extend my gratitude to Dr. Jose A. Gonzalez and Shuqin Wen in the Department of Human Ecology. They gave me generous help in conducting the experiments at Protective Clothing & Equipment Research Facility.

I acknowledge the University of Alberta for providing me the opportunity to work on this special interdisciplinary program, as well as the funding support from her and the Natural Sciences and Engineering Research Council of Canada.

Here, I want to thank my parents for their unconditional love and support. I also thank my boyfriend Tan Dawei, for his trust and care, which helped me surpass the difficult times in writing this thesis. Finally, I would like to thank all my dear friends, Qing, Xin, Dong, Xiao, Dodo, Linlin, Lidan and so many, who enriched my life and gave me their best wishes to my success in this work.

Table of Contents

List of Tables

List of Figures

List of Symbols

T temperature, K

T_m mean temperature in the microclimate, K

T_f film temperature in the boundary air flow, K

ρ density; water vapor concentration, kg/m^3

q heat flux, W/m^2

j mass flux, kg/m^2

k thermal conductivity, W/m K

D diffusion coefficient, m^2/s

h heat transfer coefficient, W/m^2 K

K mass transfer coefficient, m/s

C_p specific heat at constant pressure, J/kg K

V wind speed, m/s

P pressure, Pascal

L length, m

l thickness of layer, m

p porosity

R_{ct} total thermal resistance, m^2 K/W

R_{cf} fabric thermal resistance, m^2 K/W

R_{ct0} bare skin/plate thermal resistance, m^2 K/W

R_{et} total evaporative resistance, m^2 Pa/W

R_{ef} fabric evaporative resistance, m^2 Pa/W

R_{et0} bare skin/plate evaporative resistance, m^2 Pa/W

ΔH_{vap} enthalpy change of vaporization, J/kg

σ Stefan–Boltzmann constant, W/m^2 K^4

ε emissivity

ν kinematic viscosity, m^2/s

| τ | tortuosity |
| α | thermal diffusivity |

Subscripts

S	skin
MC	microclimate
F	fabric
E	environment
f	forced; fiber
n	natural
$cond$	conduction
$conv$	convection
rad	radiation
$mass$	mass transfer
eff	effective
air	air
vap	water vapor
sat	saturated
sur	fiber surface
c	characteristic
cr	critical
1	microclimate-fabric interface
2	fabric-environment interface

Dimensionless groups

Gr	Grashof number
Pr	Prandtl number
Ra	Rayleigh number
Re	Reynolds number
Nu	Nusselt number

CHAPTER 1: INTRODUCTION

Protective clothing is designed to protect the wearers from a variety of hazards in industry, military, or sports field where a stressful environmental condition usually comes along. The protection and the thermal comfort are two important considerations in the design of thermal protective clothing. Specifically, the purpose of protection provided by clothing is to isolate the human body from environmental hazards, while thermal comfort is associated with a thermal balance between the heat generation and the heat loss from human body. These two aspects are sometimes contradictive and can hardly be achieved at the same time [1]. On one hand, overprotection, for example, when a clothing system is constructed with thick layers of less breathable materials, will inevitably inhibit the heat and evaporative loss from human body to the environment, thus breaking the thermal balance of human body; on the other hand, insufficient protection may not be able to meet the requirement to protect human body against hazardous exposures even though it may help to maintain the thermal balance. As a result, a compromise between the minimum necessary protection and the best possible comfort has always been considered for the design of protective clothing [2].

The direct consequence of failure to maintain the thermal comfort of human body is the breakdown of the thermoregulation system. This is a dangerous situation at workplaces, which usually arises gradually without the notice of the wears due to wearing the bulky protective clothing. Not only can this situation reduce the wearer's mental capacity and work performance, but also lead to severe accidents. Therefore, thermal comfort has been brought forward as an important issue with the application of protective clothing. To study the thermal comfort properties, the fundamental mechanism of heat and moisture transfer through a clothing system needs to be explored.

In this work, a mathematical model was established on a skin-clothing-environment system to understand the heat and mass transfer through a single-layer fabric system. Two important clothing properties associated with the thermal comfort, thermal resistance and evaporative resistance, were calculated from the model. Experiments on selected fabric systems were conducted using a sweating guarded hotplate (SGHP), and good agreement was found between the measured thermal and evaporative resistances and the model prediction. Using this model, the effects and significances of environmental conditions, air gap and material properties on the thermal resistance and evaporative resistance were investigated by a parametric study.

1.1 Literature Review

Human beings are homoiotherms, they maintain their core body temperature at about 37 ℃ by balancing the amount of metabolic heat and heat loss [3]. But the ability of a human body to regulate the core temperature to a narrow range is limited. For example, a nude human body has the capacity of regulating its core temperature between 36.4 ℃ and 37.6 ℃ when the ambient temperature is between approximately 12.8 ℃ and 60 ℃ in dry air [4]. Out of this temperature range, a nude human body can hardly maintain the safe core temperature, thus the thermoregulation of the body will fail quickly. Clothing, which forms a barrier between the environment and the human body, makes it possible for human beings to stay and work under stressful environmental conditions for a long time. However, the additional need to provide protection to human body against environmental hazards increases the challenges of human body to dissipate heat and sweat from the skin to the environment through the clothing, leading to thermal discomfort. The consequent heat-related threats are sometimes fatal and were considerably underestimated for decades [5]. Thermal comfort, therefore, was brought into growing concern related to the occupational health and safety when people wear protective clothing.

1.1.1 Environmental Ergonomics

Ergonomics is an applied science concerned with designing and arranging tools people use so that the people and tools interact most efficiently and safely. Environmental Ergonomics is a study that addresses the problems of maintaining human comfort, health and performance in stressful environments [6]. Research in this field covers numerous investigations of physiology, thermal comfort, heat and cold stresses, clothing and protective clothing, thermal manikins and modeling. A good review on these topics can be found in Yutaka [6]. The development of selected aspects related to thermal comfort and its interaction with wearing clothing and protective clothing are summarized as follows.

Thermal Comfort

One common definition of human comfort is "freedom from pain, a state of physiological, psychological, and physical harmony between a human being and the environment" [7]. Comfort associated with clothing properties have been categorized into three types. The first category is called thermo-physiological comfort or thermal comfort, which refers to "the attainment of a comfortable thermal and wetness state" [8], and it involves the transport of heat and moisture through a fabric. The second category is sensorial comfort, defined as "the elicitation of various neural sensations when a textile comes into contact with the skin" [8]. The third category is body-movement comfort, defined as "the ability of a textile to allow freedom of movement, reduced burden, and body shaping, as required" [8]. Among these factors, thermal comfort is predominant [9, 10]. Two most important thermo-physiological properties related to thermal comfort are the thermal resistance and the evaporative resistance, defined as follows.

Thermal resistance, also known as thermal insulation, represents the ability of a fabric system to resist heat transfer. Heat is always transferred from high temperature to low temperature whenever there is a temperature difference

between two regions in proximity. There are three modes of heat transfer: conduction, convection and radiation. For a fabric system including the boundary air layer, the total thermal resistance (R_{ct}) is defined under the "dry condition" where moisture transfer is absent [11].

Evaporative resistance represents the ability of a fabric system to resist the transfer of moisture (mass transfer). Mass is always transferred from high concentration to low concentration. Different from heat, mass can be transmitted by two modes: diffusion and convection. For a fabric system including the boundary air layer, the total evaporative resistance (R_{et}) is defined under the "wet condition" in the presence of mass transfer [11].

These two thermal comfort properties can be experimentally measured by a SGHP according to standard ASTM (American Society for Testing and Materials) F 1868: Standard Test Method for Thermal and Evaporative Resistance of Clothing Materials Using a Sweating Hot Plate or standard ISO (International Organization for Standardization) 11092: Physiological Effects -- Measurement of Thermal and Water-vapor Resistance under Steady-state Conditions (Sweating Guarded-hotplate Test). The reproducibility of this test method has been investigated by a couple of interlaboratory studies in the U.S. by Gibson *et al.* [12] and by McCullough *et al.* [13].

The ratio between the thermal resistance and the evaporative resistance is of particular significance to the "optimum clothing-physical effect" [14], and is defined as the water vapor permeability index (I_{mt})

$$I_{mt} = \frac{SR_{ct}}{R_{et}}. \tag{1-1}$$

S here is a conversion factor to normalize the different units of the thermal and

evaporative resistances, which equals 60 Pa/K. According to standard ISO 11092, R_{et} in Eqn. (1-1) is determined under "isothermal condition" where the environmental temperature equals the hotplate temperature. I_{mt} is a dimensionless quantity and ranges between 0 and 1. The fabric is vapor impermeable if $I_{mt} = 0$, while $I_{mt} = 1$ indicates that the fabric has the same thermal resistance and evaporative resistance provided by an air layer of the same thickness. According to Verdu, *et al.* [14], a fabric system was considered to provide optimum thermal comfort if $I_{mt} \approx 0.3$.

Heat and Cold Stresses

Heat and cold stresses are two concepts to assess the thermal environment and its heat exchange between the human bodies. The common idea that heat stress is produced only in warm or hot conditions is in fact mistaken, because the metabolic heat that cannot escape out of the clothing will be stored in the body. Heat stress, therefore, can be created even in cold environmental conditions [5]. Likewise, cold stress will be produced whenever the heat generation from human body is less than the heat loss. The accumulative heat or cold stress will lead to a temperature rise or drop in the body core. As a result, the thermoregulation of human body will fail, and severe consequences can follow. It is reported that people will be deprived of effectiveness or capability when their core temperature approaches 39.5°C, and over 42°C is usually fatal; cardiac disturbances will be triggered if the core temperature goes below 33°C, and fatalities might occur below 25°C [15]. The issue of heat and cold stresses has become closely related to the occupational safety due to the application of protective clothing, and a lot of relevant investigations have been carried out lately.

Holmér *et al.* [16] studied the wind effects for cold protective clothing, and

proposed an equation for predicting the thermal insulation of clothing ensemble as a function of wind, walking and air permeability from a lot of thermal manikin tests. Later, Havenith and Nilsson [17] expanded the experimental database on clothing insulation provided by regular workwear and cold-weather clothing. They introduced some corrections for the effect of body movement and air flow on clothing insulation. Those corrections were then incorporated in standard ISO 11079: Ergonomics of the Thermal Environment -- Determination and Interpretation of Cold Stress when using Required Clothing Insulation (IREQ) and Local Cooling Effects.

Holmér *et al.* [18] also studied the wind effect on evaporative heat exchange through clothing. Two equations were proposed to determine the reduction of the total thermal insulation as a combined result of environmental wind and walking. Later, Holmér [19] discussed the heat exchange by sweat evaporation in protective clothing under hot condition. In this work, thermal insulation and evaporative resistance were introduced as the main factors for the performance of protective clothing in hot environment. Indices for physiological strain including heat storage rate and tolerance time during work were also introduced. These findings provided improvements to the standard ISO 7933: Ergonomics of the Thermal Environment -- Analytical Determination and Interpretation of Heat Stress using Calculation of the Predicted Heat Strain.

Clothing and Protective Clothing

Clothing serves both as a barrier to the outside environment and a transporter of heat and moisture from the body to the surrounding environment. Protective clothing is the clothing designed to provide occupational safety to the wearers from environmental hazards such as thermal, chemical, biological hazards, etc. [20]. The clothing structure and fabric properties can be improved to assist the thermoregulation of the human body more effectively so that thermal comfort is

reached according to its end-use conditions. From the literature, experiments including bench scale tests, manikin tests and human trials were conducted on the properties of clothing and protective clothing, so that the factors that influence the thermal balance of human body could be investigated from the experimental data. Those factors were found to be body activities, the microclimate (the air gap between skin and clothing), fabric properties (the abilities for the fabric to dissipate heat and moisture) and environmental conditions, but few studies are available to quantitatively explain how these factors affect the thermal comfort provided by a clothing system.

An equation for the heat balance when wearing protective clothing was proposed by Havenith [3], which stated that heat storage equaled the heat production subtracting the heat loss from human body. The heat production was mainly determined by the metabolic activity, while the heat loss was the sum of heat transfer due to conduction, radiation, convection, evaporation and respiration. By this equation, if the heat storage was zero, then heat balance was achieved; otherwise, positive heat storage within the body would result in a temperature rise in the human body, and negative heat storage would lead to a temperature drop. Relevant parameters in heat exchange, such as environmental temperature, air humidity, wind speed, and clothing insulation were introduced. The effect of clothing on heat and mass transfer, given by the thermal insulation and evaporative resistance, were discussed based on their experimental data. It was found that the clothing thickness was the main factor contributing to the clothing insulation and evaporative resistance. Experiments also showed that the air flow had a strong and nonlinear effect on the reduction in the insulation of surface air layer. In addition, the thickness of air layer between the human body and the clothing, which was directly related to the garment fit, was found to contribute to the total thermal and evaporative resistances. Later, Havenith [21] took a deeper look into the relevant clothing factors affecting human body's thermoregulation. It was found that the protective function of the clothing and the thermoregulation

of the body were sometimes contradictive, and this conflict led to discomfort and thermal stress. Skin temperature, in this work, was found to be the main signal that was sent to the brain to produce a sensation of thermal comfort or discomfort. These works provided a comprehensive study of the factors that contribute to the thermal comfort associated with wearing protective clothing.

Havenith *et al*. [22] studied the clothing thermal insulation for the actual conditions at the workplaces. In order to provide a complete investigation into the real situations, they conducted an experimental study by human trials for the various effects on clothing insulation, including clothing fit, body movement, wind effect, and the combined effect of body movement and wind. It was found that body movement and posture had a significant effect on the intrinsic clothing insulation, while wind speed mainly affected the thermal resistance of boundary air layer. Tight-fit clothing (small air gap between skin and clothing) showed a reduction in clothing insulation as high as 31% than loose-fit ones.

Fan *et al*. [23] used a SGHP to investigate the temperature and water content distribution within the porous fibrous battings sandwiched by an inner and an outer layer of thin covering fabrics, which simulated a down jacket. The hotplate simulated the sweating human skin and was maintained at 33°C with relative humidity at 100%, and the fabric was exposed to the ambient with temperature at -20°C and relative humidity at 65%. Based on the experimental results for four fabric systems, it was found that temperature distribution reached an equilibrium state after the first half hour of the tests irrespective of the types of fabrics, and its distribution within the fabric was affected by the moisture absorbed by the textile fibers. The water content in the fabric was found to be accumulating with time, and the distribution of water content was a combined result of moisture absorption, condensation and liquid water movement.

Chen *et al*. [24] studied the effect of garment fit on the thermal insulation and evaporative resistance of a clothing system. The thermal resistance and evaporative resistance of three different types of garments with five different sizes were measured using a self-designed sweating manikin. It was found that both quantities increased with the thickness of the air gap between the human body and garment when the air gap was small. The rate of their increase gradually decreased with increasing air gap thickness. A noticeable phenomenon was discovered in this paper, namely that, when the air gap exceeded a certain value, thermal insulation and evaporative resistance might decrease with increasing air gap. In another word, there was an air gap thickness that corresponded to a local maximum thermal resistance and maximum evaporative resistance. The authors attributed this observation to the natural convection and forced convection involved in this system. They experimentally determined that a 10mm air gap corresponded to a local maximum under no wind condition, while a 6mm air gap corresponded to a local maximum under windy condition with air speed of 2 m/s.

Barker *et al*. conducted a series of experimental studies on the comfort properties of heat-resistant protective clothing in different environmental conditions. Thermal comfort and sensorial comfort were studied by corresponding instruments. The thermal comfort properties for both dry and wet conditions were measured by a SGHP on six heat resistant workwear systems in the first part [25] and the results were reported in the second part [26]. It was found that the comfort performance of the heat-resistant protective workwear can be enhanced with minimal skin contact and high liquid absorption capacity.

A study on the effect of clothing thermal properties on the comfort sensations of wearers during sport activities was carried out by Fan and Tsang [27] recently. The clothing thermal properties they studied included thermal resistance,

evaporative resistance and moisture accumulation within clothing. Experiments were conducted subjectively by a self-designed sweating manikin and objectively by human trials on five set of sportswear. It was found that the moisture accumulation within the clothing would reduce the permeability sensation of the clothing, increasing human sweating and the evaporative resistance of the clothing. Remarkably, the subjective comfort sensation was found related to the sensorial comfort rather than the thermal comfort properties of clothing before sports activity; the overall comfort sensation during and after sports activity was found highly related to the evaporative resistance and the moisture accumulation within clothing. The thermal resistance of sportswear was found to be a less critical property to achieve comfort under mild environmental conditions.

1.1.2 Heat and Mass Transfer Models

A lot of research has been conducted to understand the heat and mass transfer through textiles. Some of these works focused only on the heat transfer within the fabric so as to study the thermal properties of fabrics [28, 29]; some focused only on the mass transfer through the fabric in order to study the factors that affect water vapor transport [31-33]; others focused on the sweating condition and addressed both heat and moisture transfer. These models and studies were different in their focuses of study, assumptions, fabric systems, and the problem solving methods. In this part, previous studies in this area are reviewed, and the significance and deficiency of each work are discussed.

Henry's model

In 1939, a theoretical model accounting for the vapor diffusion in an absorbing porous media was established by Henry [30]. Heat discharged during the absorption process was also considered. Henry assumed the thermal properties of

the solid, gas and vapor in the porous media to be constant, then he established the governing differential equations for the temperature and water vapor concentration through the porous media. Analytical solutions of this problem were two coupled linear functions, which were analogous to the solutions to a coupled vibration problem. They showed that the water vapor and heat were transferred spontaneously through an absorbing porous media in the form of "waves". Each vapor "wave" was accompanied by a proportional temperature "wave"; meanwhile, each temperature "wave" resulted in a secondary vapor "wave". Later, in 1948, Henry studied further into the coupled processes by making simplifications to the previous equations, particularly for the situation when the coupling is very week or very strong [31]. Numerical treatment was provided by applying this model to a compressed cotton package under different temperature and humidity conditions.

Henry's model could be esteemed as the first model that focused on the heat conduction and mass diffusion through an absorbing media. His studies provided initiatory knowledge in understanding the coupled nature of heat and mass transfer through porous materials, which was later widely applied in the research of textile materials. As pointed out by the author, the results could only be applied to small variations in vapor concentration and temperature due to the assumptions of constant material properties, which might not be valid if the variations were large.

Nordon and David's model

Nordon and David [32] made an improvement to Henry's model by considering the moisture sorption as a two-stage process into the hygroscopic fibers under transient relative humidity condition. Such process included a rapid first stage of Fickian diffusion and a second stage of slower moisture change. Later, David and Nordon [33] carried out a case study by applying this model to wool beds

and conducting corresponding experiments. Agreement was found between the model predictions and the experimental observations.

This model mainly explained how the moisture content changed within an absorbing fabric under varying relative humidity on the fabric boundary, as well as the heat discharged with the moisture sorption. The effect of varying temperature in the boundary condition on this system was not shown by this work.

Li *et al*.'s model

Based on the previous models, Li and Holcombe [34] established a mathematical model describing the dynamic heat and moisture transport through hygroscopic clothing under transient relative humilities, and they combined it with a physiological model to account for its interaction with the human thermoregulation system. Particularly, they considered the time dependent process of water vapor exchange between fibers and air in the fabric. The heat and moisture transport was assumed to be coupled with the sorption by the fibers. The sorption was considered to follow the previously suggested two-stage process [32] for strongly hygroscopic fibers, but only pure Fickian diffusion for weakly hygroscopic fibers, where hygroscopicity is the ability of textile fibers to absorb moisture [35, 36]. This assumption was experimentally proved by Li *et al*. [37] in another work. This model was applied to a system consisting of five components from inner body to outer environment: body core, skin, microclimate, single-layer fabric and the environment. The predicted temperature and the relative humidity in different regions of this system met good agreement with their experimental data.

This model innovatively interfaced a physiological model with a numerical heat

and mass transfer model, therefore able to capture various effects on the heat and moisture transfer, such as textile properties, ambient conditions and physical activities. Once the ambient conditions and physical activity were specified, this model could predict the skin temperature, the temperature and moisture profiles throughout a single-layer fabric. However, like Nordon and David's model, this model was designed to work under varying relative humidity at a certain environmental temperature, and all the thermal properties were taken as constants, which may not be applicable under the situation of varying temperature. Another, the role of the physiological model for predicting the thermal comfort was not shown.

Fan *et al*.'s model

Based on Henry's model [30, 31] and recent works from Li *et al*. [37, 38], Fan *et al*. [35] established a model where, for the first time, radiative heat transfer in the porous fibrous batting was considered, as well as the effect of water accumulation on the effective thermal conductivity of fabric. This work focused on heat and moisture transfer with condensation in a system including a human body, an air gap, a sandwiched hygroscopic fibrous batting (a thick fibrous batting sandwiched by two thin fabrics), and the cold environment. Transient changes in temperature, moisture concentration through the fibrous batting were solved. Numerical results of this model showed that the effect of water content on the effective thermal conductivity of batting and radiative heat transfer were significant when there was a large difference between the boundary temperatures. In addition, condensation was found less likely to occur in higher hygroscopic fabrics within a certain period of time; and it could be reduced by increasing the evaporative resistance of the inner fabric or reducing the evaporative resistance of the outer fabric.

This model applied over a variety of cold ambient conditions, but no

corresponding experiments were carried out to describe the perceptional condensation. Another, this paper provided the method to reduce the water condensation in the fabric system but neglected the wearing discomfort it might bring to the human body. For example, increasing the water vapor resistance of the inner fabric can prevent the water vapor from entering the batting on one hand, but will also increase the skin wetness on the other hand, thus creating an uncomfortable thermal sensation to the human body.

Min *et al*.'s model

Based on the work from Li *et al*. [34] and Fan *et al*. [35], Min *et al*. [39] set up a mathematical model that simulated the steady state heat and moisture transfer from skin to environment through a fabric system including a microclimate layer and a single fabric layer. Some assumptions were made to simplify the fabric model in this research, and liquid condensation was ignored. Numerical results of this model showed that microclimate played a significant role in the heat and moisture transfer from skin to environment. Within the microclimate, the radiation and conduction contributed approximately 20% each to the total heat flux, and the contribution of moisture diffusion was about 60% of the total heat flux. For the first time, a surface diffusion term was introduced in this paper accounting for the vapor diffusion along fiber surfaces. Its magnitude (10^{-6} to 10^{-4} m^2/s in this paper) was suggested to be ten times the pore diffusion if it was caused by multilayer physisorption (or physical adsorption), but negligible if the it was caused by chemisorption (or chemical adsorption). The effects of environmental temperature, microclimate thickness, fabric thickness and surface diffusion on the heat and mass transfer throughout this system were studied. It was found that the microclimate was the most significant factor.

Limitations exist in this work. First of all, all material parameters including air and water vapor properties were assumed to be constant. Secondly, there was no

forced convection in the environment. In addition, natural convection that might occur in the microclimate was neglected. Hence the model was only applicable to certain environmental conditions and clothing system geometries. Finally, how to relate this model to thermal comfort properties (thermal and evaporative resistances) was not addressed.

1.2 Overview of this Research

In this work, a study of the heat and mass transfer from the human body to the environment through a single-layer fabric system is carried out systematically, and the issue of thermal comfort is addressed through the calculation of thermal and evaporative resistances. The organization of the thesis is as follows:

1) In Chapter 2, a model is established to understand the coupled heat and mass transfer through a single-layer fabric system.

2) In Chapter 3, experiments are conducted to prove the validity of this model.

3) In Chapter 4, thermal and evaporative resistances are calculated for a variety of environmental conditions and parameters of the clothing system, their dependence on these parameters are analyzed.

4) In Chapter 5, the results of the current work are summarized and possible future directions are provided.

CHAPTER 2: HEAT AND MASS TRANSFER MODEL

In this chapter, a coupled heat and mass transfer model is developed to study the performance of a single-layer fabric system. Fig. 2-1 shows the system, which includes a flat bottom surface, an air gap (also referred to as the microclimate or MC), a fabric layer and the environment. The bottom surface is used to mimic human skin and is maintained at a constant temperature T_S and relative humidity ϕ_S. The environmental conditions are given by ambient temperature T_E, relative humidity ϕ_E and a parallel air flow of velocity V. The MC and fabric layer transfer heat and moisture from skin to the environment, and are of thicknesses l_1 and l_F respectively. The goals here are, given a fabric system and the ambient conditions at the skin and in the environment, calculating the energy to maintain the skin conditions and predicting the thermal comfort properties of the fabric system from the results. In particular, thermal comfort properties are quantified by the thermal resistance and evaporative resistance. The total thermal resistance R_{ct} is given by

$$R_{ct} = \frac{T_S - T_E}{q_{dry}},\tag{2-1}$$

Here q_{dry} is the total heat flux through the layers, under the condition that there is no mass transfer, which is referred to as the "dry condition". R_{ct}, as defined above, includes the thermal resistance of the fabric system as well as the boundary air layer above the fabric. To describe the performance of the fabric system alone, it is often helpful to subtract a "bare skin" thermal resistance R_{ct0} from the R_{ct}, where R_{ct0} is the thermal resistance in the absence of the fabric system. In other words, R_{ct0} can be calculated from Eqn. (2-1) with q_{dry} being interpreted as the heat flux from a bare skin exposed to the ambient air. So-defined fabric thermal resistance R_{cf} is therefore

$$R_{cf} = R_{ct} - R_{ct0}. \tag{2-2}$$

The total evaporative resistance R_{et} is used to quantify the effect of moisture transfer. In particular, under the condition that the skin surface is fully saturated with water, which is referred to as the "wet condition", R_{et} is defined by

$$R_{et} = \frac{P_S - P_E}{q_{tot} - (T_S - T_E)/R_{ct}}, \tag{2-3}$$

where q_{tot} is the total heat flux in the wet condition. P_S is the water vapor saturated pressure on the skin surface, which depends on T_S, and P_E is the water vapor partial pressure in the ambient. The term $(T_S - T_E)/R_{ct}$, which is the heat flux under dry condition, has been subtracted from the total heat flux q_{tot} to obtain the heat flux due to sweat evaporation, so that R_{et} solely captures the effect of the moisture. The fabric evaporative resistance R_{ef} is defined similarly to Eqn. (2-2), i.e.,

$$R_{ef} = R_{et} - R_{et0}, \tag{2-4}$$

where R_{et0} is the "bare skin" evaporative resistance, it can be calculated from Eqn. (2-3) for the situation where a bare skin is exposed to the ambient air.
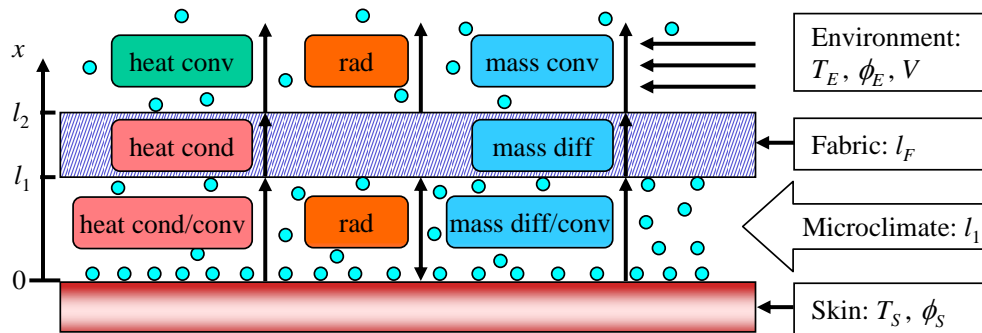
Figure 2-1 Schematic of the fabric system

In order to calculate the thermal and evaporative resistances above, it is necessary to obtain the heat flux by modeling the heat and mass transfer throughout the fabric system. In the following, the fundamental assumptions, formulations and numerical scheme to solve the heat and mass transfer problem are to be presented.

2.1 Assumptions

In Fig. 2-1, the heat and mass transfer modes in each layer of this system are demonstrated. Heat transfer occurs when there is an imbalance in temperature between the skin surface and the environment while mass transfer occurs when a gradient exists in the moisture concentration. Within the MC layer, heat conduction, radiation and mass diffusion can be present. Natural convection in MC can also exist, depending on the value of Rayleigh number Ra_L compared with the critical value $Ra_{L,cr}$, which is 1708 for the case of a horizontal rectangular enclosure [40]. In all calculations, whether Ra_L exceeds $Ra_{L,cr}$ is checked, and if it does, natural convection is included. Within the porous fabric layer, heat conduction and mass diffusion are present; radiation is negligible due to the densely packed weaving structure of the fabric [39]. Above the fabric surface, in addition to radiation, heat and mass convection exist due to the forced flow. Natural convection is negligible compared with forced convection in the current study. This is confirmed by checking two criteria for the flow, details are given in Appendix A.

The horizontal dimension of the system is assumed to be much larger than the vertical (x) direction, so that heat and mass transfer are one-dimensional. In addition, the system is considered to have reached steady state, therefore all the physical quantities are functions of position x only. Perfect contact is assumed at each interface of this system. Therefore, the temperature and moisture

18

concentration at the interfaces are continuous. Continuity also applies to heat and mass fluxes on the interfaces.

For the model to be able to capture the performance of the fabric system under a broad range of ambient temperature and relative humidity conditions, it is in general inappropriate to assume constant values for the properties of the air and water vapor present in this system. Here, all the thermal properties of air and water vapor are taken to be functions of temperature. These properties include density $\rho_{air}(T)$, specific heat $C_p(T)$, thermal conductivity $k_{air}(T)$ and Prandtl number $\Pr(T)$ of air. The temperature dependence of each parameter is obtained by fitting available experimental data [41] with a 4th order polynomial. The expressions for these polynomials are given in Appendix B. Expressions for the saturation pressure of water vapor $P_{sat}(T)$ [42] and binary diffusion coefficient (mass diffusivity) of water vapor in air $D_{vap}(T)$ [41] are obtained from empirical formula. Coefficients associated with solid bodies (e.g., thermal conductivity of textile fibers, emissivity of skin and fabric surfaces) are less sensitive to temperature, thus being taken as constant. The performance of the fabric system is then studied for ambient temperature ranged from -50 ℃ to 100 ℃, relative humidity ranged from 0 to 100%, and wind speed ranged from 1 to 30 m/s. For these environmental conditions, the enthalpy change of vapor is estimated to be at most 5% of the enthalpy of vaporization, and therefore is neglected.

Finally, phase change (e.g., condensation) of water vapor is not considered in the current work. However, it can be particularly significant when the environmental temperature is below zero Celsius. While the calculation of thermal resistance R_{ct} is under dry condition and applies to temperature well below zero Celsius, the calculation for evaporative resistance R_{et} is restricted to the case where the temperature everywhere is above zero.

2.2 Formulation of the Boundary Value Problem (BVP)

Based on the above assumptions, the BVP can be formulated for the temperature distribution $T(x)$ and the moisture concentration distribution $\rho(x)$ throughout the fabric system. ρ here is the mass of water vapor per unit volume, and it is related to temperature and relative humidity, as shown in Appendix C. In the following, the expressions for heat and mass fluxes in each layer are first given. The governing equations and boundary conditions (BCs) are then specified that allow the determination of thermal and evaporative resistances for the system under consideration (See Fig. 2-1).

2.2.1 Heat and Mass Fluxes

<u>MC layer</u>: ($0 \leq x < l_1$)

As explained earlier, if the Rayleigh number Ra_L in the MC layer is less than the critical value of $\mathrm{Ra}_{L,cr} = 1708$, natural convection does not occur, and the total heat flux in MC includes contributions from conduction (q_{cond}), radiation (q_{rad}) and mass diffusion (q_{mass}) given by

$$q_{MC} = q_{cond} + q_{rad} + q_{mass} = -k_{MC}(T)\frac{dT}{dx} + \varepsilon_{eff}\sigma\left[T_S^4 - T_1^4\right] + j_{MC}\Delta H_{vap} ,$$

$$(\mathrm{Ra}_L < \mathrm{Ra}_{L,cr}) \ (2\text{-}5)$$

where $k_{MC}(T) = k_{air}(T)$ is the thermal conductivity of the air in the MC layer. ε_{eff} is the effective emissivity of the air space between skin and the lower fabric surface, and is given by [41]

$$\varepsilon_{eff} = \frac{1}{\varepsilon_S^{-1} + \varepsilon_F^{-1} - 1} , \qquad (2\text{-}6)$$

where ε_S and ε_F are the emissivity of skin and that of the fabric surface, respectively. In Eqn. (2-5), σ is the Stefan–Boltzmann constant (5.67×10^{-8}

20

W/m² K⁴), T_S is the skin temperature, and T_1 is the temperature at $x = l_1$, i.e., on the MC-fabric interface. T_1 is an unknown and is part of the solution. j_{MC} is the mass flux of the moisture and ΔH_{vap} is the enthalpy of vaporization at the skin surface.

If the Rayleigh number Ra_L reaches 1708, natural convection occurs in the MC, and Eqn. (2-5) needs to be modified to

$$q_{MC} = q_{conv} + q_{rad} + q_{mass} = h_{n,MC}\left(T_S - T_1\right) + \varepsilon_{eff}\sigma\left[T_S^4 - T_1^4\right] + j_{MC}\Delta H_{vap} ,$$

$$(Ra_L \geq Ra_{L,cr}) \ (2\text{-}7)$$

where $h_{n,MC}$ is the average heat transfer coefficient for natural convection in the MC enclosure. An empirical expression of this parameter is given by [43]

$$Nu_{MC} = \frac{h_{n,MC}l_1}{k_{air}} = 1 + 1.44\left[1 - \frac{1708}{Ra_L}\right]^+ + \left[\left(\frac{Ra_L}{5830}\right)^{1/3} - 1\right]^+ , \ (Ra_L < 10^8) \ (2\text{-}8)$$

where Nu_{MC} is the Nusselt number in the MC, $\left[x\right]^+$ takes zero if $x < 0$, and takes x if $x \geq 0$. Ra_L is the average Rayleigh number in the MC given by

$$Ra_L = \frac{g\beta\left(T_S - T_1\right)l_1^2}{\nu^2}Pr .$$

$$(2\text{-}9)$$

Here $g = 9.81\,m/s^2$ is the gravitational acceleration, β is the coefficient of thermal expansion, it equals the reciprocal of air temperature by treating air as an ideal gas. ν is the kinematic viscosity of the air, and Pr is the Prandtl number of air. They are both functions of temperature given by in Appendix B. In order to evaluate $h_{n,MC}$, the aforementioned temperature dependent parameters will be calculated at the mean temperature in the MC: $T_{m,MC} \equiv \left(T_S + T_1\right)/2$.

In the absence of natural convection, the mass flux in the MC layer j_{MC} can be expressed according to the Fick's law, i.e.,

$$j_{MC} = -D_{MC}(T)\frac{d\rho}{dx}, \ (\text{Ra}_L < \text{Ra}_{L,cr}) \tag{2-10}$$

where $D_{MC}(T) = D_{vap}(T)$ is the binary diffusion coefficient (mass diffusivity) of water vapor in air. An empirical formula for $D_{vap}(T)$ was developed by Marrero and Mason [41]:

$$D_{vap}(T) = 1.87 \times 10^{-10} \frac{T^{2.072}}{P_{atm}}, \tag{2-11}$$

where P_{atm} is the total pressure in atmospheres (atm) and T is the temperature in Kelvin (K). In this work, P_{atm} is assumed to be the standard atmospheric pressure which equals 1 atm.

In the presence of natural convection, however, the mass flux is given by

$$j_{MC} = K_{n,MC}(\rho_S - \rho_1), \ (\text{Ra}_L \geq \text{Ra}_{L,cr}) \tag{2-12}$$

where ρ_S and ρ_1 are the water vapor concentration at the skin surface and that on the MC-fabric interface respectively, and $K_{n,MC}$ is the temperature-dependent mass transfer coefficient corresponding to mass convection in MC and should be evaluated at the mean temperature $T_{m,MC} \equiv (T_S + T_1)/2$. For air-water vapor mixtures, a relation between mass transfer coefficient $K_{n,MC}$ and heat transfer coefficient $h_{n,MC}$ can be obtained using the Chilton-Colburn analogy [41]

$$K_{n,MC} = \frac{h_{n,MC}}{\rho_{air}C_p\left(\dfrac{\alpha_{air}}{D_{vap}}\right)^{2/3}}, \tag{2-13}$$

where $\alpha_{air} = k_{air}/(\rho_{air}C_p)$ is the thermal diffusivity of air.

<u>Fabric layer</u>: ($l_1 \leq x \leq l_2$)

The total heat flux in the fabric layer has components from heat conduction and moisture diffusion, i.e.,

$$q_F = q_{cond} + q_{mass} = -k_{eff,F}(T)\frac{dT}{dx} + j_F \Delta H_{vap}, \qquad (2\text{-}14)$$

where $k_{eff,F}$ is the effective thermal conductivity of the porous fabric material, and is given by

$$k_{eff,F} = (1-p)k_f + pk_{air}(T). \qquad (2\text{-}15)$$

Here k_f, k_{air} and p are respectively the thermal conductivity of solid fiber, that of air and the porosity. k_f is taken to be constant within the studied temperature range, while k_{air} depends on the local temperature.

Mass flux through the fabric pores is given by

$$j_F = -D_{eff,F}(T)\frac{d\rho}{dx}, \qquad (2\text{-}16)$$

where $D_{eff,F}(T)$ is the effective diffusion coefficient of water vapor in the fabric layer. According to Min *et al.* [39], it consists of two parts

$$D_{eff,F}(T) = D_{vap}\frac{p}{\tau} + KD_{sur}, \qquad (2\text{-}17)$$

The first part accounts for ordinary molecular diffusion of vapor in pores, where p is the porosity of the fabric, and τ is the tortuosity defined as the ratio of the actual length of flow path to the straight length or thickness of a sample/unit cell along the macroscopic pressure gradient. Through experimental studies, an empirical relation between τ and p is given by $\tau = 0.8(1-p)+1$ [44]. The second part in Eqn. (2-17) accounts for surface diffusion due to adsorption and desorption of water along fiber surfaces, where K is the equilibrium constant and

D_{sur} is the surface diffusion coefficient [45]. Min *et al.* [39] has used the range from 1×10^{-6} m^2/s to 1×10^{-4} m^2/s for hygroscopic fibers, but the actual value of KD_{sur} has not been quantified experimentally. As will be shown later, comparison between model and experiment data suggests that surface diffusion does not play an important role in this system.

Environment layer: ($x > l_2$)

Due to the air flow, heat transfer above the fabric in the environment is governed by forced heat and mass convections, in addition to radiation, i.e.,

$$q_E = q_{conv} + q_{rad} + q_{mass} = h_{f,E}\left(T_2 - T_E\right) + \varepsilon_F \sigma \left(T_2^4 - T_E^4\right) + j_E \Delta H_{vap}, \quad (2\text{-}18)$$

where T_2 and T_E are the temperature on the fabric-environment interface and the ambient temperature, respectively. In particular, T_2 is the temperature at $x = l_2$ and is part of the solution. $h_{f,E}$ is the heat transfer coefficient corresponding to forced convection over a flat plate in the environment, which can be determined from [41]

$$\mathrm{Nu}_E = \frac{L h_{f,E}}{k_{air}} = 0.664 \, \mathrm{Re}_L^{0.5} \, \mathrm{Pr}^{1/3}, \quad (\mathrm{Re}_L < 5 \times 10^5) \qquad (2\text{-}19a)$$

$$\mathrm{Nu}_E = \frac{L h_{f,E}}{k_{air}} = \left(0.037 \, \mathrm{Re}_L^{0.8} - 871\right) \mathrm{Pr}^{1/3}, \quad (5 \times 10^5 \leq \mathrm{Re}_L \leq 10^7) \quad (2\text{-}19b)$$

where Re_L is the average Reynolds number over a flat plate given by

$$\mathrm{Re}_L = \frac{VL}{\nu}. \qquad (2\text{-}20)$$

V is the velocity of the flow, L is the characteristic length of the fabric surface and ν is the temperature dependent kinematic viscosity of air. (19a) corresponds to the case where the flow over the entire fabric surface is laminar, while (19b) corresponds to the case where the flow over part of the surface has turned

turbulent. All the thermal parameters pertinent to the calculation of $h_{f,E}$, i.e., ν, k_{air} and Pr should be evaluated at the film temperature: $T_{f,E} \equiv (T_2 + T_E)/2$.

Mass flux in the environment due to mass convection is

$$j_E = K_{f,E}(\rho_2 - \rho_E),$$ (2-21)

where ρ_2 and ρ_E are the vapor concentration at the fabric-environment interface and in the environment, respectively. $K_{f,E}$ is the mass transfer coefficient in the environment and can be related to $h_{f,E}$ by the Chilton-Colburn analogy [41]

$$K_{f,E} = \frac{h_{f,E}}{\rho_{air} C_p \left(\dfrac{\alpha_{air}}{D_{vap}} \right)^{2/3}}.$$ (2-22)

2.2.2 Governing Equations

At steady state, the heat and mass fluxes are independent of time throughout the system. Therefore the equations that govern the distribution of temperature and water vapor concentration can be obtained by applying the principle of conservation of energy to an infinitesimal element in the corresponding region. The resulting differential equations are

In the MC: ($0 \leq x < l_1$)

$$\frac{d}{dx}\left[-k_{MC}(T)\frac{dT}{dx} \right] = 0, \; (\mathrm{Ra}_L < \mathrm{Ra}_{L,cr})$$ (2-23)

$$\frac{d}{dx}\left[-D_{MC}(T)\frac{d\rho}{dx} \right] = 0, \; (\mathrm{Ra}_L < \mathrm{Ra}_{L,cr})$$ (2-24)

In the fabric: ($l_1 \leq x \leq l_2$)

$$\frac{d}{dx}\left[-k_{eff,F}(T)\frac{dT}{dx}\right] = 0, \tag{2-25}$$

$$\frac{d}{dx}\left[-D_{eff,F}(T)\frac{d\rho}{dx}\right] = 0. \tag{2-26}$$

Note that if natural convection occurs in the MC layer, differentials of (2-7) and (2-12) result in the identities of $0 = 0$, and hence these equations are not included here.

2.2.3 Boundary Conditions

The four second order ordinary differential equations (ODEs) (2-23)-(2-26) require eight boundary conditions. These are given by the continuity of temperature and water vapor concentration on the skin-MC and MC-fabric interfaces, as well as continuity of heat flux and mass flux on the MC-fabric and fabric-environment interfaces. They are

$$T(0) = T_S, \qquad T\left(l_1^-\right) = T\left(l_1^+\right) \equiv T_1, \tag{2-27, 2-28}$$

$$\rho(0) = \rho_S, \qquad \rho\left(l_1^-\right) = \rho\left(l_1^+\right) \equiv \rho_1, \tag{2-29, 2-30}$$

$$q_{MC}\left(l_1\right) = q_F\left(l_1\right), \qquad q_F\left(l_2\right) = q_E\left(l_2\right), \tag{2-31, 2-32}$$

$$j_{MC}\left(l_1\right) = j_F\left(l_1\right), \qquad j_F\left(l_2\right) = j_E\left(l_2\right). \tag{2-33, 2-34}$$

In Eqns. (2-28) and (2-30), l_1^- means approaching l_1 from the bottom, i.e., from the MC, while l_1^+ means approaching l_1 from the top, i.e., from the fabric layer. Hence $T(l_1^-)$ and $\rho(l_1^-)$ are to be evaluated using temperature and water vapor concentration in MC, while $T(l_1^+)$ and $\rho(l_1^+)$ are to be evaluated using those in the fabric layer.

The BVP for $T(x)$ and $\rho(x)$ is now completely defined by Eqns. (2-23)-(2-34). Solving this BVP will allow us to determine the heat and mass fluxes in the system, and in turn calculate the thermal resistance and evaporative resistance. It should be noted that if natural convection does occur in the MC, then Eqns. (2-23) and (2-24) reduce to the identities of $0=0$, and hence cannot be used to determine $T(x)$ and $\rho(x)$ in the MC. However, in this case, q_{MC} and j_{MC} do not rely on the distributions $T(x)$ and $\rho(x)$. Rather, they depend on the temperature T_1 and the water vapor concentration ρ_1 on the MC-fabric interface, according to Eqn. (2-7) and Eqn. (2-12) respectively. Therefore, T_1 and ρ_1 need to be determined for the evaluation of thermal and evaporative resistances in the presence of natural convection in the MC.

2.3 Solving the BVP

First, for the situation where no natural convection is present in the MC layer ($0 \leq x < l_1$), integrating Eqn. (2-23) once, the following equation is obtained

$$-k_{MC}(T)\frac{dT}{dx} = C_1 , \qquad (2\text{-}35)$$

where C_1 is an integration constant. Its physical meaning is the conductive heat flux in the MC layer. Further integration of (2-35) results in $\int_{T_S}^{T} -k_{MC}(T)dT = \int_0^x C_1 dx$, or

$$x = -\frac{1}{C_1}\int_{T_S}^{T} k_{MC}(T)dT , \quad (0 \leq x < l_1) \qquad (2\text{-}36)$$

Note that BC (2-27) is automatically satisfied by Eqn. (2-36). At the MC-fabric interface where $x = l_1$, letting $T(l_1^-) \equiv T_1$, one obtains

$$l_1 = -\frac{1}{C_1}\int_{T_S}^{T_1} k_{MC}(T)dT . \qquad (2\text{-}37)$$

Similarly, integrating Eqn. (2-24) once results in

$$-D_{MC}(T)\frac{d\rho}{dx} = C_2 , \qquad (2\text{-}38)$$

where C_2 is an integration constant, corresponding to the diffusive mass flux in the MC layer. Substituting Eqn. (2-38) into Eqn. (2-35) yields $d\rho = \frac{C_2}{C_1}\frac{k_{MC}(T)}{D_{MC}(T)}dT$, which can be integrated to be $\int_{\rho_S}^{\rho} d\rho = \int_{T_S}^{T}\frac{C_2}{C_1}\frac{k_{MC}(T)}{D_{MC}(T)}dT$, or

$$\rho = \rho_S + \frac{C_2}{C_1}\int_{T_S}^{T}\frac{k_{MC}(T)}{D_{MC}(T)}dT . \quad (0 \le x < l_1) \qquad (2\text{-}39)$$

At the skin-MC interface where $x = 0$, BCs (2-27) and (2-29) are satisfied automatically by Eqn. (2-39). At the MC-fabric interface where $x = l_1$, letting $T(l_1^-) \equiv T_1$ and $\rho(l_1^-) \equiv \rho_1$ in Eqn. (2-39), one obtains

$$\rho_1 = \rho_S + \frac{C_2}{C_1}\int_{T_S}^{T_1}\frac{k_{MC}(T)}{D_{MC}(T)}dT . \qquad (2\text{-}40)$$

In the fabric layer ($l_1 \le x \le l_2$), integrating (2-25) once to get

$$-k_{eff,F}(T)\frac{dT}{dx} = C_3 , \qquad (2\text{-}41)$$

where C_3 is an integration constant, corresponding to the conductive heat flux in the fabric layer. Integration of (2-41) results in $\int_{T_1}^{T} -k_{eff,F}(T)dT = \int_{l_1}^{x} C_3 dx$, i.e.,

$$x = l_1 - \frac{1}{C_3}\int_{T_1}^{T} k_{eff,F}(T)dT , \quad (l_1 \le x \le l_2) \qquad (2\text{-}42)$$

which satisfies BC (2-28) automatically. At the fabric-environment interface where $x = l_2$, letting $T(l_2^-) \equiv T_2$ in (2-42), one obtains

$$l_2 = l_1 - \frac{1}{C_3} \int_{T_1}^{T_2} k_{eff,F}(T) dT .\tag{2-43}$$

Similarly, integrating Eqn. (2-26) once results in

$$-D_{eff,F}(T) \frac{d\rho}{dx} = C_4 ,\tag{2-44}$$

where C_4 is an integration constant, corresponding to diffusive mass flux in the fabric layer. Substituting Eqn. (2-44) into Eqn. (2-41) yields $d\rho = \frac{C_4}{C_3} \frac{k_{eff,F}(T)}{D_{eff,F}(T)} dT$, which can be integrated to be $\int_{\rho_1}^{\rho} d\rho = \int_{T_1}^{T} \frac{C_4}{C_3} \frac{k_{eff,F}(T)}{D_{eff,F}(T)} dT$, or

$$\rho = \rho_1 + \frac{C_4}{C_3} \int_{T_1}^{T} \frac{k_{eff,F}(T)}{D_{eff,F}(T)} dT . \quad (l_1 \le x \le l_2)\tag{2-45}$$

At the MC-fabric interface where $x = l_1$, BCs (2-28) and (2-30) are satisfied automatically by Eqn. (2-45). At the fabric-environment interface where $x = l_2$, letting $T(l_2^-) \equiv T_2$ and $\rho(l_2^-) \equiv \rho_2$ in (2-45), one obtains

$$\rho_2 = \rho_1 + \frac{C_4}{C_3} \int_{T_1}^{T_2} \frac{k_{eff,F}(T)}{D_{eff,F}(T)} dT .\tag{2-46}$$

So far, four out of the eight BCs have been used, as Eqns. (2-37), (2-40), (2-43) and (2-46). It should be noted that T_1, T_2, ρ_1 and ρ_2 are unknown, and their values are determined from the solution of the BVP. Together with C_1, C_2, C_3 and C_4, there are eight unknowns, and four more equations are required, which come from the BCs (2-31)-(2-34). Using Eqns. (2-5), (2-14), (2-35) and (2-41), BC (2-31) becomes

$$C_1 + \varepsilon_{eff} \sigma \left[T_S^4 - T_1^4 \right] = C_3 ,\tag{2-47}$$

where the terms associated with mass diffusion are canceled due to equal mass flux. With Eqns. (2-14), (2-18) and (2-41), BC (2-32) becomes

$$C_3 = h\left[T_2 - T_E\right] + \varepsilon_F \sigma\left[T_2^4 - T_E^4\right]. \qquad (2\text{-}48)$$

Similarly, using Eqns. (2-10), (2-16), (2-21), (2-38) and (2-44), the BCs (2-33) and (2-34) for continuity of mass flux can be reduced to

$$C_2 = C_4 \qquad (2\text{-}49)$$

and

$$C_4 = K_{f,E}\left(\rho_2 - \rho_E\right). \qquad (2\text{-}50)$$

Solution to the eight equations (2-37), (2-40), (2-43), (2-46) and (2-47)-(2-50) determines the unknown constants T_1, T_2, ρ_1 , ρ_2 , C_1, C_2, C_3 and C_4, and therefore determines the temperature and moisture concentration distributions, as well as the heat and mass fluxes in all layers.

If natural convection does occur in the MC, then C_1 and C_2 are not defined, since conductive heat flux and diffusive mass flux are now replaced by convective heat and convective mass fluxes. Therefore BCs (2-37) and (2-40) are not relevant and are removed from the calculation. Also, Eqns. (2-47) and (2-49) should be replaced by

$$h_{n,MC}\left(T_S - T_1\right) + \varepsilon_{eff}\sigma\left(T_S^4 - T_1^4\right) = C_3, \qquad (2\text{-}51)$$

$$K_{n,MC}\left(\rho_S - \rho_1\right) = C_4. \qquad (2\text{-}52)$$

Together with Eqn. (2-43), (2-46), (2-48) and (2-50), these are six equations for the six unknowns T_1, T_2, ρ_1 , ρ_2 , C_3 and C_4.

2.4 Numerical method

To solve the eight variables $T_1, T_2, \rho_1, \rho_2, C_1, C_2, C_3, C_4$ in the eight Eqns. (2-37), (2-40), (2-43), and (2-46)-(2-50), a vector function $\boldsymbol{f}(\boldsymbol{z}) \equiv \{f_1, f_2, f_3, f_4, f_5, f_6, f_7, f_8\}^T$ is defined with variable $\boldsymbol{z} \equiv \{T_1, T_2, \rho_1, \rho_2, C_1, C_2, C_3, C_4\}^T$ and

$$f_1 \equiv C_1 l_1 + \int_{T_S}^{T_1} k_{MC}(T) dT, \tag{2-53a}$$

$$f_2 \equiv C_1 (\rho_1 - \rho_S) - C_2 \int_{T_S}^{T_1} \frac{k_{MC}(T)}{D_{MC}(T)} dT, \tag{2-53b}$$

$$f_3 \equiv C_3 (l_2 - l_1) + \int_{T_1}^{T_2} k_{eff,F}(T) dT, \tag{2-53c}$$

$$f_4 \equiv C_3 (\rho_2 - \rho_1) - C_4 \int_{T_1}^{T_2} \frac{k_{eff,F}(T)}{D_{eff,F}(T)} dT, \tag{2-53d}$$

$$f_5 \equiv C_1 - C_3 + \varepsilon_{eff} \sigma \left[T_s^4 - T_1^4 \right], \tag{2-53e}$$

$$f_6 \equiv C_3 - h_{f,E} \left[T_2 - T_E \right] - \varepsilon_F \sigma \left[T_2^4 - T_E^4 \right], \tag{2-53f}$$

$$f_7 \equiv C_2 - C_4, \tag{2-53g}$$

$$f_8 \equiv C_4 - K_{f,E} \left[\rho_2 - \rho_E \right], \tag{2-53h}$$

The problem then reduces to finding the vector $\boldsymbol{z}$ that satisfies $\boldsymbol{f}(\boldsymbol{z}) = 0$. The Newton-Raphson scheme is adopted to solve this equation iteratively. In particular, $\boldsymbol{z}_n$ at step n of the iteration is the solution to the following matrix equation

$$\boldsymbol{J}(\boldsymbol{z}_n - \boldsymbol{z}_{n-1}) = 0 - \boldsymbol{f}_{n-1}, \tag{2-54}$$

where $\boldsymbol{J}$ is the Jacobian with its element defined by $J_{ij} = \partial f_i / \partial z_j$. Numerically, $\boldsymbol{J}$ at step n is calculated by slightly perturbing $\boldsymbol{z}_n$ and calculating the

corresponding variation in f_n. Iteration continues until the Euclidean norm of the vector on the right hand side of Eqn. (2-54) becomes smaller than a tolerance, which is taken to be 1×10^{-5} here. The solution generally converges quickly, within a few steps of iteration.

After convergence is achieved, the Rayleigh number Ra_L in the MC layer is calculated and checked against the critical value $\text{Ra}_{L,cr} = 1708$. If Ra_L exceeds $\text{Ra}_{L,cr}$, then it implies that natural convection will occur in MC, and the previous calculation without considering natural convection in MC is not self-consistent. The calculation is then redone by solving a new equation system $f(z) = 0$, where $z \equiv \{T_1, T_2, \rho_1, \rho_2, C_3, C_4\}^T$ and $f \equiv \{f_3, f_4, f_5, f_6, f_7, f_8\}^T$, with C_1 in f_5 replaced by $h_{n,MC}(T_S - T_1)$ and C_2 in f_7 replaced by $K_{n,MC}(\rho_S - \rho_1)$ according to Eqns. (2-51) and (2-52). The numerical solution is performed using MATLAB, and the codes are attached in Appendix E.

CHAPTER 3: EXPERIMENT

3.1 Method

A standard SGHP (Sweating guarded hotplate, Model SGHP-8.2, manufactured by Measurement Technology Northwest from Seattle, WA, USA) was equipped to evaluate the thermal and evaporative resistances of the fabric systems (Fig. 3-1). The guarded hotplate, which serves as the skin simulator, was housed in an environmental chamber (Lunaire Environmental Steady Sate/Stability Test Chamber, Model No. CEO910W-4, manufactured by Thermal Product Solutions from Williamsport, PA., USA) where temperature, relative humidity, and wind speed can be controlled and maintained at a steady state. Its parameters are specified in Table 3-1. Experiments were conducted under two conditions. One corresponded to the "dry condition" which did not involve moisture transfer. In this case, the test plate was guarded by a lower guard and a ring guard to maintain a constant temperature of 35°C and thus the heat flow was one dimensional in the vertical direction. Under specific ambient temperature and wind speed in the environment, the amount of heat loss was automatically recorded by the data acquisition system and used in the calculation of the thermal resistance. Another condition corresponded to the case where a water reservoir was connected to the hotplate to feed water, and was referred to the "wet condition". A vapor permeable liquid barrier was placed on the top of the heated hotplate (at 35°C) to simulate the sweating human skin at 100% relative humidity (RH). The amount of heat required to maintain the surface condition of the hotplate, together with the thermal resistance obtained under "dry condition", were used to calculate the evaporative resistance.

Two commonly used fabrics in workwear and protective clothing were selected in the experiments: Denim and Nomex®. The fabric information and specifications of material parameters are provided in Table 3-2 and 3-3,

respectively. Three specimens for each fabric were cut to the dimension of 12×12 square inches (30.48×30.48 square cm). Before testing, all specimens were pre-conditioned in a standardized environment (21°C and 65% RH) for 24 hours to ensure a consistent fiber condition. To create the MC layer between the hotplate and fabric, a spacer was used and the fabric specimen was held on top of the space by a firm wire interlaced across the spacer ring. The spacers were made of acrylic Plexiglas and the wire was 100% nylon monofilament. Three different spacers of thickness 3mm, 6mm and 11.6mm were used in the experiment, as shown in Fig. 3-2(a). The fabric system was mounted onto the hotplate (Fig. 3-2(b)) with all edges taped down to the rim of the hotplate to prevent flapping and energy loss from edges. Experiments were operated under standard conditions according to the part C of standard ASTM F1868 [11].
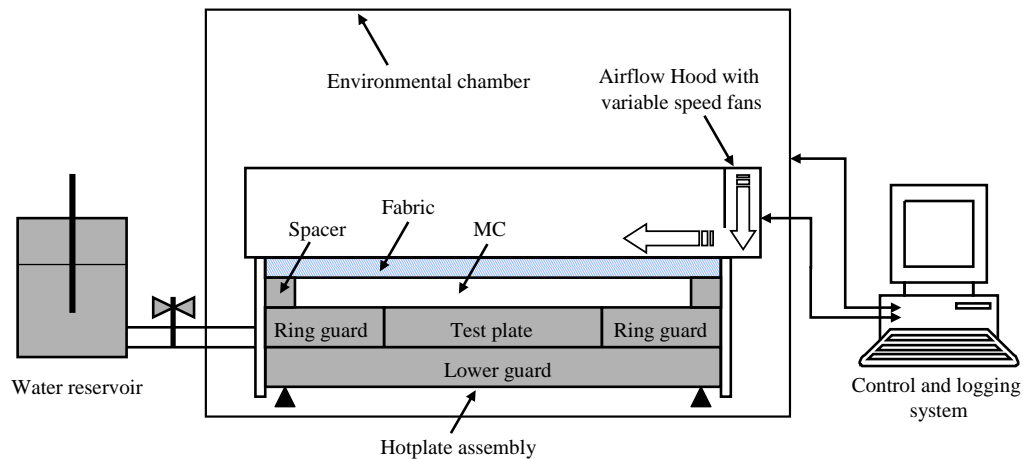
Figure 3-1 Experimental set-up.

Figure 3-2 (a) Spacers (Air gap simulator), (b) Standard SGHP.

Table 3-1 Parameters of the hotplate (skin simulator)

Properties	Values
Temperature, T_S (K)	308.15
Relative humidity, ϕ_S (100%)	0.65 (in dry); 1 (in wet)
Emissivity, ε_S	0.95 [41]
Enthalpy of vaporization at T_S, ΔH_{vap} (J/kg)	2.419×10^6 [41]
Dimension (inches$\times$inches)	12×12

Table 3-2 Fabric information

Fabric name	Fiber content	Fabric pattern	Fabric count (warp/cm)$\times$(weft/cm)
Denim	100% cotton	3/1 twill	26×17
Nomex®	100% flame-resistant aramid	plain weave	19×17

Table 3-3 Parameters of the fabrics

Fabric	Denim	Nomex[®]
k_f , Thermal conductivity of fiber (W/m K)	0.243 [46]	0.25 [47]
l_F , Thickness (mm)	1.34	0.87
m, Mass of fabric[*1] (kg/m^2)	456×10^{-3} (13.4 oz/yd^2)	254.3×10^{-3} (7.5 oz/yd^2)
ρ_f , Fiber density (kg/m^3)	1520 [46]	1460 [46]
p , Porosity[*2]	0.777	0.8
τ , Tortuosity[*2]	1.178	1.159
ε_F , Surface emissivity	0.68 [48]	0.77 [49]

[*1] Mass of fabric is tested according to ASTM D 3776[50]

[*2] Calculations of fabric porosity and tortuosity are shown in Appendix D

3.2 Results

Tests were conducted for the above two fabrics with spacers of different thickness. During each test, recording of environmental parameters and energy input started after all experimental conditions reached steady state, and the thermal or evaporative resistance was calculated from the average of the recorded values over a period of 30 minutes. The measured thermal and evaporative resistances were compared with calculations from the heat and mass transfer model presented in Chapter 2.

3.2.1 Tests under dry condition

Ambient conditions in dry tests are specified in Table 3-4. The total thermal resistance of the fabric system R_{ct} associated with different air gap thicknesses are measured and compared with the model prediction. Raw experimental data are given in Table 3-5 and the comparison to model predictions is illustrated in Figs. 3-3 and 3-4.

Table 3-4 Ambient conditions in dry tests

Properties	Values
Ambient temperature, T_E (°C)	25
Ambient relative humidity, ϕ_E (100%)	0.65
Ambient wind velocity, V (m/s)	1

Table 3-5 Experimental R_{ct} values (m^2 K/W)

Sample	No air gap		3mm air gap		6mm air gap		11.6mm air gap	
	Denim	Nomex®	Denim	Nomex®	Denim	Nomex®	Denim	Nomex®
1	0.0873	0.0792	0.158	0.169	0.188	0.192	0.215	0.202
2	0.0873	0.0789	0.158	0.167	0.180	0.193	0.209	0.199
3	0.0831	0.0788	0.156	0.167	0.170	0.194	0.197	0.203
Mean	0.0859	0.0790	0.158	0.167	0.179	0.193	0.207	0.201
STD×10^{-3}	2.40	0.200	1.20	1.10	9.00	0.900	9.20	2.20
CV%	2.82	0.260	0.790	0.680	5.03	0.440	4.46	1.08

Figure 3-3 Tested and predicted R_{ct} values for Denim under dry condition.

Figure 3-4 Tested and predicted R_{ct} values for Nomex® under dry condition.

It can be seen from Figs. 3-3 and 3-4 that both the measured and predicted R_{ct} values increase with the air gap thickness. The increase is nonlinear and the rate of increase becomes smaller for larger air gap. However the predicted R_{ct} values are generally larger than the experimental data. This can be explained by noting that in the model, the air flow is assumed to be laminar when it enters the region above the fabric system. In the experiments, however, the instrument produces a "semi-turbulent" flow [51] that enters the test hotplate, resulting in larger heat loss than laminar flow at the same speed and smaller thermal resistance.

The effect of different flow type is particularly significant on the boundary air layer. This is quantified by the thermal resistance of a bare plate R_{ct0} for which no fabric system is present. Specifically, R_{ct0} is predicted to be 0.0770 m^2 K/W from the model, while the measurement gives 0.0561 m^2 K/W. In order to minimize the influence of different flow, comparison is made between the tested

and predicted fabric thermal resistance R_{cf}, where R_{ct0} is subtracted from R_{ct}. This is illustrated in Figs. 3-5 and 3-6.
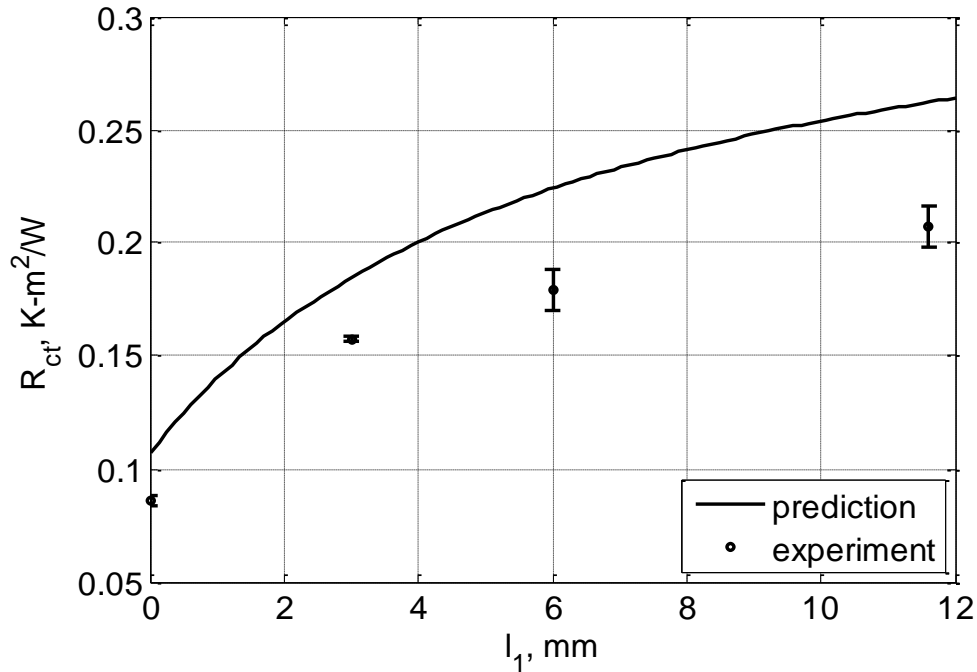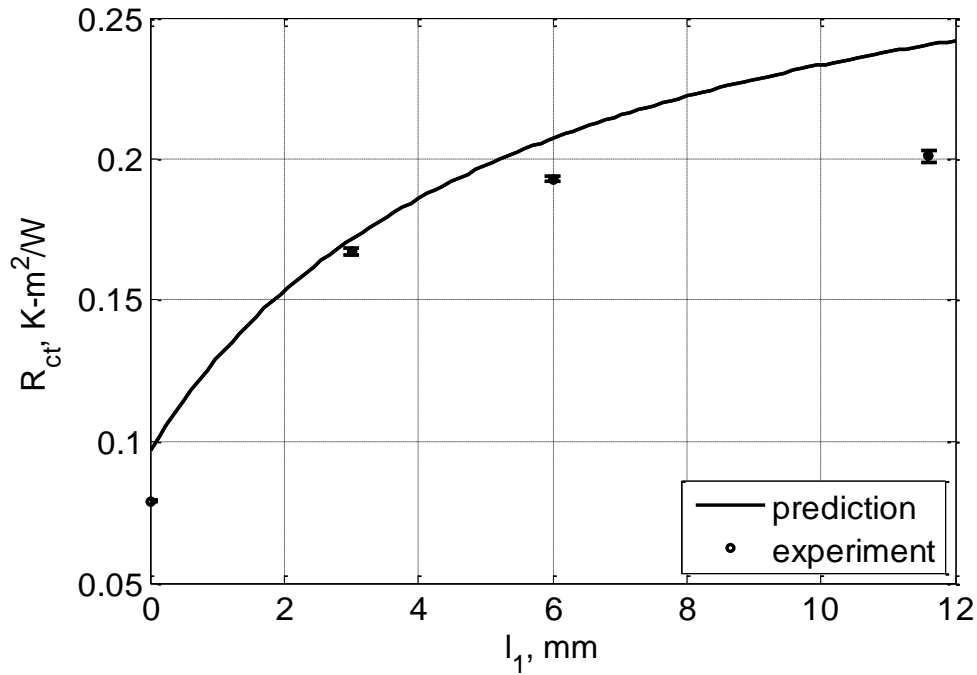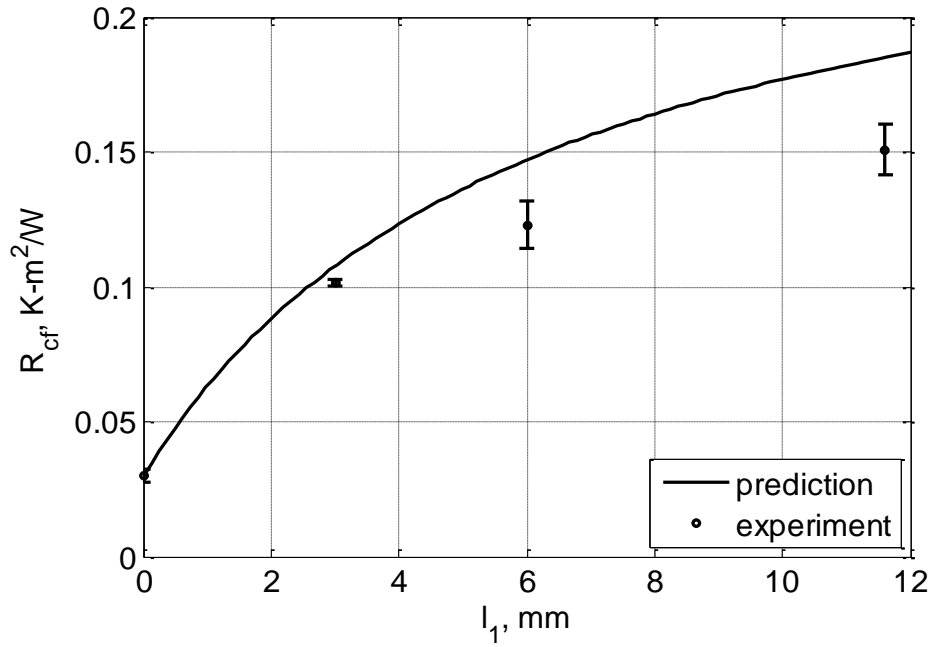

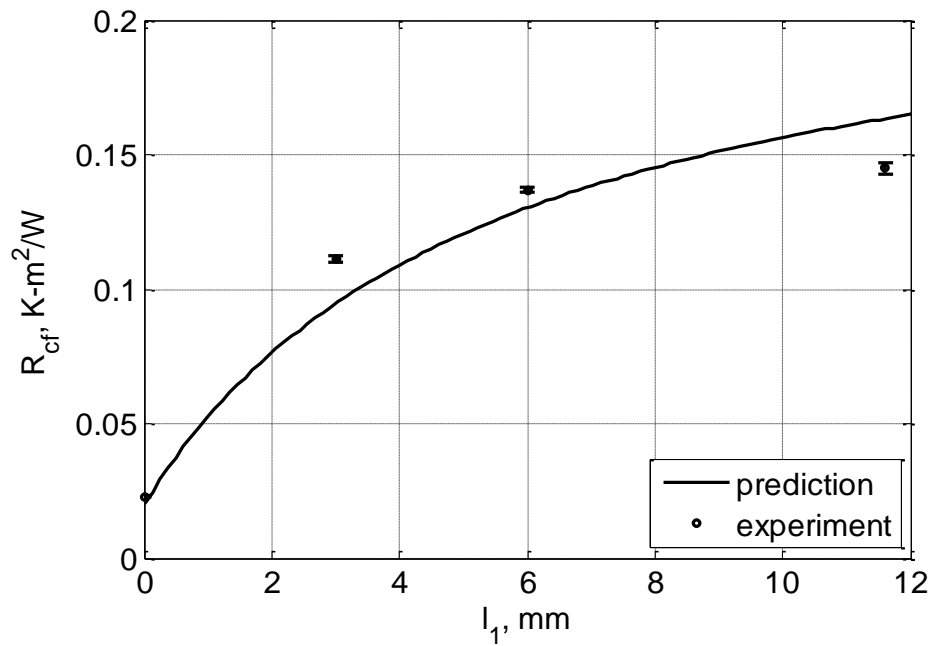Figure 3-5 Tested and predicted R_{cf} values for Denim under dry condition.

Figure 3-6 tested and predicted R_{cf} values for Nomex® under dry condition.

As shown in Figs. 3-5 and 3-6, the predicted R_{cf} are in good agreement with the experimental data for both fabrics. The largest discrepancies between predictions and experimental data appear at 11.6mm air gap for both fabrics, i.e., 19.1% for Denim and 11.9% for Nomex®. The increasing discrepancy with air gap thickness can be attributed to the horizontal heat loss from the sides of the spacers, which has been reported in a previous study on the hotplate testing method [52]. Fig. 3-7 demonstrates the scenario. In Fig. 3-7(a), where the fabric layer is in direct contact with the test plate, the ring guard and lower guard prevent heat loss from the sides so that heat transfer is one dimensional in the vertical direction. When a spacer is introduced, as shown in Fig. 3-7(b), heat can be transferred through the sides of the spacer because the material of the spacer does not provide as good insulation as the guards, thus more energy needs to be generated to maintain the surface temperature of the hotplate. This causes discrepancy between model and experiment, and such discrepancy increases with the thickness of the spacer.
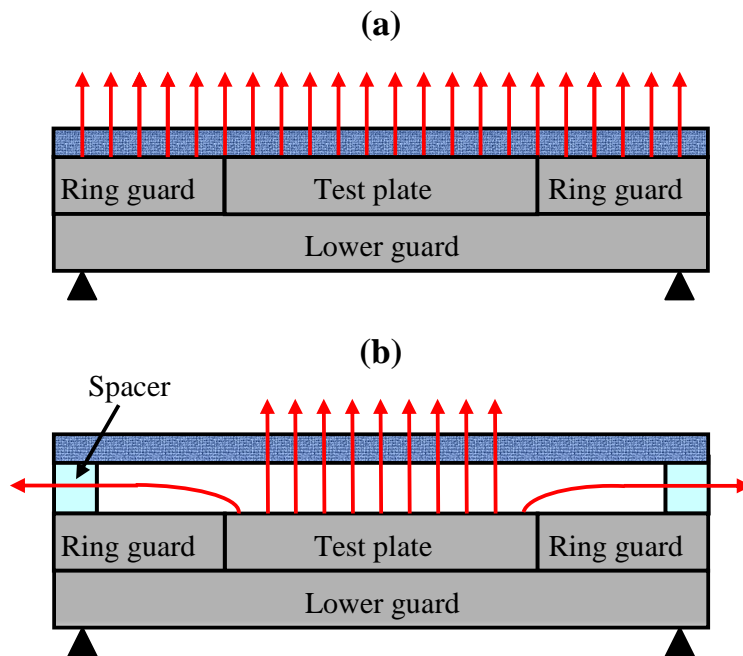
(a)

(b)

Figure 3-7 Heat flow in the experiments: (a) no side heat loss for a system without spacer, (b) side heat loss for a system with a spacer.

3.2.2 Tests under wet condition

Ambient conditions in wet tests are specified in Table 3-6. The total evaporative resistance R_{et} associated with different air gap thickness is calculated from the model and compared with experimental data. The surface diffusivity is taken to be zero in the theoretical calculation, i.e., $KD_{sur} = 0$. Raw experimental data are recorded in Table 3-7 and the comparison to model prediction is illustrated in Figs. 3-8 and 3-9.

Table 3-6 Ambient conditions in wet tests

Properties	Values
Ambient temperature, T_E ($^{\circ}$C)	25
Ambient relative humidity, ϕ_E (100%)	0.65
Ambient wind velocity, V (m/s)	1

Table 3-7 Experimental R_{et} values (m^2 Pa/W)

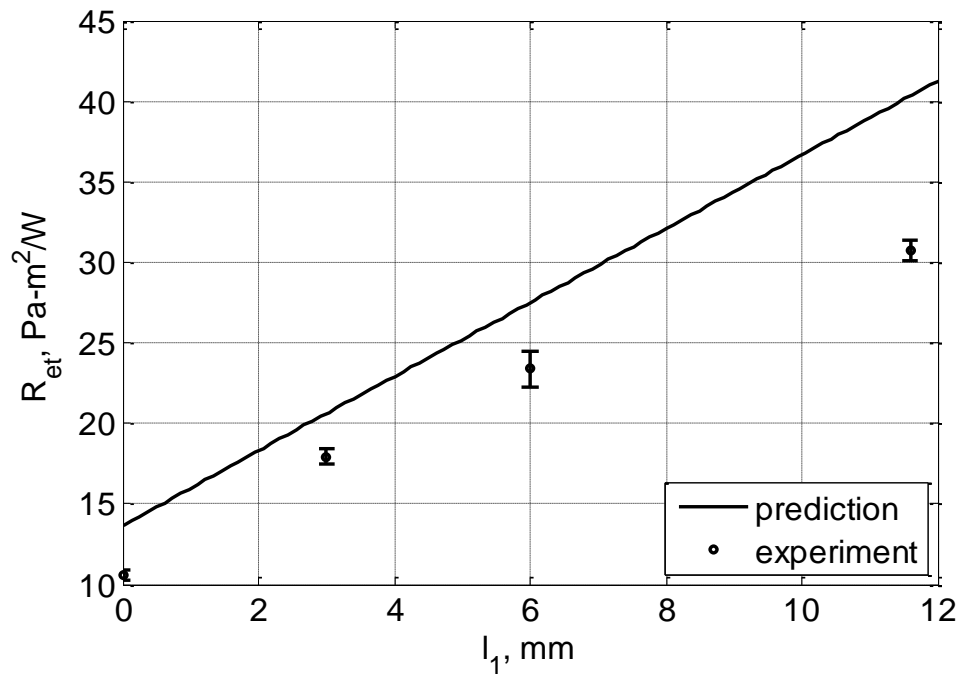| Sample	No air gap		3mm air gap		6mm air gap		11.6mm air gap	
	Denim	Nomex$^{\circledR}$	Denim	Nomex$^{\circledR}$	Denim	Nomex$^{\circledR}$	Denim	Nomex$^{\circledR}$
1	10.5	8.88	18.3	16.1	22.2	20.5	30.2	26.5
2	11.0	8.62	18.2	17.4	23.6	21.0	31.32	25.8
3	10.40	8.77	17.4	17.5	24.4	20.8	30.72	26.7
Mean	10.6	8.76	18.0	17.0	23.4	20.8	30.7	26.3
STD	0.318	0.129	0.508	0.763	1.11	0.216	0.590	0.474
CV%	2.99	1.47	2.83	4.48	4.74	1.04	1.92	1.80

Figure 3-8 Tested and predicted R_{et} values for Denim under wet condition.
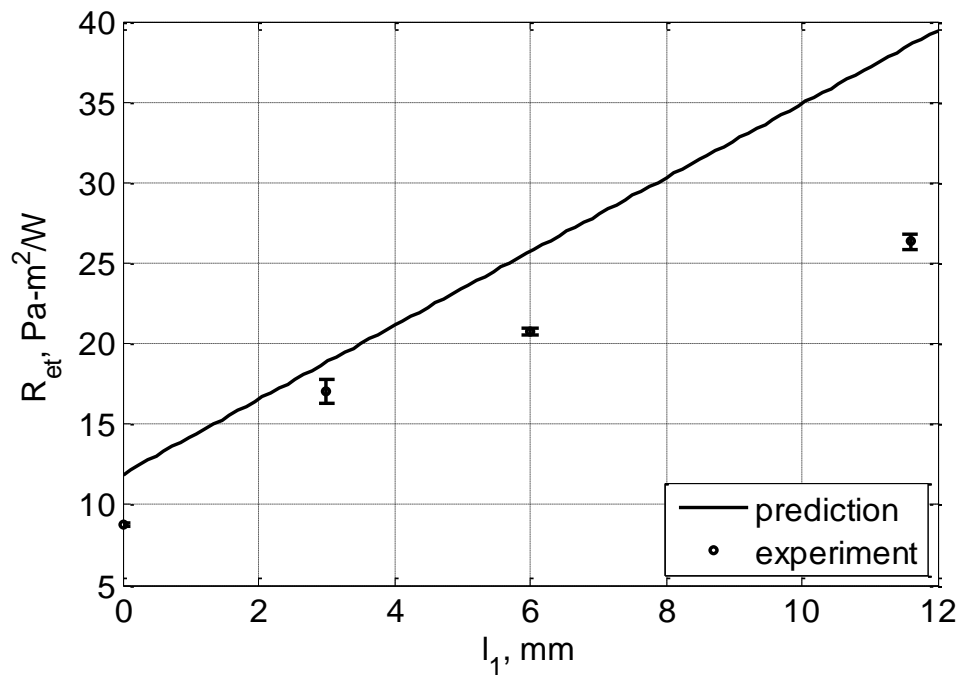
Figure 3-9 Tested and predicted R_{et} values for Nomex® under wet condition.

Both the measured and predicted total evaporative resistance R_{et} in Figs. 3-8 and 3-9 increases almost linearly with the air gap thickness. However, like in the comparison of R_{ct}, the model predictions of R_{et} are generally higher than the experimental data, due to the difference in flow type between experimental set-up and the model. Mass convection above the fabric system in the experiments is driven by "semi-turbulent" flow [51] rather than by laminar flow assumed in the model, hence resulting in greater mass transfer and smaller evaporative resistance.

To minimize this effect, the fabric evaporative resistance R_{cf} was calculated and compared with the experimental data. The evaporative resistance of bare plate R_{et0}, 9.04 m^2 Pa/W from model prediction and 4.63 m^2 Pa/W from experiment, are subtracted from R_{et} to obtain R_{cf}. The comparison of R_{cf} is illustrated in Figs. 3-10 and 3-11.
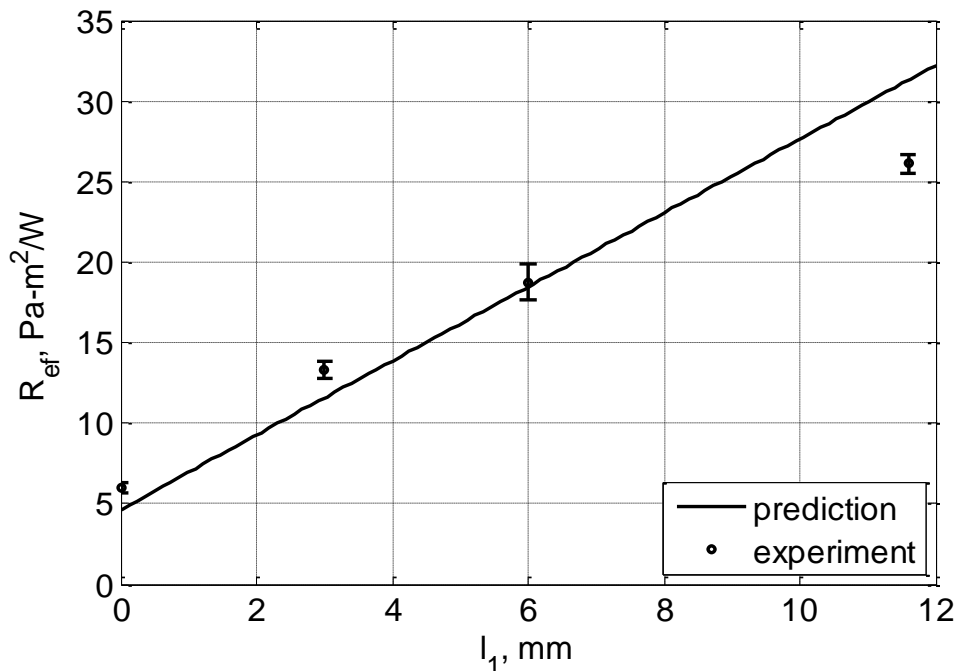
Figure 3-10 Tested and predicted R_{ef} values for Denim under wet condition.
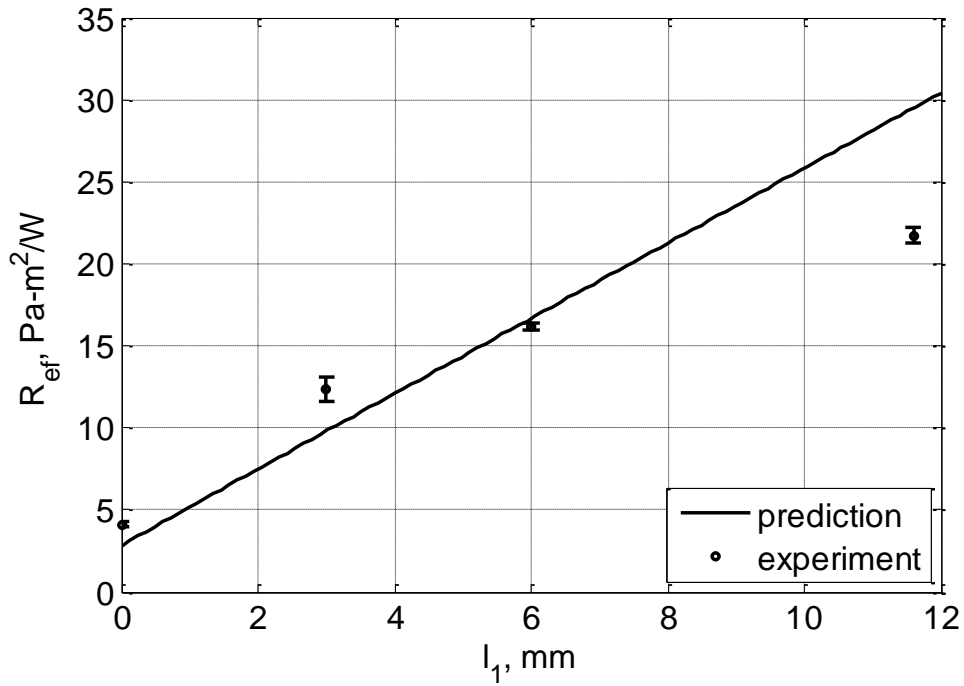
Figure 3-11 Tested and predicted R_{ef} values for Nomex® under wet condition.

In Figs. 3-10 and 3-11, good agreement is found between model and experimental data for R_{ef} except for very large air gap thickness, with the largest errors showing up at the 11.6mm air gap, i.e., 16.6% for Denim and 26.4% for Nomex®. Side heat loss present at large air gap is accompanied by a small amount of horizontal mass flow developed from the hotplate to the sides of the spacer, which can further result in condensation onto the spacer due to the sudden temperature drop experienced by the adjacent water vapor. As a result, mass transfer is greater than that predicted in the one-dimensional model. Therefore, the measured R_{ef} is smaller than the predicted one at large air gap thickness.

In the above calculations, because of the lack of quantification for surface diffusivity, the value for KD_{sur} is taken to be zero. $KD_{sur} = 1 \times 10^{-5}$ m²/s

suggested by Min *et al.* [39] was used in a separate calculation. However, no significant difference is found for the comparison, suggesting that surface diffusivity is not important in the current experimental assembly. To account for its effect on evaporative resistance in general, parametric study on this quantity is performed in the next chapter.

3.3 Summary

Comparison is made for both thermal and evaporative resistances calculated from the heat and mass transfer model and measured from the experiments. Due to the difference in external flow, discrepancy exists between the measurement and model prediction of the total thermal (R_{ct}) and evaporative (R_{et}) resistances. Comparison of fabric thermal (R_{cf}) and evaporative (R_{ef}) resistances shows good agreement except for very large air gap, which can be due to side heat loss and liquid condensation in the experiments. These results show that the heat and mass transfer model presented in Chapter 2 is capable of accurately predicting thermal and evaporative resistances for the single-layer fabric system. In the next chapter, this model is applied in a parametric study on the effect of environmental conditions and parameters of a fabric system on its thermal performance.

CHAPTER 4: PARAMETRIC STUDY

In this chapter, parametric study is conducted using the developed model to address the effect of environmental conditions, MC and fabric thicknesses and material parameters on the thermal and the evaporative resistances. In all the calculations, the skin temperature is fixed at $T_S = 35^oC$ and its emissivity is $\varepsilon_S = 0.95$ [41]. Under wet condition, the skin surface is fully saturated with relative humidity is $\phi_S = 100\%$. The characteristic length in the forced convection in the environment is taken to be $L = 0.3048$ m, which is the length of the hotplate in the experiment. All other parameters to be studied are listed in Table 4-1. While studying the effect of each parameter, all other parameters are assumed to be constant as specified. The MC thickness, which is closely related to the garment fit feature, is selected over a range of geometries in Table 4-1, where a 0.001 mm air gap is used to mimic the case of zero air gap since setting the air gap to be exactly zero causes problem in the numerical solution; 3 mm, 6 mm and 12 mm are selected to study the effect of MC for certain "tight-fit" [3] fabric systems.

Table 4-1 Parameters used to calculate thermal and evaporative resistances

Parameter	Range of variation	Constant when varying other parameters
Ambient temperature, T_E (^oC)	[-50, 100] (dry); [0, 100] (wet)	25
Air speed, V (m/s)	[1,30]	1
Ambient RH, ϕ_E (100%)	[0, 100]	0.65 (wet only)
Air gap thickness, l_1 (mm)	[0.001, 30]	0.001, 3, 6 or 12; see individual figure
Fabric thickness, l_F (mm)	[0.001, 6]	1
Fiber conductivity, k_f (W/m K)	[0.01, 1]	0.25
Porosity, p	[0.1, 0.99]	0.7
Fabric emissivity, ε_F	[0.01, 0.99]	0.7
Surface diffusivity, KD_{sur} (m^2/s)	[10^{-6}, 10^{-4}]	0

4.1 Thermal resistance

This section reports the model predictions for total thermal resistances R_{ct} and fabric thermal resistance R_{cf} under dry condition. How they change with varying environmental conditions and fabric properties is analyzed, and their implication to thermal comfort is addressed.

4.1.1 Effect of environmental conditions

Because the bare skin thermal resistance R_{ct0} depends on the environmental conditions (ambient temperature and wind speed), discussions are carried out for both R_{ct} and R_{cf}.

Ambient temperature

Fig. 4-1 shows the effect of ambient temperature T_E on R_{ct} for systems with the same fabric but different MC thicknesses. The plot shows an overall decreasing trend in R_{ct} with T_E, except for the case of 12 mm air gap, where R_{ct} first increase and then decreases after T_E reaches 17.2°C. In addition, the decreasing branch of R_{ct} with T_E is almost linear for all cases. The distinct behavior observed for 12 mm air gap is due to the fact that when the ambient temperature is below 17.2°C, natural convection takes place in the MC of this system. This is confirmed by calculating the Rayleigh number at this temperature, which equals the critical Rayleigh number of 1708. For other MC thicknesses, natural convection does not occur for the entire range of T_E. It can also be seen from Fig. 4-1 that for most environmental temperature, increasing air gap thickness results in significant increase in R_{ct}. For example, at T_E = 17.2°C, by introducing a 3 mm, 6 mm, and 12 mm MC into a fabric without air gap (l_1 = 0.001 mm), R_{ct} is increased by 78.2%, 118%, and 158% respectively. However, due to the natural convection in the MC, a system with a 12mm air gap does not always provide higher thermal resistance than a system with a 6mm air gap, i.e., in this figure,

the former has higher thermal resistance only when the ambient temperature exceeds -22.5°C. Therefore adding MC thickness does not always result in better insulation, which is sensitive to the ambient temperature.
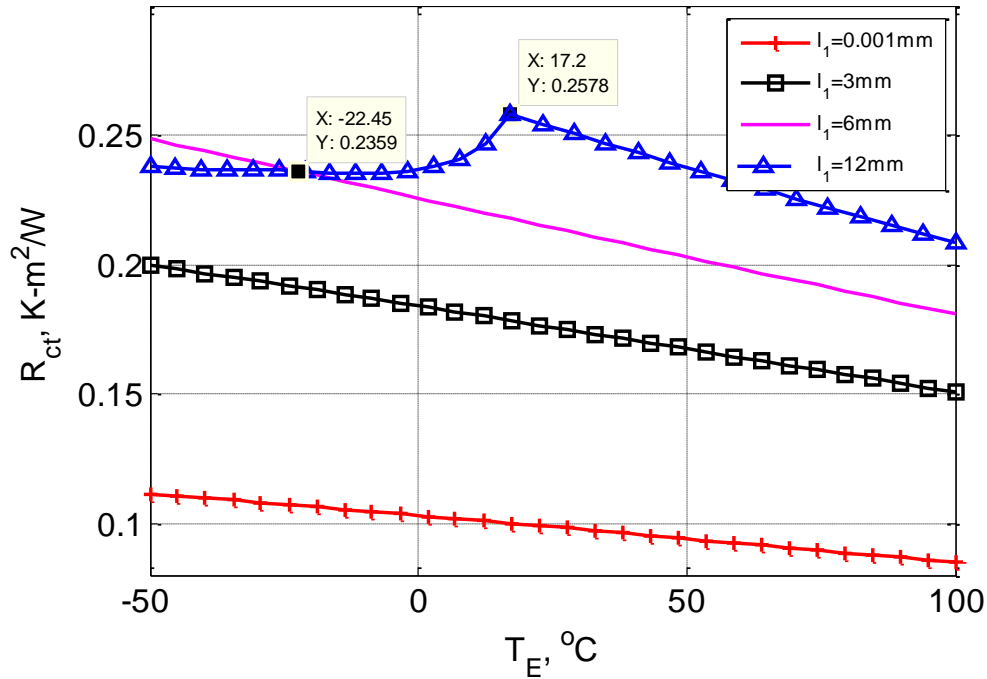
Figure 4-1 Effect of ambient temperature on the total thermal resistance.

In order to examine the heat transfer modes within the fabric systems under different conditions, systems with different air gap thickness and ambient temperature were compared and illustrated in Figs. 4-2 and 4-3 respectively. In Fig. 4-2, the heat flux from each mode (conduction, convection and radiation) is plotted for the air gap, fabric and environment layers. Air gap thickness is fixed to be 3 mm in all the plots. When the environmental temperature is higher than the skin temperature, the total heat loss is negative, which indicates a heat gain from the environment. For a constant skin temperature, it is expected that more heat is transferred to the fabric as the temperature difference between the skin and the ambient increases, which is confirmed by Fig. 4-2. On the other hand, the temperature difference in Eqn. (2-1) also increases as the ambient

temperature decreases. The change in thermal resistance is hence a result of the competition between the increase in temperature difference ($T_S - T_E$) and that in heat flux q_{dry}.
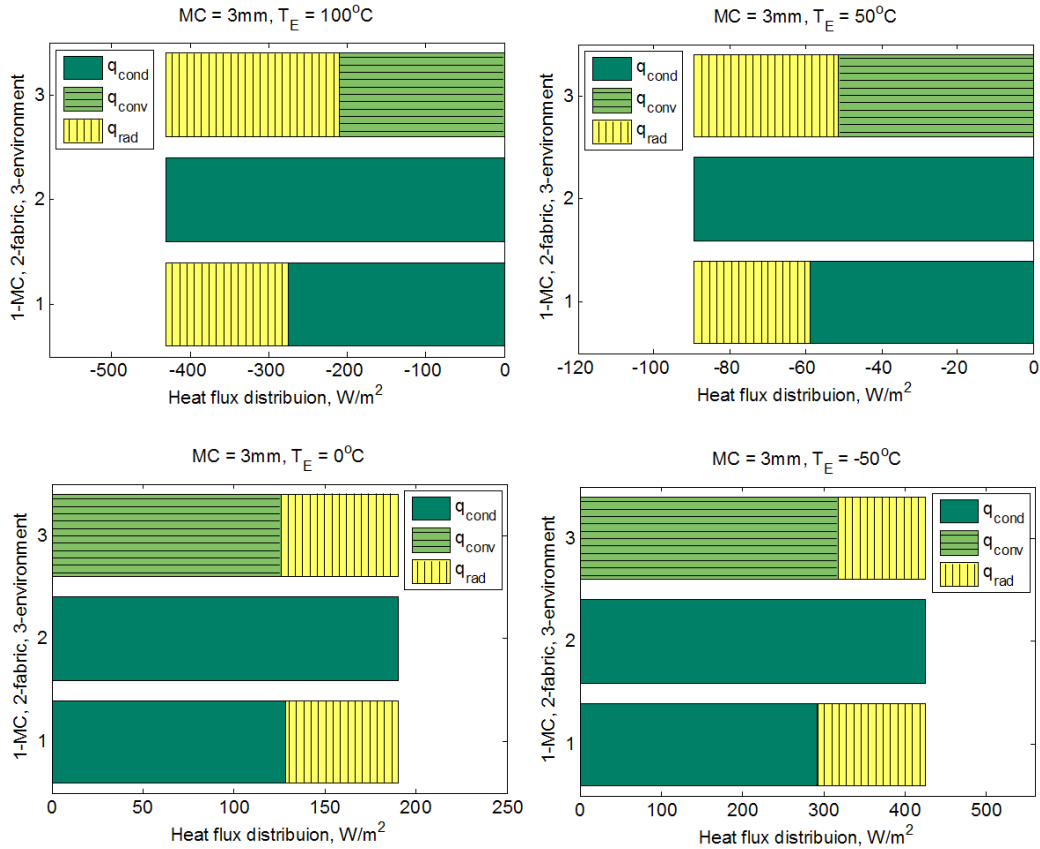
Figure 4-2 Heat flux distribution in each layer for systems under different ambient temperature.

Fig. 4-3 shows the heat flux component for the same ambient temperature $25^{\circ}C$ but different air gap thicknesses. The reduction in total heat flux with increasing air gap thickness is apparent, which indicates an increase in thermal resistance. In addition, as the air gap thickness increases, the conduction component in MC layer becomes smaller, accounting for 100%, 63.2%, 49.9% and 33.3% of the total heat flux, respectively for 0.001 mm, 3 mm, 6 mm and 12 mm MC. The decrease in the conduction component here is consistent with Fourier's law that

the heat transfer rate is inversely proportional to the thickness of the medium. At the same time, the radiation component increases correspondingly with MC thickness. This is in agreement with Stephan-Boltzmann's law because temperature difference at the two sides of the MC is increased with its thickness l_1.
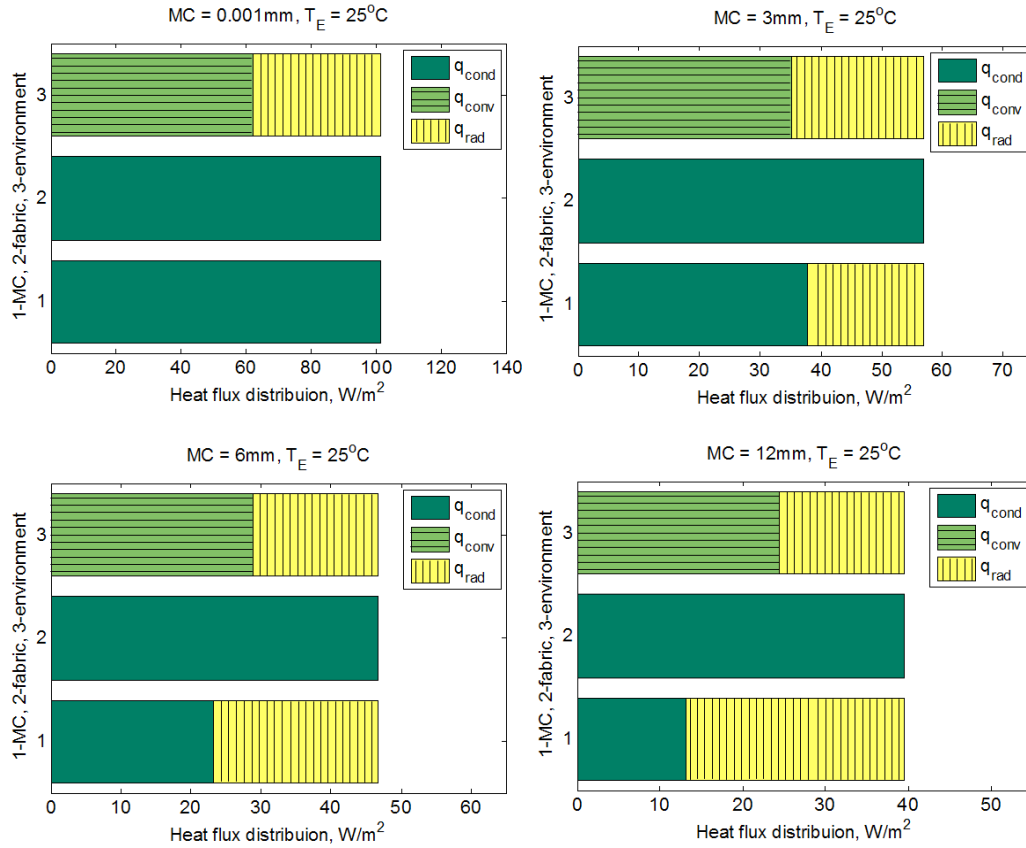
Figure 4-3 Heat flux distribution in each layer for systems with different air gap thicknesses.

The bare skin thermal resistance R_{ct0} is calculated and it decreases with the ambient temperature, as shown in Fig. 4-4. It is reduced by 28.1% as T_E increases from -50°C to 100°C. This can be explained by the fact that under dry condition R_{ct0} is given by $\left[h_{f,E} + \varepsilon_S \sigma (T_S + T_E)(T_S^2 + T_E^2)\right]^{-1}$ according to Eqns. (2-1) and (2-18). As the ambient temperature changes from -50°C to 100°C, the heat transfer coefficient $h_{f,E}$ under the current wind speed ($V = 1$ m/s) only decreases slightly

from 7.03 W/m^2 K to 6.95 W/m^2 K, while the other term $\varepsilon_S \sigma \left(T_S + T_E \right) \left(T_S^2 + T_E^2 \right)$ due to radiation increases significantly from 4.14 W/m^2 K to 8.58 W/m^2 K. They together account for the decrease in Fig. 4-4. Fig. 4-5 shows the effect of T_E on the fabric thermal resistance R_{cf}, which exhibits similar behavior as seen in Fig. 4-1. Clearly, R_{cf} of a fabric system without air gap remains almost unchanged for the entire range of ambient temperature.

Figure 4-4 Effect of ambient temperature on the bare skin thermal resistance.

Figure 4-5 Effect of ambient temperature on the fabric thermal resistance.

Air speed

The air speed in the environment is another important factor that affects thermal insulation of a fabric system, i.e., it is related to the wind chill effect on human body in cold weather. Boundary air layer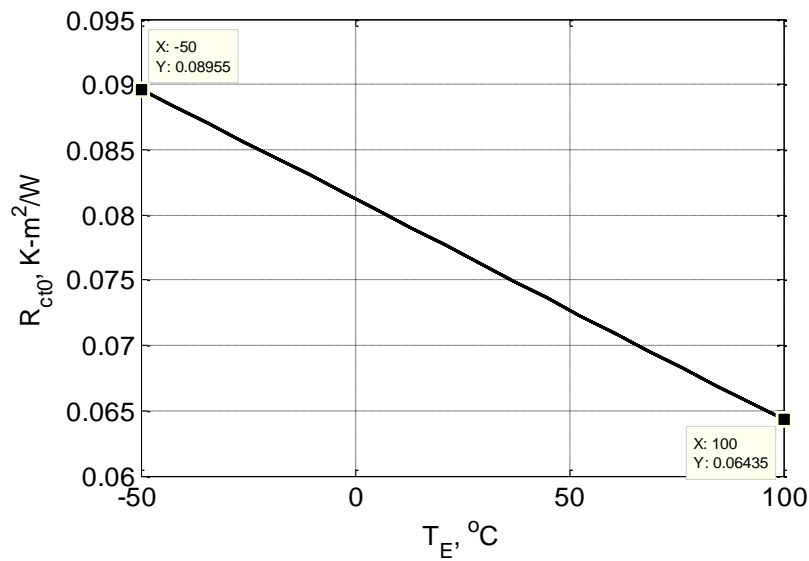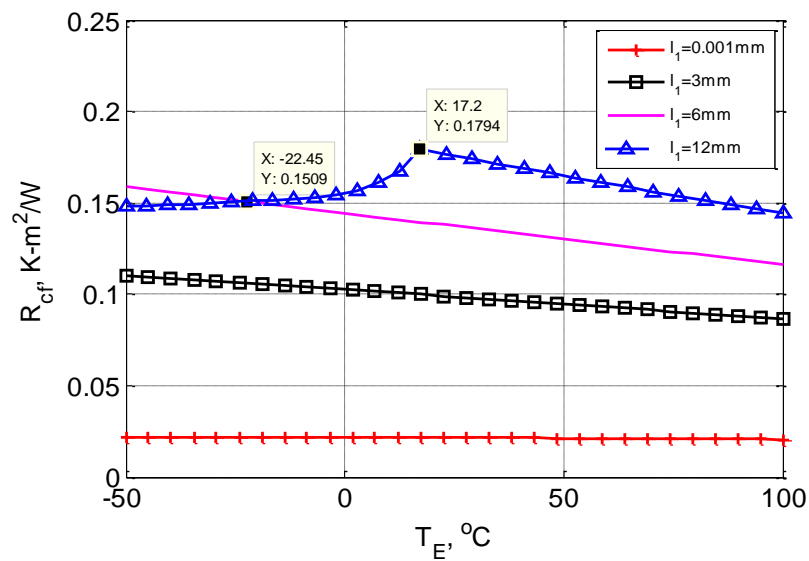 conducts heat through forced convection, which can increase significantly with the wind speed, especially when the wind changes its type from laminar to turbulent flow, as can be seen from the results below.

In the model presented in Chapter 2, natural convection was assumed negligible in the ambient. The validity of this assumption for the studied range of environmental conditions has been checked using two criteria: $Gr_L / Re_L^2 << 1$ [41] and $\left(Nu_n / Nu_f \right)^{3.5} << 1$ [53]. Detailed calculations are given in Appendix A. For the characteristic length considered here, both criteria are satisfied if the air speed V is larger than 1 m/s. The dependence of thermal resistance R_{ct} on air speed is plotted in Fig. 4-16 for a fabric system with an air gap thickness of 6 mm. It indicates that R_{ct} of the fabric system deceases with V, and the decrease is most significant for $V < 5$ m/s. An abrupt transition exists at $V_1 = 25.6$m/s, which corresponds to the onset of turbulent flow over the fabric surface. Below V_1, the flow over the entire fabric surface is laminar. V_1 here is calculated from the criterion $Re_{L,1} = V_1 \rho_{air}(T_{f,1})L / v_{air}(T_{f,1}) = 5 \times 10^5$, where L is the characteristic length for forced convection, ρ_{air} and v_{air} are the density and kinematic viscosity of air respectively, and their values are evaluated at the film temperature $T_{f,1} = \left(T_2 + T_E \right) / 2$, where T_2, the temperature at the fabric-environment interface, is an unknown that has to be solved iteratively. Due to the increased convection driven by turbulent flow, R_{ct} deceases at a greater rate beyond V_1.
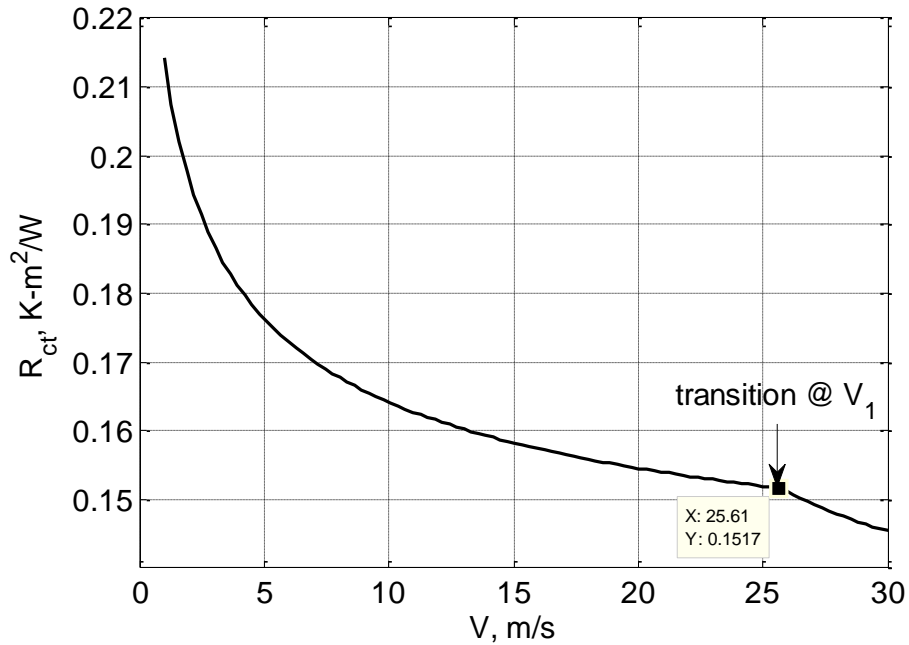
Figure 4-6 Wind effect on the total thermal resistance of a fabric system with 6 mm MC.

Fig. 4-7 shows the bare skin thermal resistance R_{ct0} as a function of V. The trend is very similar to Fig. 4-6, but the transition point from laminar to turbulent flow is a little higher than V_1, which is at $V_2 = 26.5$ m/s. V_2 is calculated from $\mathrm{Re}_{L,2} = V_2 \rho_{air}(T_{f,2})L / \nu(T_{f,2}) = 5 \times 10^5$, where ρ_{air} and ν are now evaluated at the film temperature of $T_{f,2} = (T_S + T_E)/2$. The different transition speeds found in Figs. 4-6 and 4-7 are due to the different film temperatures $T_{f,1}$ and $T_{f,2}$ used in evaluating the air properties ρ_{air} and ν. To be more specific, $\rho_{air}(T)$ is a decreasing function of temperature while $\nu(T)$ increases with temperature. Their ratio $\rho_{air}(T)/\nu(T)$ consequently decreases with temperature. Since $T_{f,2} > T_{f,1}$, $\rho_{air}(T_{f,2})/\nu(T_{f,2}) < \rho_{air}(T_{f,1})/\nu(T_{f,1})$, and therefore $V_2 > V_1$. In addition, the wind effect shown here explains the experimental finding in Fig. 5 from Havenith *et al.* [3], where the dependence of air layer insulation on wind speed was found to be

quantitatively consistent with Fig. 4-7 for the wind speed from 1 m/s to 5 m/s, experimental data beyond 5 m/s was not available from their work.
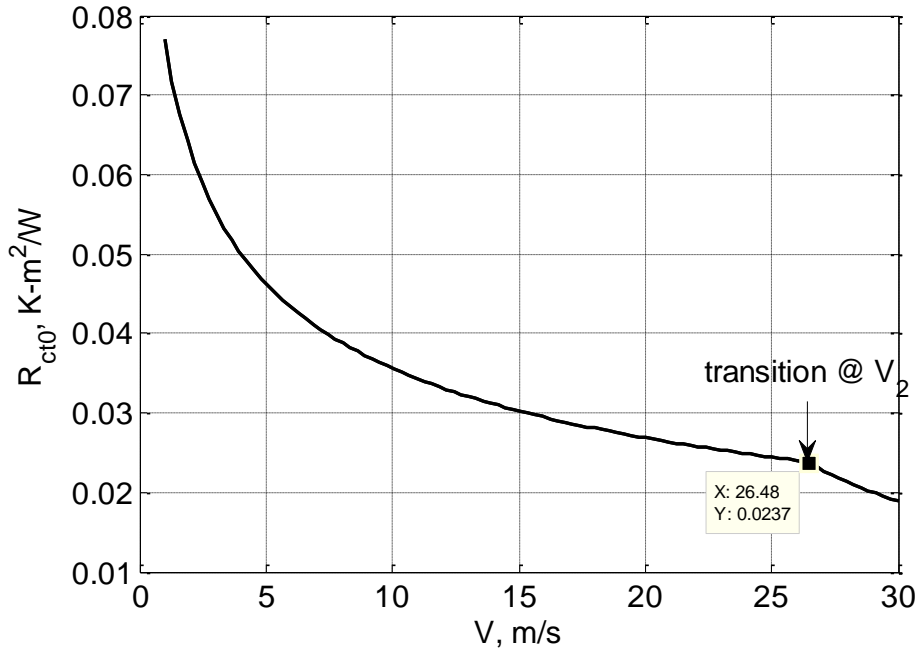
Figure 4-7 Wind effect on the bare skin thermal resistance.

The dependence of fabric resistance R_{cf} of the same system on air speed is shown in Fig. 4-8, where both transition points V_1 and V_2 can be seen. Between V_1 and V_2, the flow over part of the fabric surface has turned turbulent, while the flow over the bare skin is still laminar; therefore, there is a sudden drop in R_{cf}. Beyond V_2, R_{cf} remains almost unchanged. The overall variation of R_{cf} with respect to the wind speed is not significant. Specifically, by increasing the wind speed from 1 m/s to 30 m/s, R_{cf} is reduced by only 7.73%. This suggests that the reduction in R_{ct} is mostly due to decrease in the bare skin thermal resistance R_{ct0}, which is consistent with the experimental findings from Havenith *et al.* [22].
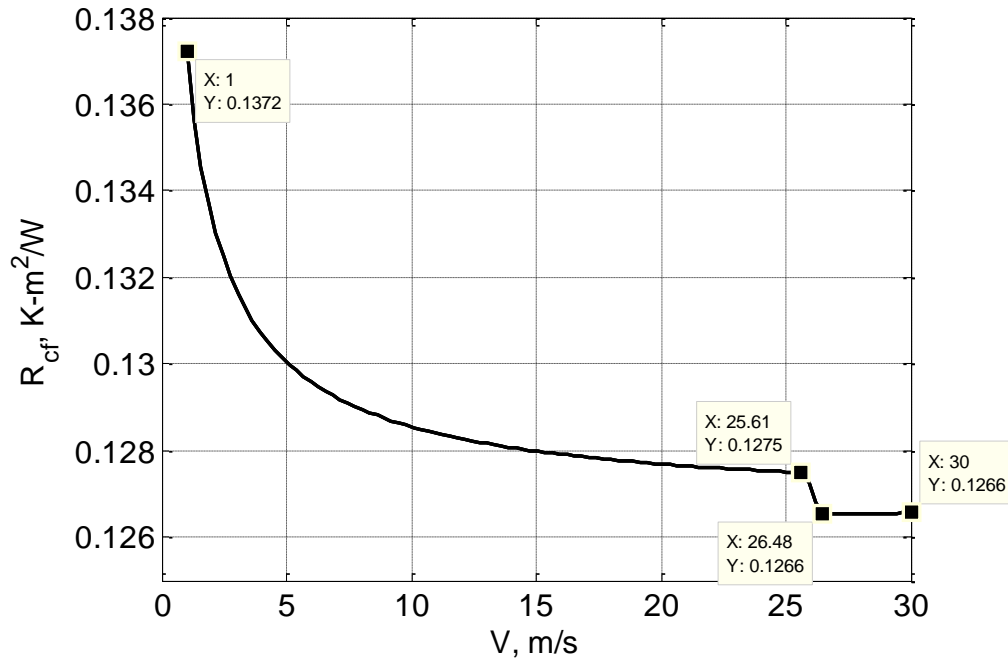
Figure 4-8 Wind effect on the fabric thermal resistance of a fabric system with 6 mm MC.

The wind effect on R_{ct} for four fabric systems with different MC thickness is illustrated in Fig. 4-9, which exhibits similar behavior as seen in Fig. 4-6. The transition speeds V_1 for different fabric systems are slightly different due to the different film temperature used in the calculation of Reynolds number for the boundary layer above the fabric. Specifically, film temperature above the fabric with thicker MC is smaller and therefore V_1 is smaller. In general, increasing MC thickness provides better insulation. For example, at the wind speed of 5m/s in Fig. 4-9(a), by introducing a 3mm MC to a fabric system without air gap ($l_1 =$ 0.001 mm), R_{ct} is increased by 127% from 0.0608 m^2 K/W to 0.138 m^2 K/W. However, under a low temperature condition, a 12 mm MC does not always provide higher thermal insulation than 6 mm MC due to natural convection in MC. This can be seen from Fig. 4-9(b), where a 12 mm MC indeed provides less thermal insulation than 6 mm MC at T_E = -10°C when wind speed V is greater than 6 m/s.
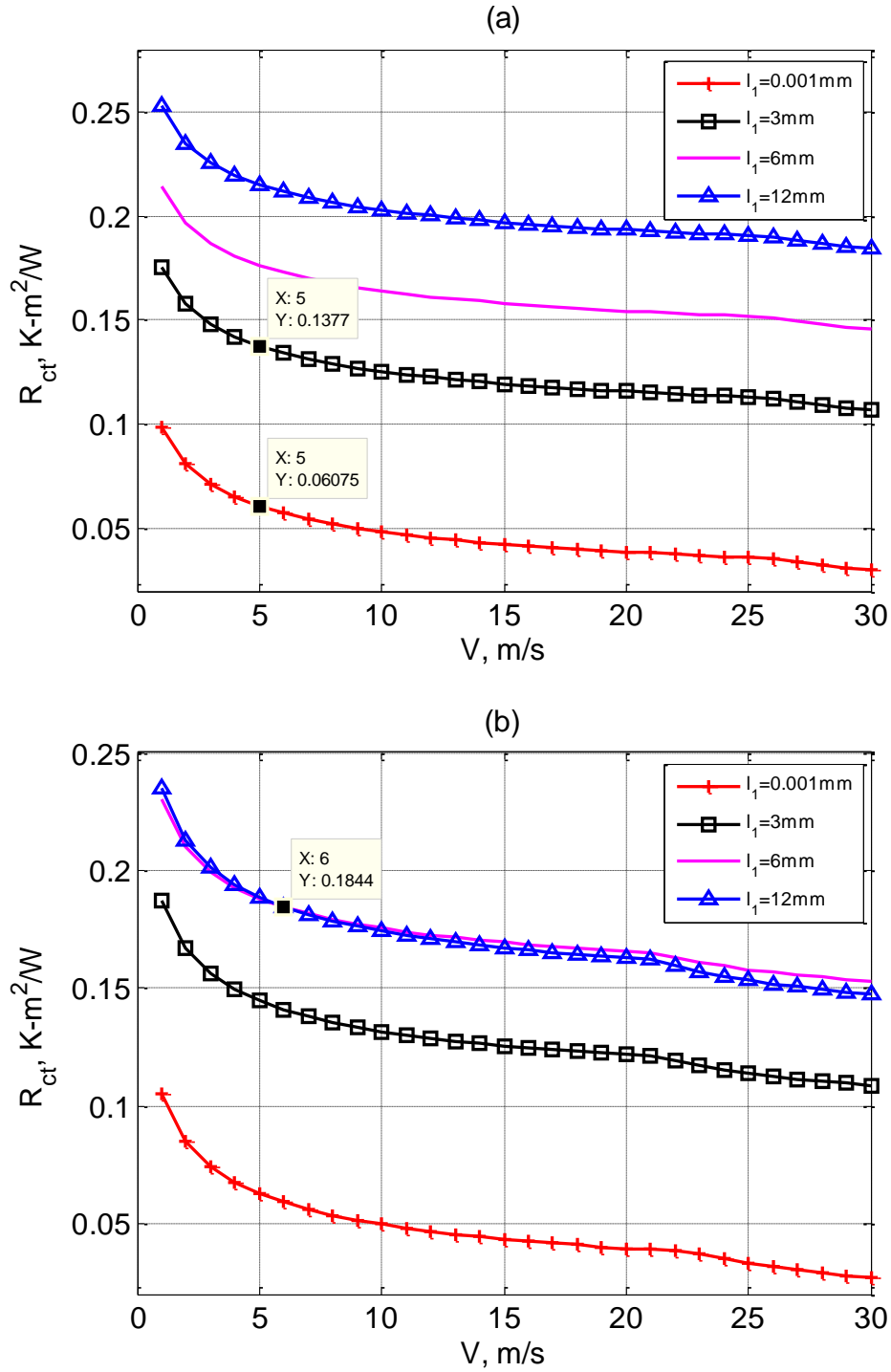
Figure 4-9 Wind effect on the total thermal resistance of systems with different MC thickness: (a) under ambient temperature of 25°C, (b) under ambient temperature of -10°C.

4.1.2 Effect of fabric properties

In the following, effect of fabric properties on thermal resistance is studied, while environmental conditions (ambient temperature and wind speed) are kept unchanged. In this case, R_{ct0} is a constant independent of the variations in fabric properties, that is, R_{ct} and R_{cf} differ only by a constant value. Therefore only the dependence of R_{ct} is presented here.

MC thickness

The effect of MC thickness on the total thermal resistance is illustrated in Fig. 4-10, which demonstrates the following characteristics. For each curve, R_{ct} first increases significantly with increasing MC thickness. At a critical thickness, R_{ct} reaches a local maximum value and starts decreasing afterwards. This critical thickness corresponds to the onset of natural convection in the MC layer, confirmed from the calculation of the Rayleigh number. The total thermal resistance gradually builds up again after the critical point, but at a much slower rate. Similar experimental observation was reported by Fan *et al*. [24]. It is also clear from Fig. 4-10 that the value of the critical thickness is sensitive to the ambient temperature. For the specific fabric used here, under the ambient temperature of 25°C, 10°C and -50°C, the corresponding critical thickness is found to be 14.6 mm, 8.64 mm and 6.76 mm, respectively. The lower the ambient temperature, the easier it is for natural convection to occur in the MC, and hence the smaller the critical thickness. Therefore, for cold weather protective clothing, proper fit may provide a maximum thermal performance.
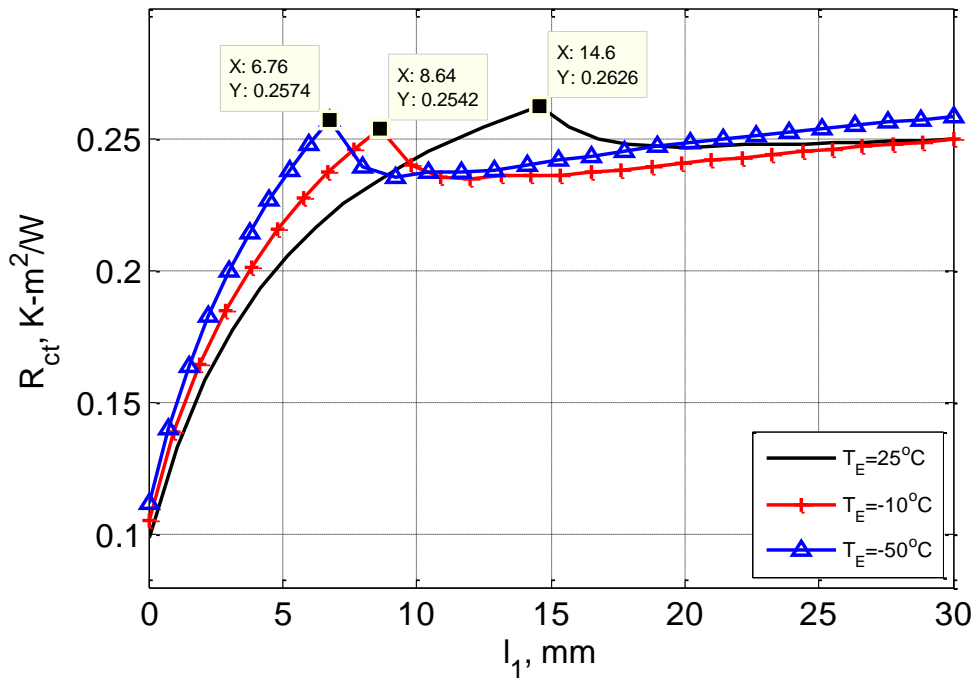
Figure 4-10 Effect of MC thickness on the total thermal resistance.

Fabric thickness

Fig. 4-11 shows the dependence of R_{ct} on the fabric thickness l_F, which is nearly linear for the entire range of l_F and four different MC thicknesses. The predictions agree well with previous research, where in some cases fabric thermal insulation exhibits a linear relation with fabric thickness [54, 55]. Normally, the increase of the fabric thickness implies more trapped air and therefore produces more thermal insulation. For example, by increasing the fabric thickness from 0.001 mm to 6 mm, R_{ct} for the fabric without air gap ($l_1 = 0.001$ mm) is increased by 74.3%. As air gap thickness increases, the curve shifts upwards significantly, specifically, by introducing a 3 mm and 6 mm MC into a fabric system without air gap, R_{ct} can be increased by 88.0% and 132% respectively. This indicates a relatively smaller influence of the fabric thickness than the MC thickness on the total thermal insulation, which agrees with the findings from Min *et al.* [39]. In addition, as the MC thickness increases, the effect of fabric thickness on thermal insulation

becomes smaller. Specifically, for the fabric without air gap, by varying l_F from 0.001 mm to 6 mm, R_{ct} is increased by 74.1%. However, with a MC of 12 mm, increase in R_{ct} is only 26.3% for the same range of variation in l_F.
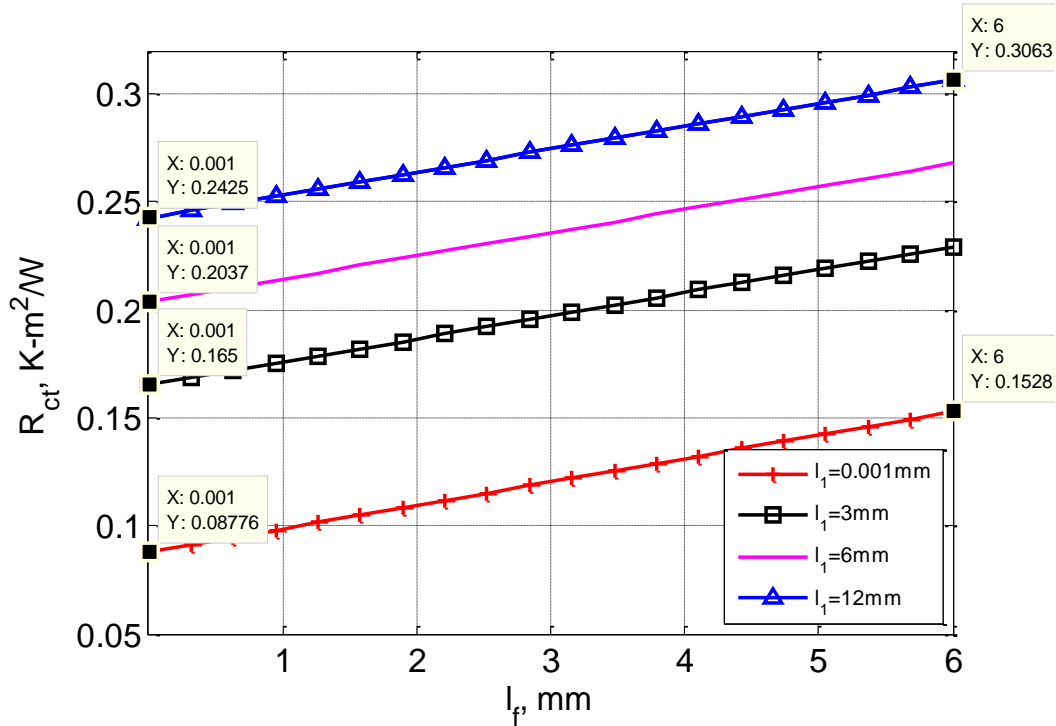
Figure 4-11 Effect of fabric thickness on the total thermal resistance.

Fiber conductivity

In Fig. 4-12, an overall non-linear decrease of R_{ct} with conductivity of fiber k_f is shown. R_{ct} exhibits most significant decrease with k_f before it reaches 0.2 W/m K, while increasing k_f beyond 0.2 W/m K does not change R_{ct} significantly. The relatively weak influence of the fiber conductivity is due to the porous structure of the fabric layer, where air occupies most of the volume and dominates in the effective thermal conductivity of the porous media. By comparing the results for different MC thicknesses, it can be seen that the effect of MC thickness is much stronger than that of fiber conductivity. Specifically, by reducing k_f from 1 W/m K to 0.01 W/m K for the fabric without air gap ($l_1 = 0.001$ mm), R_{ct} can be increased by 48.8%; while by introducing a MC of 3 mm, R_{ct} can be increased by

84.9%. In addition, as the MC thickness increases, the effect of thermal conductivity of fiber on thermal insulation becomes smaller.
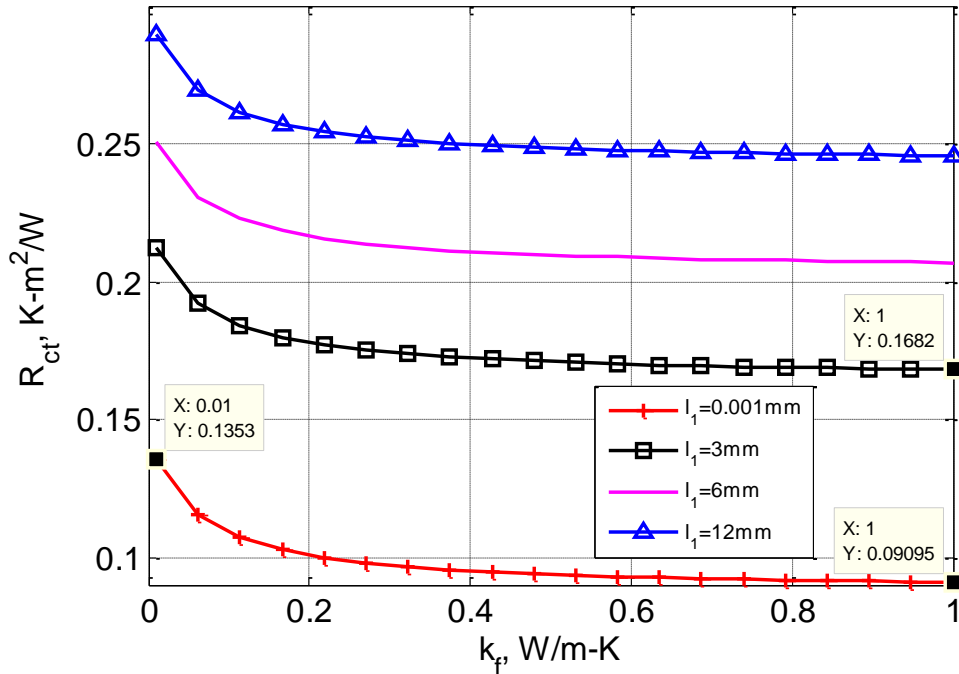
Figure 4-12 Effect of thermal conductivity of fiber on the total thermal resistance.

Porosity

The fabric porosity represents the relative air volume trapped (voids) in the fabric structure. Since fabric fibers normally have higher thermal conductivity than air, with larger fabric porosity, the effective thermal conductivity of the fabric becomes smaller and results in smaller conductive heat flux in the fabric; therefore, R_{ct} increases according to Eqn. (2-1). This influence is demonstrated in Fig. 4-13. For a fabric without air gap ($l_1 = 0.001$ mm), by increasing the porosity from 0.3 to 0.95, R_{ct} will be increased by 23.5%. Similar to the effect of thermal conductivity of fiber, the influence is weakened as the air gap thickness increases. The results obtained from the model indicate that the change of fabric porosity and fiber conductivity will have a minimal impact on thermal insulation value for a clothing system with large air gap.
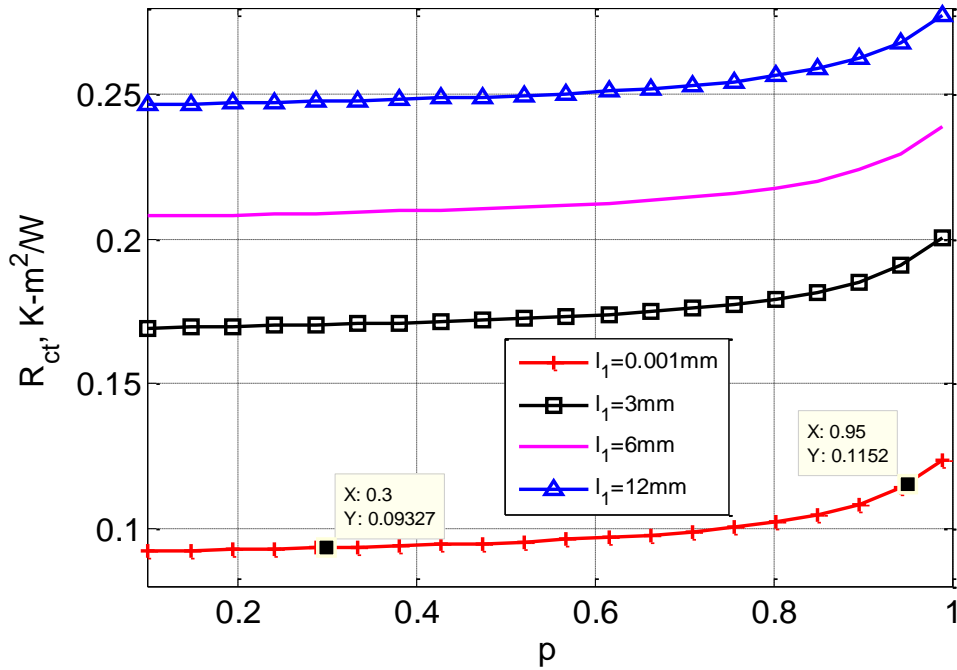
Figure 4-13 Effect of porosity on the total thermal resistance.

Surface emissivity

It is particularly interesting to see that varying the surface emissivity ε_f of the fabric layer has a strong effect on R_{ct}, shown in Fig. 4-14. As the surface emissivity decreases, radiation heat transfer also decreases, thus increasing the thermal resistance of the fabric. This indicates that much better insulation can be achieved by modifying the surface properties of the fabric (e.g., through certain finishing or coating), without changing the bulk fabric properties. Different from the previous three parameters (fabric thickness, fiber conductivity and porosity), the effect of surface emissivity on the thermal resistance becomes more significant as air gap thickness increases. For a fabric system without air gap, by reducing ε_f from 0.99 to 0.01, R_{ct} is increased by 76.5%. However, with the introduction of a 6mm and 12mm MC, increase in R_{ct} is 107%, 188% respectively for the same range of variation in ε_f. Such observations can be explained as following. With increasing MC thickness, the contribution of conduction to the

61

total heat flux reduces while the contribution of radiation becomes dominant, as discussed in Fig. 4-3. Since the radiative heat flux depends strongly on the surface emissivity, the thermal resistance R_{ct} for a fabric system with larger MC is more sensitive to changes in surface emissivity.
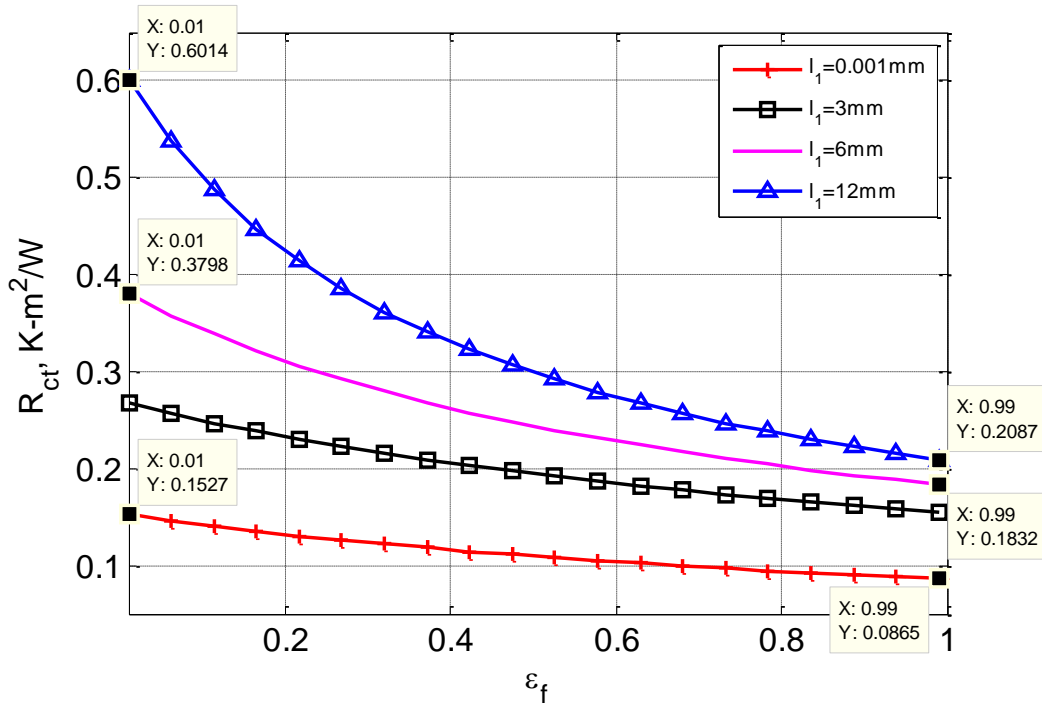
Figure 4-14 Effect of fabric surface emissivity on the total thermal resistance.

4.2 Evaporative resistance

When heat stress is produced, sweating is an efficient way to chill the human body by dissipating excessive heat in the core body from skin by evaporation. Evaporative resistance R_{et}, as a measure of mass transfer, is an important quantity associated with wet thermal comfort. Following the formulation in Chapter 2, the total evaporative resistance R_{et} and fabric evaporative resistance R_{ef} are calculated given the environmental conditions and fabric properties. The sensitivity of them to these parameters is analyzed.

4.2.1 Effect of environmental conditions

Because the bare skin evaporative resistance R_{et0} depends on the environmental conditions (ambient temperature, relative humidity and wind speed), discussions are carried out for both R_{et} and R_{ef}.

Ambient temperature

The total evaporative resistance R_{et} as a function of ambient temperature T_E is shown in Fig. 4-15 for a fabric system with 6 mm MC, which exhibits a non-monotonic behavior with a singularity at about 43.7°C. To explain this, note that the total mass flux decreases with T_E. As T_E approaches 43.7°C, the denominator of Eqn. (2-4) approaches zero, and therefore R_{et} becomes singular. In addition, because the denominator of Eqn. (2-4) changes sign as T_E passes 43.7°C, R_{et} experiences a jump from negative infinity to positive infinity. Physically, this singularity is not meaningful because it corresponds to the case where mass transfer is absent, and hence R_{et} is undefined. Away from this temperature, R_{et} varies slightly with T_E. The bare skin evaporative resistance R_{et0} is shown in Fig. 4-16 and the fabric evaporative resistance R_{ef} for a system with 6 mm MC is

plotted in Fig. 4-17. They both behave similarly to R_{et} discussed in Fig. 4-15.
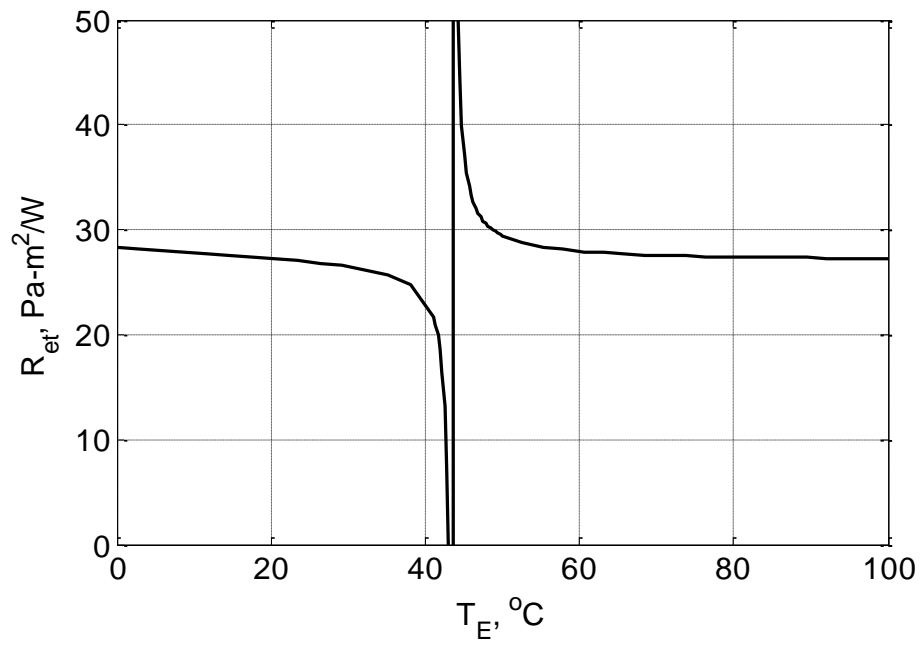
Figure 4-15 Effect of ambient temperature on the total evaporative resistance of a system with 6 mm MC.
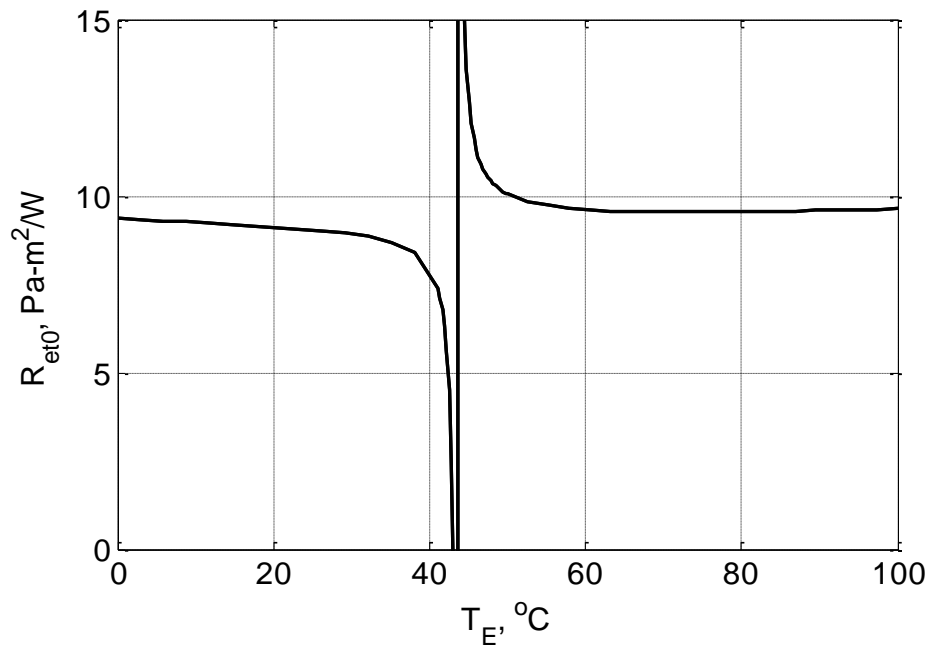
Figure 4-16 Effect of ambient temperature on the bare skin evaporative resistance.
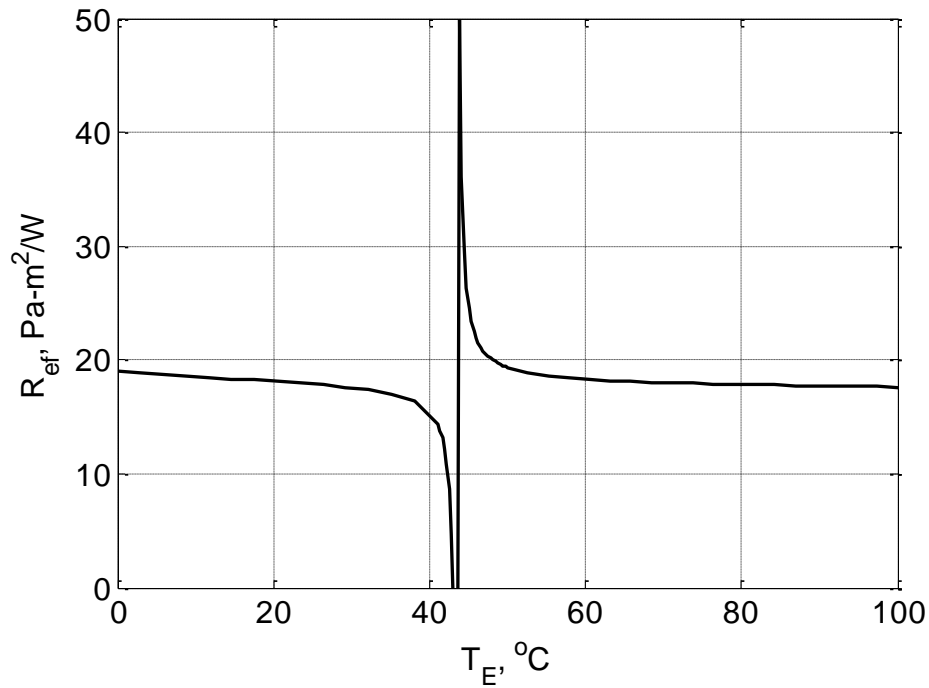
Figure 4-17 Effect of ambient temperature on the fabric evaporative resistance for a system with 6 mm MC.

Air speed

The wind effect on different fabric systems is given by Fig. 4-18. A generally decreasing trend in R_{et} is found with increasing wind speed for all fabric systems, with a relatively large decrease occurring within 5 m/s. A transition from laminar to turbulent flow exists as well for wet condition, beyond which R_{et} decreases at a faster rate. At a fixed wind speed, R_{et} can be greatly increased by increasing MC thickness. Wind effect on bare skin evaporative resistance R_{et0} shown in Fig. 4-19 is very similar to Fig. 4-18. The fabric evaporative resistance R_{ef} therefore remains almost constant for the entire range of wind speed, as can be seen from Fig. 4-20.
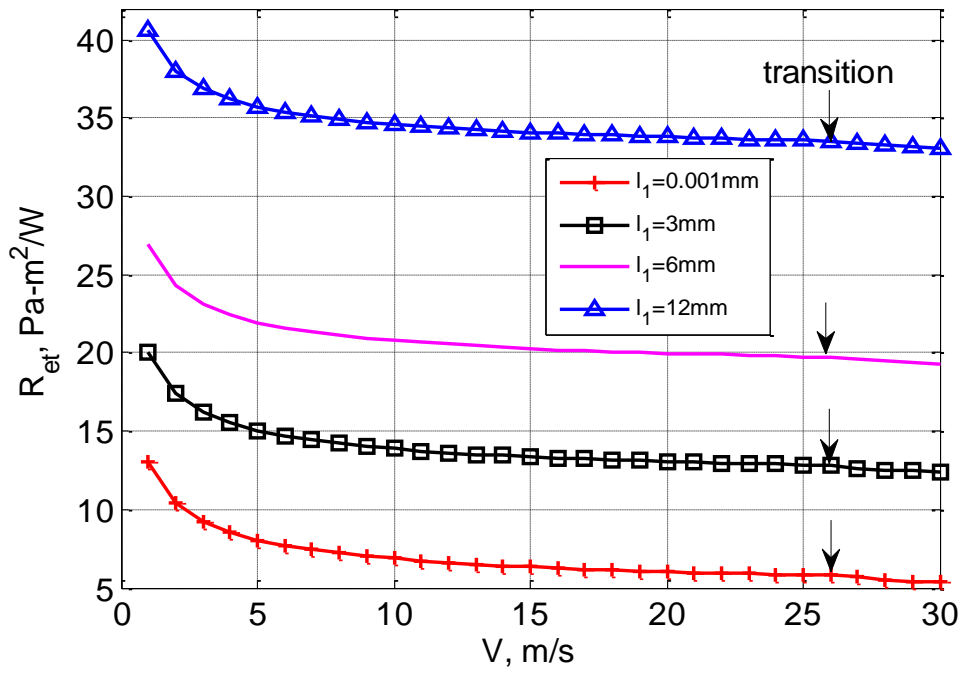
Figure 4-18 Wind effect on the total evaporative resistance.
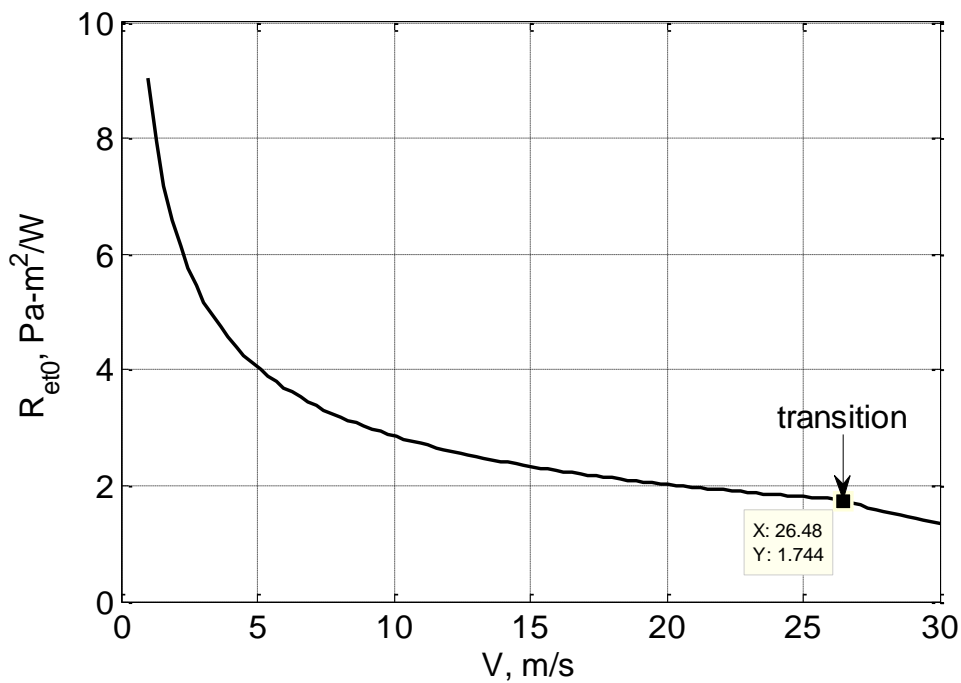
Figure 4-19 Wind effect on the bare skin evaporative resistance.
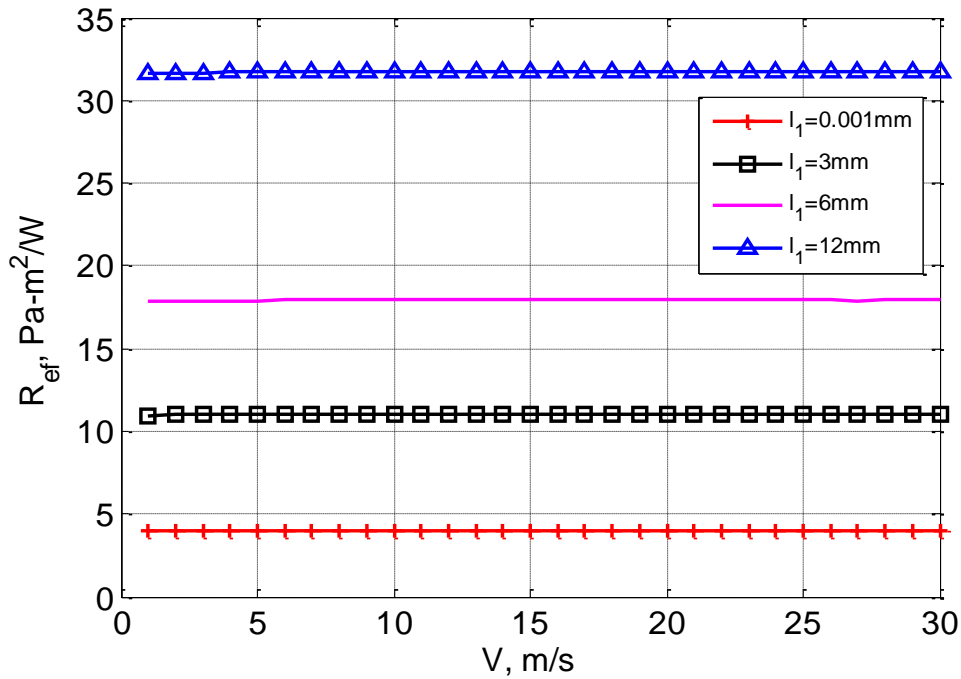
Figure 4-20 Wind effect on the fabric evaporative resistance.

Relative humidity

The effect of RH on the total evaporative resistance in Fig. 4-21 shows overall increasing R_{et} with RH. However, the variation is relatively small, with an increase of less than 4.54% from $\phi_E = 0$ to $\phi_E = 100\%$ in all cases. To account for the small increase, Eqn. (2-3) is investigated, where the numerator and the denominator both decrease with increasing ϕ_E. The predicted R_{et} shown here is the result of the competition between the two. Similar behavior is observed for the dependences of the bare skin evaporative resistance R_{et0} and fabric evaporative resistances R_{ef} on ϕ_E, shown in Figs. 4-22 and 4-23, respectively .
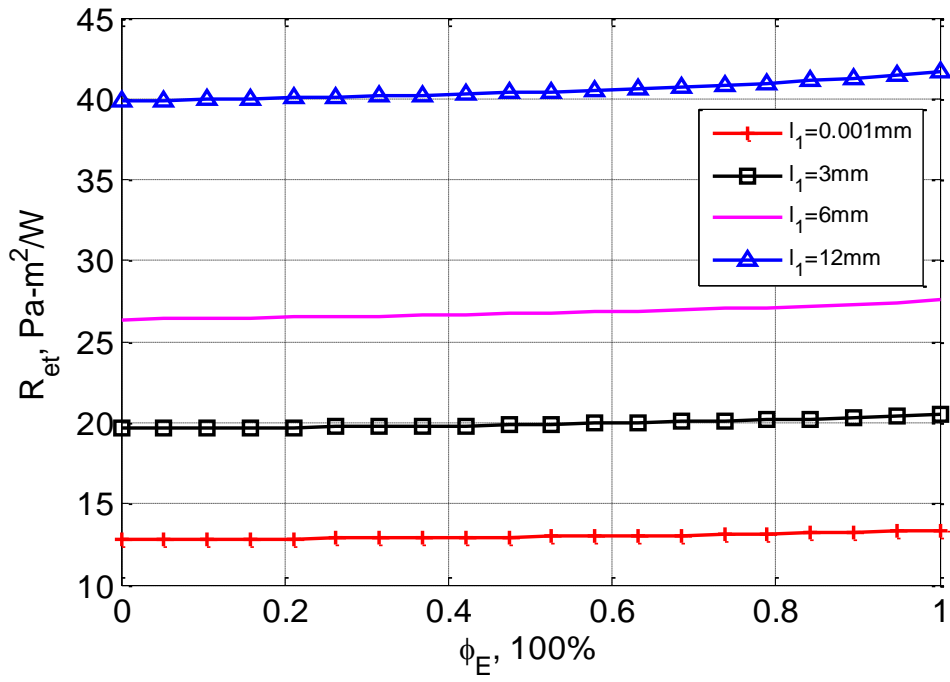
Figure 4-21 Effect of RH in the environment on the total evaporative resistance.
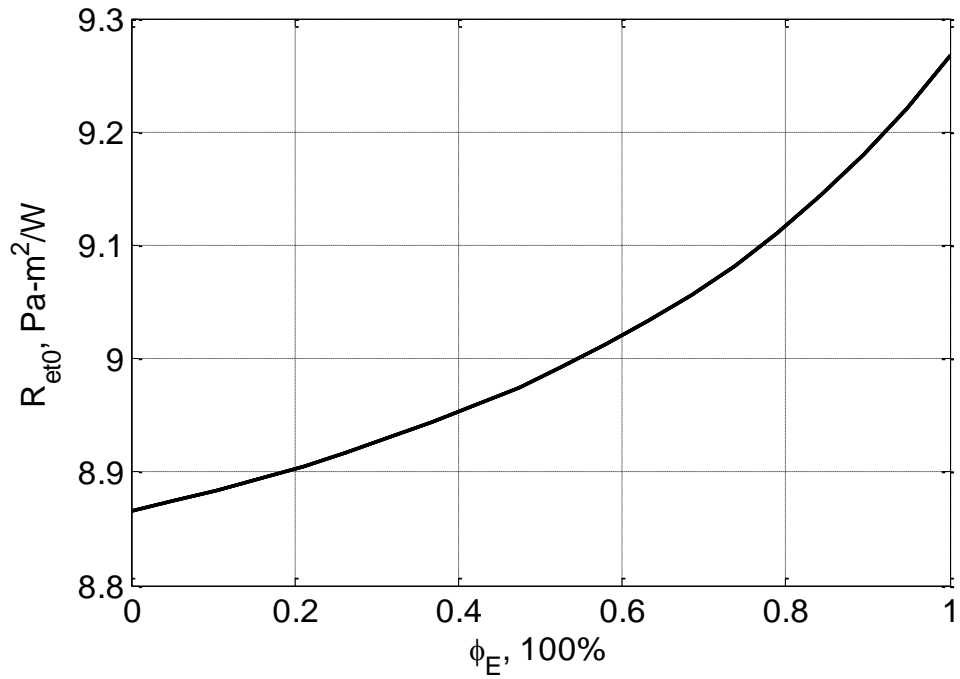
Figure 4-22 Effect of RH in the environment on the bare skin evaporative resistance.
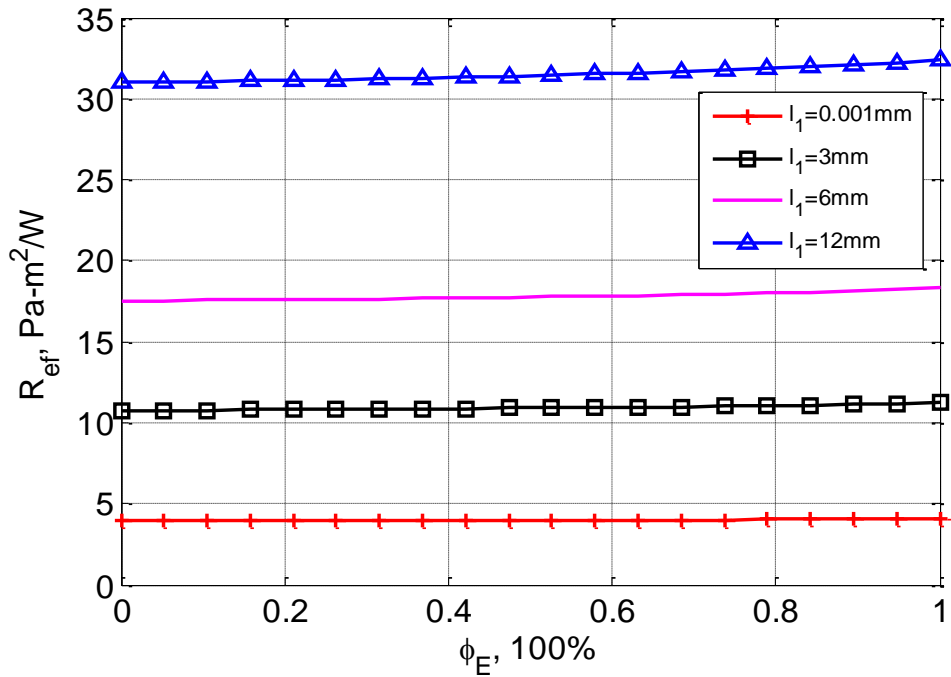
Figure 4-23 Effect of RH in the environment on the fabric evaporative resistance.

4.2.2 Effect of the fabric properties

Similar to the parameter study under dry condition, only the dependence of R_{et} on fabric properties will be presented, since R_{ef} differs from it by a constant R_{et0}.

MC thickness

The effect of MC thickness on R_{et} is illustrated in Fig. 4-24. Each curve in this figure shows an initially linear increase of R_{et} with MC thickness. This increase may continue if the ambient temperature is higher than the skin temperature and natural convection in the MC is prevented. For lower ambient temperatures, local maximum R_{et} values appear at certain critical MC thicknesses. These critical points correspond to onset of natural convection in the MC layer. Similar to the dry condition, the location of the critical MC thickness varies with ambient temperature, being 10.8 mm for 10°C and 14.7 mm for 25°C here. Beyond the

critical thickness, R_{et} experiences a sudden drop due to the onset of natural convection in the MC, and then builds up again, but at a much slower rate.
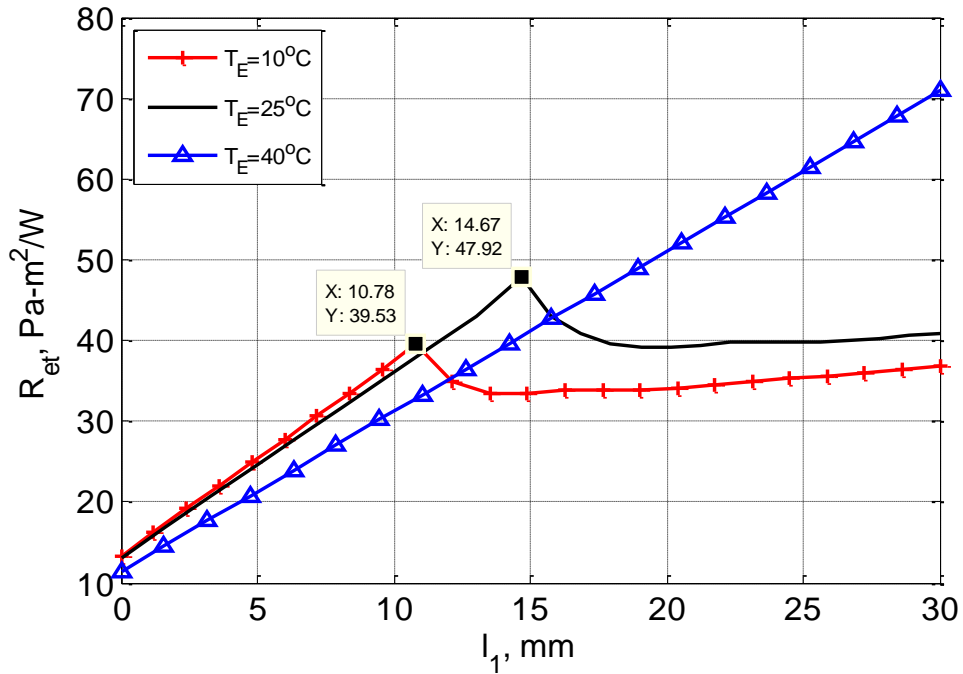
Figure 4-24 Effect of MC thickness on the total evaporative resistance.

Fabric thickness

As shown in Fig. 4-25, the fabric thickness has a strong and almost linear effect on the evaporative resistance, which is similar to its effect on the thermal resistance. Increasing MC thickness increases the absolute value of the evaporative resistance, while the relative influence of this increase is weakened with large MC thickness. For example, by increasing the fabric thickness from 0.001 mm to 6 mm, the total evaporative resistance for a fabric without air gap (l_1 = 0.001 mm) can be increased by 267%, while for fabric systems with MC thickness of 6 mm and 12 mm, the corresponding increase is 108% and 67.4% respectively.
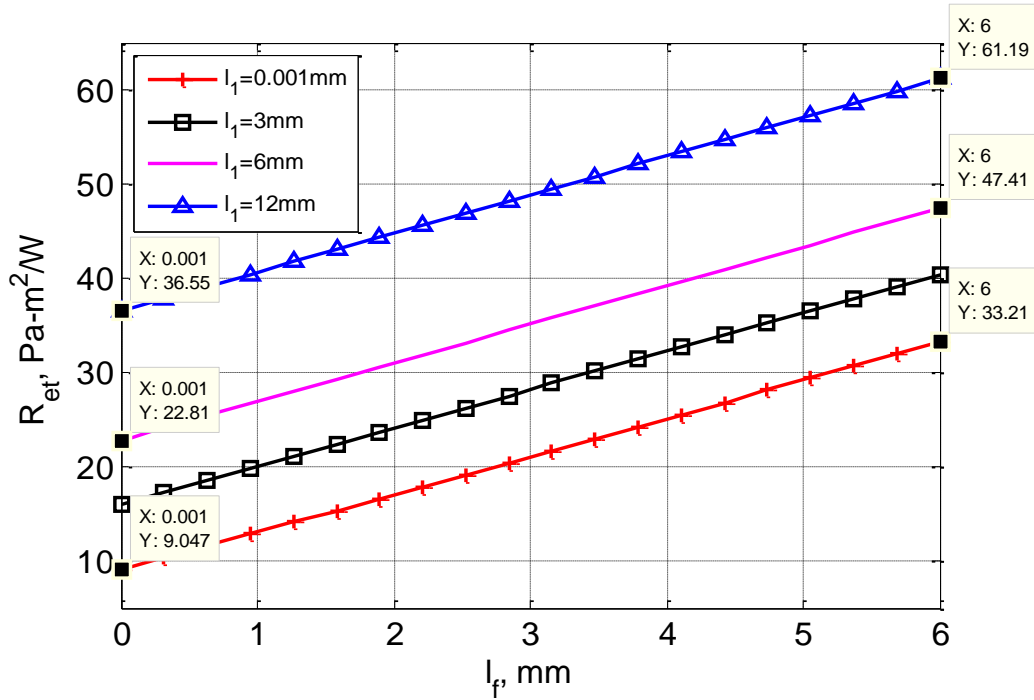
Figure 4-25 Effect of fabric thickness on the total evaporative resistance.

Porosity

A non-linear decrease of evaporative resistance with porosity is observed and shown in Fig. 4-26. The smallest evaporative resistance is reached when the porosity approaches unity, corresponding to pure air. The percentage of decrease over the entire range of porosity is significant. For example, for a fabric system without air gap ($l_1 = 0.001$ mm), the percentage of decrease is 44.4% by increasing the fabric porosity from 0.3 to 0.95. Again, the relative influence of decrease is weakened with large MC thickness over the same range. For example, by introducing a MC of 6 mm and 12 mm, the corresponding decrease is 27.5%, and 19.9%, respectively.
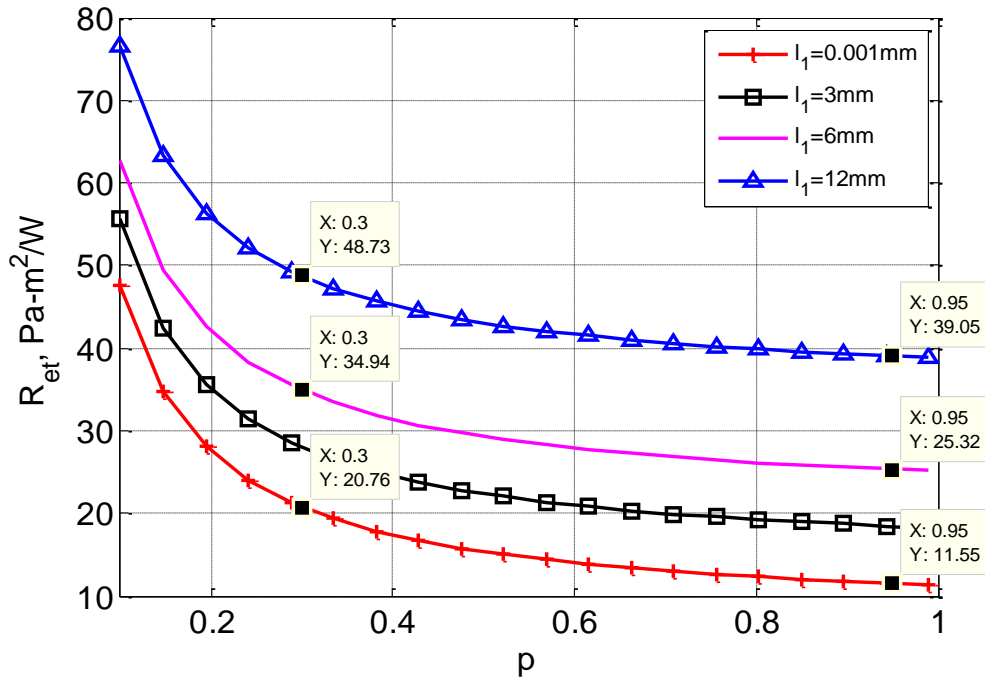
Figure 4-26 Effect of fabric porosity on the total evaporative resistance.

Surface Diffusivity

The effective diffusivity D_{eff} of the fabric layer determines the rate of mass transfer through the fabric, thus affecting the evaporative resistance. Since D_{eff} is the summation of the molecular diffusivity of water vapor $D_{vap} p / \tau$ and the surface diffusivity KD_{sur} along the fibers, the effect of D_{eff} on R_{et} relies on the relative magnitude of these two components. In Fig. 4-27, the surface diffusivity KD_{sur} ranging from 1×10^{-6} m^2/s to 1×10^{-4} m^2/s suggested by Min *et al.* [39] is used to calculate the corresponding R_{et}. Increasing KD_{sur} reduces R_{et} for all cases. In particular, for a fabric system without air gap ($l_1 = 0.001$ mm), increasing KD_{sur} by two orders of magnitude results in about 25.1% of reduction in R_{et}. But the effect of KD_{sur} becomes smaller with increasing MC thickness. For example, by introducing a MC of 6 mm and 12 mm, the corresponding decrease is 12.5%, and 8.27%, respectively.
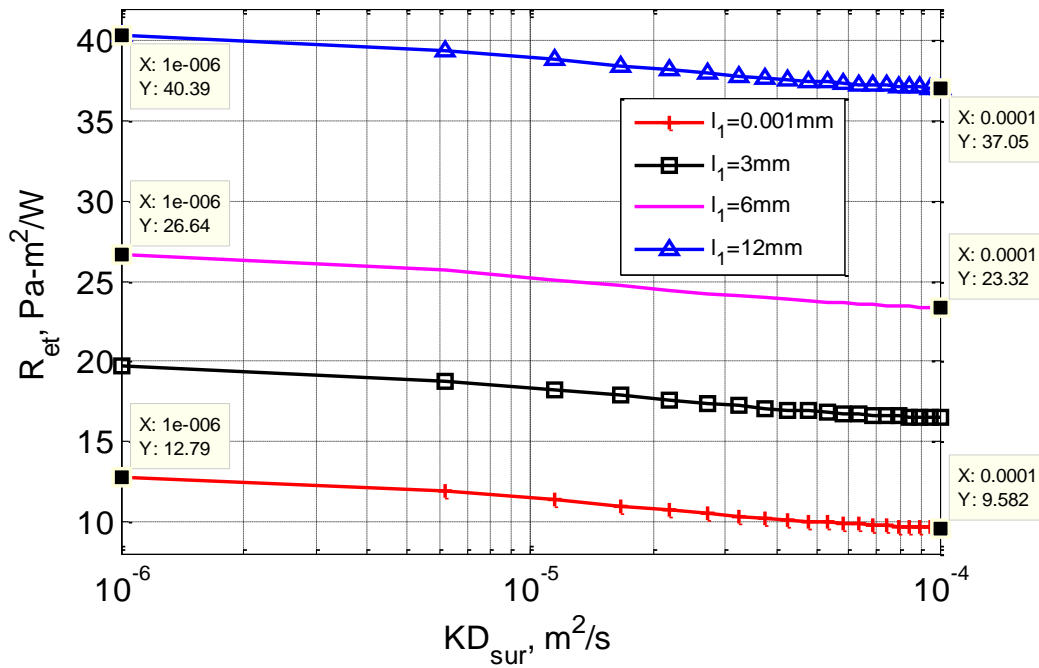
Figure 4-27 Effect of surface diffusivity on total evaporative resistance.

Finally, parameter study has also been carried out for fiber conductivity and fabric emissivity, which shows negligible effect on the evaporative resistance.

4.3 Summary

In this chapter, an elaborate parametric study is carried out on the thermal resistance and evaporative resistance. Environmental conditions and fabric properties that affect these two thermal comfort properties are studied. Their impact on the thermal and evaporative resistances is important in improving the performance of protective clothing.

Table 4-2 Sensitivity of thermal resistance to environmental conditions and fabric properties[*]

	Ambient temperature [°C]	Wind speed [m/s]	Thickness of MC [mm]	Thickness of fabric [mm]	Thermal conductivity [m²K/W]	Porosity	emissivity of fabric
Range	-50~100	1~30	0.001~10	0.001~10	0.01~1	0.3~0.95	0.1~0.99
Variation in R_{ct}	-23.9%	-69.6%	146%	123%	-32.8%	23.0%	-39.1%

* Data listed in this table are for model study only, which might have limitations with actual applications

Table 4-2 summarizes the sensitivity of the thermal resistance to the variations in environmental conditions and fabric properties. It is found that:

▪ Increasing the ambient temperature or wind speed results in a decrease in the total thermal resistance.

▪ The most influential properties of the fabric system are the thickness of MC and that of the fabric. In addition, in order to provide better thermal insulation, increasing the thickness of MC is more effective than increasing the fabric thickness, not to mention the reduced body-movement comfort associated with thickening of the fabric. However, natural convection might occur in large MC under low temperature.

▪ Three other fabric properties, thermal conductivity, porosity and emissivity can also affect the thermal resistance of the fabric to a certain degree. Specifically, the thermal conductivity is related to the type of textile fibers, fabric constructed by fibers with smaller thermal conductivity generally provides better thermal insulation than that made of fibers with higher thermal conductivity. However this effect from fiber conductivity is minimized given the fact that fabrics normally consist of more air (trapped air) volume than that of fibers. Porosity is mainly related to the fabric structure. Higher fabric porosity gives rise to higher thermal resistance, thus suggesting a non-woven structure should provide a higher thermal insulation than other woven or knitted. Emissivity is not only dependent on the fiber type of the fabric but also the surface condition. Low emissivity is found to promote thermal

insulation; it can be achieved by certain finishing or coating to modify the surface properties of the fabric, without changing the bulk fabric properties.

Table 4-3 Sensitivity of evaporative resistance to environmental conditions and fabric properties[*]

	Ambient temperature [^{o}C]	Wind speed [m/s]	RH [100%]	Thickness of MC [mm]	Thickness of fabric [mm]	Porosity	Surface diffusivity [m^2/s]
Range	0~100	1~30	0-100	0.001~10	0.001~10	0.3~0.95	10^{-6}~10^{-4}
Variation in R_{et}	-	-59.0%	4.54%	176%	467%	-44.4%	-25.1%

* Data listed in this table are for model study only, which might have limitations with actual applications

Table 4-3 summarizes the sensitivity of the evaporative resistance to the variations in environmental conditions and fabric properties. It is found that:

▪ Increasing wind speed results in decrease in the total evaporative resistance, but has negligible effect on the fabric evaporative resistance. The environmental temperature and relative humidity do not demonstrate significant influences on the evaporative resistance.

▪ The most influential property of the fabric system is the thickness of fabric, the second to it is the thickness of MC. Therefore, it is not only economic to control the thickness of a fabric but also helpful in providing a small evaporative resistance. Increasing MC thickness promotes thermal insulation, but at the same time increases the evaporative resistance. For thermal protective clothing, usually a high thermal resistance and a low evaporative resistance are both required to achieve optimum thermal comfort, thus proper thickness of MC is critical to achieve high performance.

▪ High fabric porosity is found to contribute to reducing evaporative resistance. Since high porosity is also found to increase thermal resistance, adjusting fabric structure to achieve high porosity benefits the design of thermal protective clothing.

- The surface diffusivity, which is related to the hygroscopicity of fabrics, is found to contribute to the evaporative resistance to a certain degree.

- Thermal conductivity and emissivity do not contribute to the evaporative resistance. It indicates that surface treatment for reducing emissivity and enhancing thermal insulation does not affect wet comfort.

CHAPTER 5: CONCLUSION AND FUTURE WORK

A heat and mass transfer model is developed to characterize the performance of a single-layer fabric system. By considering temperature dependent properties of air and water vapor, a system of nonlinear equations are formulated to determine the temperature, moisture concentration, heat and mass fluxes throughout the system. Given the environmental condition and material parameters, the model is capable of predicting the thermal resistance R_{ct} and evaporative resistance R_{et} of the fabric system, two important quantities related to thermal comfort. Experiments are conducted using a standard SGHP, and the measured fabric thermal and evaporative resistances demonstrate good agreement with model predictions.

With the validated model, the factors that influence R_{ct} and R_{et} are investigated by a parametric study. The results show the following:

1) The thickness of the MC l_1 shows great effect on both thermal and evaporative resistances. Increasing l_1 can result in rapid increase in R_{ct} and R_{et}. Such effect, however, is limited by the possible natural convection that occurs in the MC. Specifically, if the environmental temperature is lower than the skin temperature, when l_1 exceeds a critical value, natural convection occurs, which leads to reduction in R_{ct} and R_{et}. These two quantities gradually build up again with further increase in air gap thickness, but at a much slower rate. In addition, this critical thickness varies with environmental conditions such as the ambient temperature and wind speed.

2) Thickness of the fabric layer l_F also contributes significantly to both thermal and evaporative resistances. In particular, increasing l_F causes increase in R_{ct} and R_{et} and the increase is nearly linear. With increasing MC thickness, the effect of l_F becomes smaller, indicating that MC becomes the dominating factor in R_{ct} and R_{et}.

3) Porosity of the fabric layer has a distinct effect on R_{ct} and R_{et}. Larger porosity results in increase in R_{ct} while rapid decrease in R_{et}.

4) Fiber conductivity k_f and fabric surface emissivity ε_F all show certain effect on R_{ct}, but little effect on R_{et}. Specifically, R_{ct} increases nonlinearly with decreasing k_f and ε_F. Like l_F, with increasing MC thickness, the effect of k_f becomes smaller. The effect of ε_F, however, becomes more significant as the MC thickness increases.

5) Surface diffusivity can affect R_{et}. Increasing surface diffusivity by two orders of magnitude causes about 25.1% reduction in R_{et}. Experimental quantification of surface diffusivity is not yet available.

6) In terms of environmental conditions, ambient temperature contributes significantly to R_{ct} but not R_{et}. In the regime of laminar flow, wind speed can cause rapid decrease in both R_{ct} and R_{et} within 5 m/s. Transition to turbulent flow at high speed further accelerates the reduction in R_{ct} and R_{et}.

Depending on the environmental conditions and the functions of the clothing system, proper fit and material properties should be selected. For example, for cold protective clothing, maintaining sufficiently high thermal resistance is the primary goal. Thicker MC and fabric, lower fiber conductivity, higher porosity and lower emissivity are therefore desired. However, the MC thickness should not be large enough to trigger natural convection. For heat protective clothing, it is essential for the human body to be protected from the thermal hazards while at the same time maintain the ability to dissipate sweat. In this case, the garment fit and material parameters of the fabric need to be optimized to achieve both high thermal resistance and acceptable evaporative resistance. Fabric porosity is an excellent property to achieve both requirements.

The heat and mass transfer model presented here can be extended to the study of a multi-layer fabric system. Factors not considered in the current model, e.g., air

penetration through the fabrics, skin and surface roughness, can also be included. Finally, based on this model, heat and cold stresses associated with different body activities can be evaluated. For example, the limited duration for working under certain environmental conditions can be predicted.

BIBLIOGRAPHY

1.   Rossi, R., *Interactions between protection and thermal comfort*. Textiles for protection, ed. R. Scott. Vol. 44. 2005, Cambridge, UK: Woodhead Publishing Limited. p. 233-260.

2.   Keith, S., *Comfort or protection: The clothing dilemma*. Performance of protective clothing, ed. J.S. Johnson and S.Z. Mansdorf. 1996, Philadelphia, PA,: ASTM Intl. p. 486-497.

3.   Havenith, G., *Heat Balance When Wearing Protective Clothing*. Ann. occup. Hyg., 1999. Vol. 43(5): p. 289-292.

4.   Guyton, C., *Basic Human Physiology: Normal Function and Mechanisms of Disease*. 1971: Saunders, Philadelphia. Ch. 47.

5.   Crockford, G. W., *Protective Clothing and Heat Stress: Introduction*. Annuals of Occupational Hygiene, 1999. Vol. 43(5): p. 287-288.

6.   Tochihara, Y. and Ohnaka, T., *Environmental Ergonomics - The Ergonomics of Human Comfort, Health, and Performance in the Thermal Environment* (Elsevier Ergonomics Book Series). Vol. 3. 2005, Fukuoka: Elsevier Science.

7.   Slater, K., *Human Comfort*. 1985: Thomas Plublisher, Springfield Illinois.

8.   Hatch, K. L., *Textile Science*. 1993, Minneapolis, MN: West Publishing Company. p. 26.

9.   Fan, J. and Chen, Y. S., *Measurement of clothing thermal insulation and moisture vapour resistance using a novel perspiring fabric thermal manikin*. Measurement Science and Technology, 2002. Vol. 13: p. 1115-1123.

10.   Jun, Y., Park, C. H., Shim, H. and Kang, T. J., *Thermal Comfort Properties of Wearing Caps from Various Textiles*. Textile Research Journal, 2009. Vol. 79(2): p. 179-189.

11.   ASTM, *ASTM F1868-02 Standard Test Method for Thermal and Evaporative Resistance of Clothing Materials Using a Sweating Hot Plate*. 2002.

12.   Gibson, P., Auerbach, M., Giblo, J., Teal, W. and Endrusick, T., *Interlaboratory Evaluation of a New Sweating Guarded Hot Plate Test Method (ISO 11092)*. J. Thermal Insul. and Bldg. Envs., 1994. Vol. 18: p. 182-200.

13.   McCullough. E. A., Huang, J. and Kim C., *An Explanation and Comparison of Sweating Hot Plate Standards*. Journal of ASTM International, 2004. Vol. 1(7): p. 13.

14.   Verdu, P., Rego, J. M., Nieto, J. and Blanes, M., *Comfort Analysis of Woven Cotten/Polyester Fabrics Modified with a New Elastic Fiber, Part 1 Preliminary Analysis of Comfort and Mechanical Properties.* Textile Research Journal, 2009. Vol. 79(14): p. 14-23.

15.   Bridger, R., *Introduction to Ergonomics*. 2nd ed. 2003: Taylor & Francis Group. p. 233.

16.   Holmér, I., Nilsson, H. O. and Anttonen, H., *Prediction of Wind Effects on Cold Protective Clothing*. in *RTO Human Factors and Medicine Panel (HFM) Symposium*. 2002.

17.   Havenith, G. and Nilsson, H. O., *Correction of clothing insulation for movement and wind effects, a meta-analysis*. European Journal of Applied Physiology, 2004. Vol. 92: p. 636-640.

18.   Holmér, I., Nilsson., H. O, Havenith, G., and Parsons, K., *Clothing convective heat exchange—proposal for improved prediction in standards and models* The Annals of Occupational Hygiene, 1999. Vol. 43(5): p. 329-337.

19.   Holmér, I., *Protective Clothing in Hot Environment.* Industrial Health, 2006. Vol. 44: p. 404-413.

20.   Raheel, M., *Protective Clothing System and Materials*. Occupational safety and health, ed. M. Raheel. 1994, New York: Marcel Dekker, Inc. p.1.

21.   Havenith, G., *The Interaction of Clothing and Thermoregulation.* Exogenous Dermatology, 2002. Vol. 1(5): p. 221-230.

22.   Havenith, G., Heus, R. and Lotens, W. A., *Resultant clothing insulation: a function of body movement, posture, wind, clothing fit and ensemble thickness.* Ergonomics, 1990. Vol. 33(1): p. 67-84.

23.   Fan, J., Cheng, X., and Chen, Y. S., *An experimental investigation of moisture absorption and condensation in fibrous insulations under low temperature.* Experimental Thermal and Fluid Science, 2003. Vol. 27(6): p. 723-729.

24.   Chen, Y. S., Fan, J., Qian, X. and Zhang, W., *Effect of Garment Fit on Thermal Insulation and Evaporative Resistance.* Textile Research Journal, 2004. Vol. 74(8): p. 742-748.

25.   Yoo, S. and Barker, R. L., *Comfort Properties of Heat-Resistant Protective Workwear in Varying Conditions of Physical Activity and Environment. Part I: Thermophysical and Sensorial Properties of Fabrics.* Textile Research Journal, 2005. Vol. 75(7): p. 523-530.

26.   Yoo, S. and Barker, R. L., *Comfort Properties of Heat-Resistant Protective Workwear in Varying Conditions of Physical Activity and Environment. Part II: Perceived Comfort Response to Garments and its*

Relationship to Fabric Properties. Textile Research Journal, 2005. Vol. 75(7): p. 531-541

27.   Fan, J. and Tsang, H. W. K., *Effect of Clothing Thermal Properties on the Thermal Comfort Sensation During Active Sports.* Textile Research Journal, 2008. Vol. 78(2): p. 111-118.

28.   Farnworth, B., *Mechanisms of Heat Flow Through Clothing Insulation.* Textile Research Journal, 1983. Vol. 53(12): p. 717-725.

29.   Stuart, I. M. and Holcombe, B. V., *Heat Transfer Through Fiber Beds by Radiation with Shading and Conduction.* Textile Research Journal, 1984. Vol. 54(3): p. 149-157.

30.   Henry, P. S. H., *Diffusion in Absorbing Media.* Proceedings of the Royal Society of London, 1939. Vol. 171: p. 215-241.

31.   Henry, P. S. H., *The Diffusion of Moisture and Heat through Textiles.* Discussions of the Faraday Society, 1948. Vol. 3: p. 243-257.

32.   Nordon, P. and David, H. G., *Coupled Diffusion of Moisture and Heat in Hygroscopic Textile Materials.* Int. J. Heat Mass Transfer, 1967. Vol. 10: p. 863-866.

33.   David, H. G., and Nordon, P. *Case Studies of Coupled Heat and Moisture Diffusion in Wool Beds.* Textile Research Journal, 1969. Vol. 39: p. 166-172.

34.   Li, Y. and Holcombe, B. V., *Mathematical Simulation of Heat and Moisture Transfer in a Human-Clothing-Environment System.* Textile Research Journal, 1998. Vol. 68(6): p. 389 - 397.

35.   Fan, J., Luo, Z. and Li, Y., *Heat and moisture transfer with sorption and condensation in porous clothing assemblies and numerical simulation.* International Journal of Heat and Mass Transfer, 2000. Vol. 43: p. 2989-3000.

36.   Li, Y. and Holcombe, B. V., *A Two-stage Sorption Model of the Coupled Diffusion of Moisture and Heat in Wool Fabrics.* Textile Research Journal, 1992. Vol. 62: p. 211-217.

37.   Li, Y. and Luo, Z., *Physical Mechanisms of Moisture Diffusion into Hygroscopic Fabrics during Humidity Transients.* Journal of the Textile Institute, 2000. Vol. 91(2): p. 302-316.

38.   Li, Y. and Luo, Z., *An improved Mathematical Simulation of the Coupled Diffusion of Moisture and Heat in Wool Fabric.* Textile Research Journal, 1999. Vol. 69(10): p. 760-768.

39.   Min, K., Son, Y., Kim, C., Lee, Y. and Hong K., *Heat and moisture transfer from skin to environment through fabrics: A mathematical model.* International Journal of Heat and Mass Transfer, 2007. Vol. 50: p. 5292-5304.

40.   Jiji, L. M., *Heat Convection*. 2006, Berlin, Heidelberg, New York: Springer. p. 322.

41.   Cengel, Y. A., *Heat and Mass Transfer, A Practical Approach*. 3 ed. 2007: Suzanne Jeans. p. 860, 782, 181, 815, 402, 865, 854, 510.

42.   Tetens, V. O., *Uber einige meteorologische Begriffe.* Zeitschrift für Geophysik, 1930. Vol. 6: p. 297-309.

43.   Hollands, K. G. T., Raithby, G. D. and Konicek, L., *Correlation equations for free convection heat transfer in horizontal layers of air and water.* International Journal of Heat and Mass Transfer, 1975. Vol. 18(7-8): p. 879-884.

44.   Yu, B. and Li., J., *A Geometry Model for Tortuosity of Flow Path in Porous Media.* Chinese Physics Letters, 2004. Vol. 21: p. 1569-1571.

45.   Sherwood, T. K., Pigford, R. L. and Wilke, C.R., *Mass Transfer.* 1975, New York: McGraw Hill. p. 39-43.

46.   Hearle, J. W. S. and Morton, W. E., *Physical Properties of Textile Fibres*. 2008, Manchester: Woodhead Publishing Ltd. p. 175, 165.

47.   *Technical Guide for NOMEX® Brand Fiber*. DuPont, 2001.

48.   Zhang, H., Hu, T. L. and Zhang, J. C., *Surface emissivity of fabric in the 8-14 m waveband.* The Journal of The Textile Institute, 2009. Vol. 100(1): p. 93.

49.   Cain, B. and Farnworth, B., *Two New Techniques for Determining the Thermal Radiative Properties of Thin Fabrics.* Journal of Building Physics, 1986. Vol. 9: p. 309.

50.   ASTM, *ASTM D3776 Standard Test Methods for Mass Per Unit Area (Weight) of Fabric*. 1996.

51.   *Operator's Manual for Material Evaluation Hotplate Model SGHP-8.2*, Measurement Technology Northwest, 2004: Seattle, Washington.

52.   Huang, J., *Sweating guarded hotplate test method.* Polymer Testing, 2006. Vol. 25: p. 709-716.

53.   Schltinder, E.U., *Heat Exchanger Design Handbook*, ed. B.M. Brienza, J.B. Gandy, and L. Lackenbach. 1983, Washington, New York, London: Hemisphere Publishing Corporation. 2.5.9-4.

54.   Holcombe, B. V. and Hoschke, B. N., *Dry Heat Transfer Characteristics of Underwear Fabrics.* Textile Research Journal, 1983. Vol. 53(6): p. 368-374.

55.   Bandyopadhyay, S. K., Ghose, P. K., Bose, S. K. and Mukhopadhyay, U., *The Thermal Resistance of Jute and Jute-blend Fabrics.* Journal of the Textile Institute, 1987. Vol. 78(4): p. 255-260.

56.   Burmeister, L.C., *Convective Heat Transfer*. 1982, New York, Chichester, Brisbane, Toronto, Singapore: John Wiley & Sons, Inc. p. 186.

APPENDICES

Appendix A   Convection in MC and in the environment

In the MC:

Natural convection might occur in the MC, and the Rayleigh number Ra_L in the MC (rectangular enclosure between two parallel plates) is used to determine whether natural convection takes place, which is given by

$$\text{Ra}_L = \text{Gr}_L \text{Pr} = \frac{g\beta(T_S - T_1)L_c^3}{\nu^2}\text{Pr}. \tag{A1}$$

$g = 9.81 \text{ m/s}^2$ is the gravitational acceleration, $\beta = 1/T_{m,MC} = 2/(T_S + T_1)$ is the volume expansion coefficient, L_c is the characteristic length of the enclosure which equals to the thickness of MC l_1, Pr is the Prandtl number of air, and ν is the kinematic viscosity of air. The Critical Rayleigh number for the onset of natural convection in a rectangular enclosure is $\text{Ra}_{L,cr} = 1708$. If $\text{Ra}_L < \text{Ra}_{L,cr}$, then natural convection can be neglected in the MC, otherwise natural convection has to be considered [56]. In all calculations present in this work, Ra_L is checked and compared with $\text{Ra}_{L,cr}$, and if it exceeds $\text{Ra}_{L,cr}$, natural heat convection is included.

In the environment:

In the environment, forced convection exists due to the air flow. Whether natural convection is negligible compared with the forced convection is determined by the following two criterions specified by different resources:

Criterion 1:

The ratio of Grashof number Gr_L to the square of Reynolds number Re_L in the ambient is given by [41]

$$\frac{\text{Gr}_L}{\text{Re}_L^2} = \frac{g\beta(T_S - T_\infty)\left(\dfrac{L_c}{4}\right)^3}{v^2}\Bigg/\left(\dfrac{VL_c}{v}\right)^2 , \tag{A2}$$

where $\beta = 1/T_{avg} = 2/(T_S + T_E)$ is the volume expansion coefficient, L_c is the characteristic length for a horizontal flat plate, and V is the flow speed. For a square plate, $L_c = A_s/p = L/4$, where A_s is the surface area and p is the perimeter. $\left(\text{Gr}_L/\text{Re}_L^2\right) \le 0.1$ is used as a criterion for neglecting natural convection.

Criterion 2:

Assuming natural convection and forced convection co-exist over a horizontal flat plate, the combined Nusselt number Nu can be written as [53]

$$\text{Nu}^{3.5} = \text{Nu}_F^{3.5} + \text{Nu}_N^{3.5} , \tag{A3}$$

where Nu_F and Nu_N are the Nusselt numbers for force convection and natural convection, respectively. Dividing (A3) by $\text{Nu}_F^{3.5}$, one obtains

$$\left(\frac{\text{Nu}}{\text{Nu}_F}\right)^{3.5} = 1 + \left(\frac{\text{Nu}_N}{\text{Nu}_F}\right)^{3.5} . \tag{A4}$$

If $\left(\text{Nu}_N/\text{Nu}_F\right)^{3.5} \ll 1$, then Eqn. (A4) can be written as $\left(\text{Nu}/\text{Nu}_F\right)^{3.5} \simeq 1$, i.e., forced convection dominates. $\left(\text{Nu}_N/\text{Nu}_F\right)^{3.5} \le 0.1$ is chosen as a 2nd criterion for neglecting natural convection.

For the standard testing environmental conditions ($Ts = 35^\circ\text{C}$, $T_E = 25^\circ\text{C}$, $L = 0.3048\text{m}$), by varying the flow speed V from 0.01m/s to 1m/s in the environment, it is found that:

From criterion 1: forced convection dominates when $V \ge 0.124$ m/s.

From criterion 2: forced convection dominates when $V \geq 0.102$ m/s.

Therefore, it is concluded that natural convection can be neglected for the standard testing conditions with wind speed higher than 1m/s.

In addition, for the flow speed $V = 1$ m/s over a flat plate of length $L = 0.3048$ m, by varying the environmental temperature T_E from 35°C to -50°C, the calculated values from the two criterions keep increasing, but all are smaller than 0.1. Therefore, it is further concluded that natural convection is negligible for the entire range of ambient temperature, which is -50°C to 100°C.

Based on above calculations, the assumption of negligible natural convection in the environmental flow is validated.

Appendix B Fitted polynomials for temperature dependent air parameters

Tabular values [41] for density ρ_{air}, specific heat C_p, thermal conductivity k_{air} and Prandtl number Pr of air are fitted, each by a 4$^{\text{th}}$ order polynomial of the form $f(t) = a_4 t^4 + a_3 t^3 + a_2 t^2 + a_1 t + a_0$, where t is temperature in Celsius ($^{\circ}$C). The coefficients $a_i (i = 0, 1, 2, 3, 4)$ for each parameter are listed in the following table. The fitting of these polynomials to the tabular data is shown in Fig. B-1.

Table B-1 Coefficients of the fitted polynomials for temperature dependent air properties

Air parameter	Unit	a_4	a_3	a_2	a_1	a_0
$\rho_{air}(t)$	kg/m^3	8.64×10^{-11}	-5.43×10^{-8}	1.75×10^{-5}	-4.75×10^{-3}	1.29
$C_p(t)$	J/kg K	-2.82×10^{-8}	1.23×10^{-5}	-1.15×10^{-3}	0.0451	1.01×10^3
$k_{air}(t)$	W/m K	2.98×10^{-15}	5.19×10^{-12}	-2.54×10^{-8}	7.56×10^{-5}	0.0236
Pr(t)		-2.66×10^{-11}	1.14×10^{-8}	-9.75×10^{-7}	-2.43×10^{-4}	0.736
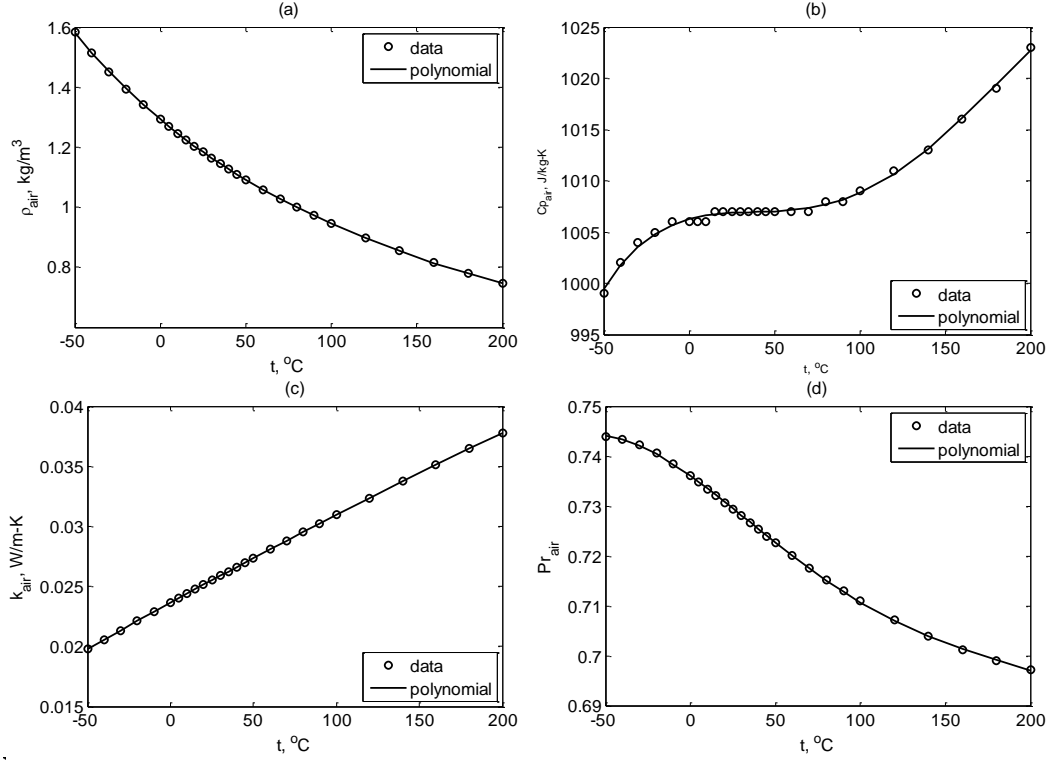
Figure B-1 Fitted polynomials to the tabular data for temperature dependent air properties.

Appendix C   Relation between water vapor concentration ρ and RH ϕ

Water vapor concentration ρ_{vap} (the symbol ρ is used in the main texts) is a function of temperature T and relative humidity ϕ. Their relation can be derived from the ideal gas law:

$$PV = \frac{m}{M} RT ,\qquad\qquad\qquad (C1)$$

where P is pressure, V is volume, m is mass, M is the molar mass of a gas, R is the universal gas constant 8.314472×10^3 J/kmol K and T is temperature. The molar mass of water vapor is $M_{vap} = 18.015$ kg/kmol. Water vapor concentration ρ_{vap} can be expressed by

$$\rho_{vap} = \frac{m_{vap}}{V} = \frac{P_{vap}M_{vap}}{RT} = \frac{P_{vap}}{R_{vap}T}, \tag{C2}$$

where P_{vap} is the partial vapor pressure, R_{vap} is the specific gas constant for water vapor, it is the ratio of R to M_{vap} and equals 461.5305 J/kg K.

The relative humidity ϕ is defined as the ratio of the partial vapor pressure P_{vap} to the saturated vapor pressure P_{sat}, therefore,

$$P_{vap}(T,\phi) = \phi P_{sat}(T), \tag{C3}$$

where P_{sat} is a function of temperature given by [42]

$$P_{sat}(T) = 610.78\exp\left[\frac{17.2694(T-273.15)}{(T-273.15)+238.3}\right], \tag{C4}$$

and T is in Kelvin (K). Substituting Eqns. (C3) and (C4) into (C2), the function for water vapor concentration ρ_{vap} is obtained, given by

$$\rho_{vap}(T,\phi) = \frac{1.3234\phi}{T}\exp\left[\frac{17.2694(T-273.15)}{(T-273.15)+238.3}\right]. \tag{C5}$$

Appendix D   Calculation of fabric porosity and tortuosity

The total mass of the fabric consists of two components: fiber and air. It can be expressed by the following equation:

$$m_{tot} = m_{fiber} + m_{air} = \rho_{fiber}V_{tot}(1-p) + \rho_{air}V_{tot}p, \tag{D1}$$

where $V_{air} = V_{tot}p$ and $V_{fiber} = V_{tot}(1-p)$ are the volumes of the air and fiber, respectively.

The total density of the fabric is

$$\rho_F = \frac{m_F}{V_F} = \rho_{fiber}(1-p) + \rho_{air}\, p \ . \tag{D2}$$

Therefore,

$$p = \frac{\rho_{fiber} - \rho_F}{\rho_{fiber} - \rho_{air}} \ . \tag{D3}$$

Under standard atmospheric condition, the porosity of a specific fabric is a constant and can be obtained given the value of ρ_{fiber}, ρ_F and ρ_{air}. Taking Denim as an example, $\rho_{fiber} = 1520$ kg/m^3 [46], $\rho_{air} = 1.184$ kg/m^3 and ρ_F is obtained by measuring the fabric mass M_F and thickness l_F according to ASTM standards, i.e.,

$$\rho_F = \frac{M_F}{l_F} = \frac{0.456\ kg\,/\,m^2}{0.00134\ m} = 339\ kg\,/\,m^3 \ .$$

So

$$p = \frac{1520 - 339}{1520 - 1.184} = 0.777 \ .$$

According to the empirical equation to calculate fabric tortuosity from the porosity [44], the tortuosity τ of Denim can be obtained by:

$$\tau = 0.8 \times (1 - p) + 1 = 1.18 \ .$$

Appendix E   MATLAB codes

1. Main function

The following code calculates R_{ct}, R_{cf}, R_{et} and R_{ef} given a particular set of parameters: T_E, V, ϕ_E, l_1, l_F, k_f, p, ε_F, KD_{sur}.

Varying one of the parameters generates the dependence of thermal and evaporative resistances on this parameter, as shown in the plots in Chapter 4.

```
% % solve the heat and mass transfer problem in a single layer
fabric system
% % include temperature dependent material parameters
% % wet condition
```

```matlab
% % parameters are defined in Table 4-1

clear;
clc;

%% parameters
% universal constants
sigma = 5.67e-8;        % Stefen-Boltzmann constant [W/(m^2*K^4)]

% geometry
l1 = 6e-3;              % thickness of MC [m]
lf = 1e-3;              % thickness of fabric [m]
l2 = l1 + lf;           % thickness of MC + fabric [m]
L = 30.48e-2;           % characteristic length [m]

% fabric properties
kfiber = 0.25;          % thermal conductivity of fiber [W/(m*K)]
p = 0.7;                % porosity [dimensionless]
tau = 0.8*(1-p)+1;      % tortuosity [dimensionless]
epsF = 0.7;             % emissivity of fabric [dimensionless]
KDsur = 0*1e-5;         % surface diffusivity [m^2/s]

% skin properties/conditions
epsS = 0.95;            % emissivity of skin [dimensionless]
Ts = 35 + 273.15;       % skin temperature [K] 309.5(=36.5C)-
>308(=35C)
delta_H = 2.419e6;      % enthalpy of water vapor at skin
temperature [J/kg]

% ambient conditons
Te = 25 + 273.15;       % ambient temperature [K]
phi = 0.65;             % ambient relative humidity [100%]
v = 1;                   % air speed of the forced convection [m/s]

% numerical parameters
tol = 1e-5;             % tolerance to control convergence
delta = 1e-6;           % increment to calculate Jacobian


%% solve the 4 constants to determine temperature distribution
para0 = [sigma, l1, l2, L, kfiber, p, tau, epsF, epsS, Ts, Te,
v]';

% first assume no natural convection in MC
k = 2;
nc(k) = 0;
nc(k-1) = 1;

while nc(k) ~= nc(k-1)

    % initial guesses of variable z
    T1_0 = 306;         % temperature at x = l1 [K]
    T2_0 = 303;         % temperature at x = l2 [K]
    C1_0 = 0;           % integration constant [W/(m^2)]
```

```matlab
    C3_0 = 10;                 % integration constant [W/(m^2)]


    z = [T1_0, T2_0, C1_0, C3_0]';
    f = funf0(z, para0, nc(k))';
    df = 0 - f;

    % Newton-Raphson method to calculate z that satisfies f(z)=0
    count = 1;
    while norm(df) > tol
        J = zeros(4);
        for iz = 1: length(z)
            z_ptb = z;
            z_ptb(iz) = z(iz) + delta;          % give a small
perturbation to z(i)
            f_ptb = funf0(z_ptb, para0, nc(k))';  % calculate f
after perturbation
            J(:,iz) = (f_ptb - f)/delta;        % this is ith
column of the Jacobian
        end
        if nc(k) == 1
            J=J(2:4,[1,2,4]); df=df(2:4);
        end
        dz = J\df;
        if nc(k) == 1
            dz=[dz(1),dz(2),0,dz(3)]';
        end
        z = z + dz;
        f = funf0(z, para0, nc(k))';
        df = 0 - f;
        count = count + 1;
        if count > 100
            disp('iteration exceeds 100, stopped'); break;
        end
    end


    % solution
    T1 = z(1);          % temperature at x = l1 [K]
    T2 = z(2);          % temperature at x = l2 [K]
    C1 = z(3);          % integration constant [W/(m^2)]
    C3 = z(4);          % integration constant [W/(m^2)]

    % check consistency of assumption
    k = k + 1;
    [RaL_MC, hn_MC] = funhn_MC(Ts, T1, l1);
    if RaL_MC < 1708
        nc(k) = 0;
    else
        nc(k) = 1;
    end
end
%% total thermal resistance Rct
Rct = (Ts - Te)/C3;                      % total thermal resistance
[K-m^2/W] --DD, Sept.1
Rct_MC = (Ts - T1)/C3;
Rct_F = (T1 - T2)/C3;
Rct_E = (T2 - Te)/C3;
```

```matlab
%% bare plate thermal resistance Rcto
Tave = (Ts + Te)/2;                     % film temperature in the
ambient [K]
qconv_bp = funh(Tave, L, v)*(Ts-Te); % convection heat flux in
the environment [W/(m^2)]
qrad_bp = epsS*sigma*(Ts^4 -Te^4);    % radiation heat flux in the
environment [W/(m^2)]
qdry_bp = qconv_bp + qrad_bp;         % total heat flux in the
environment [W/(m^2)]
Rct0 = (Ts - Te)/qdry_bp;             % bare plate thermal
resistance [K-m^2/W]

%% thermal resistance of fabric system Rcf
Rcf = Rct - Rct0;                     % thermal resistance of
fabric system[K-m^2/W]



%% solve the 8 constants to determine temperature distribution
and water vapor concentration
para = [sigma, l1, l2, L, kfiber, p, tau, epsF, epsS, Ts, Te, v,
phi, KDsur]';

% first assume no natural convection in MC
k = 2;
nc(k) = 0;
nc(k-1) = 1;

while nc(k) ~= nc(k-1)

    % initial guesses of variable z
    T1_0 = 306;        % temperature at x = l1 [K]
    T2_0 = 303;        % temperature at x = l2 [K]
    rou1_0 = 0.02;     % water vapor concentration at x = l1
[kg/m^3]
    rou2_0 = 0.02;     % water vapor concentration at x = l2
[kg/m^3]
    C1_0 = 10;         % integration constant [W/(m^2)]
    C2_0 = 0.001;      % integration constant [kg/(m^2*s)]
    C3_0 = 10;         % integration constant [W/(m^2)]
    C4_0 = 0.001;      % integration constant [kg/(m^2*s)]

    z = [T1_0, T2_0, rou1_0, rou2_0, C1_0, C2_0, C3_0, C4_0]';
    f = funf(z, para, nc(k))';
    df = 0 - f;

    % Newton-Raphson method to calculate z that satisfies f(z)=0
    count = 1;
    while norm(df) > tol
        J = zeros(8);
        for iz = 1: length(z)
            z_ptb = z;
            z_ptb(iz) = z(iz) + delta;        % give a small
perturbation to z(i)
            f_ptb = funf(z_ptb, para, nc(k))';  % calculate f
after perturbation
```

```matlab
            J(:,iz) = (f_ptb - f)/delta;         % this is ith
column of the Jacobian
        end
        if nc(k) == 1
            J=J(3:8,[1,2,3,4,7,8]); df=df(3:8);
        end
        dz = J\df;
        if nc(k) == 1
            dz=[dz(1),dz(2),dz(3),dz(4),0,0,dz(5),dz(6)]';
        end
        z = z + dz;
        f = funf(z, para, nc(k))';
        df = 0 - f;
        count = count + 1;
        if count > 100
            disp('iteration exceeds 100, stopped'); break;
        end
    end

    % solution
    T1 = z(1);          % temperature at x = l1 [K]
    T2 = z(2);          % temperature at x = l2 [K]
    rou1 = z(3);      % water vapor concentration at x = l1 [kg/m^3]
    rou2 = z(4);      % water vapor concentration at x = l2 [kg/m^3]
    C1 = z(5);          % integration constant [W/(m^2)]
    C2 = z(6);          % integration constant [kg/(m^2*s)]
    C3 = z(7);          % integration constant [W/(m^2)]
    C4 = z(8);          % integration constant [kg/(m^2*s)]

    % check consistency of assumption
    k = k + 1;
    [RaL_MC, hn_MC] = funhn_MC(Ts, T1, l1);
    if RaL_MC < 1708
        nc(k) = 0;
    else
        nc(k) = 1;
    end
end

%% calculate x in terms of T
rouS = rouvap(Ts,1);   % saturated water concentration at skin
surface [kg/m^3]
nint = 100;
T_1 = linspace(Ts, T1, nint);
T_2 = linspace(T1, T2, nint);
x1(1) = 0;
x2(1) = l1;
rou_1(1) = rouS;
rou_2(1) = rou1;
for j = 2:nint
    x1(j) = -1/C1*quadl(@(t)funkMC(t), Ts, T_1(j));
    x2(j) = l1-1/C3*quadl(@(t)funkF(t, p, kfiber), T1, T_2(j));
    rou_1(j) = rouS + C2/C1*quadl(@(t)funkMC_Dvap(t), Ts, T_1(j));
    rou_2(j) = rou1 +
C4/C3*quadl(@(t)funkF_Deff(t,p,tau,kfiber,KDsur), T1, T_2(j));
end
```

```matlab
%% find heat flux distribution in each layer
% parameters
[RaL_MC, hn_MC] = funhn_MC(Ts, T1, l1); % heat transfer
coefficient for natural convection in MC [W/(m^2*K)]
Kn_MC = funKn_MC(Ts, T1, l1);           % mass transfer
coefficient for natural convection in MC [m/s]
eps12 = (1/epsF + 1/epsS - 1)^(-1);     % emissivity in MC
[dimensionless]
Tf = (T2 + Te)/2;                       % film temperature in the
ambient [K]
hf_E = funh(Tf, L, v);                  % heat transfer
coefficient for forced convection above fabric [W/(m^2*K)]
Kf_E = funKw(Tf, L, v);                 % mass transfer
coefficient of forced convection above fabric [m/s]
rouE = rouvap(Te,phi);                  % saturated water
concentration in ambient air [kg/m^3]

% in the MC layer
qrad_MC = eps12*sigma*(Ts^4 - T1^4);    % radiation heat flux in
the MC [W/(m^2)]
if RaL_MC > 1708
    qnconv_MC = hn_MC*(Ts-T1);          % natural heat convection
heat flux in the MC [W/(m^2)]
    qnmass_MC = delta_H*Kn_MC*(rouS-rou1);% natural mass
convection heat flux in the MC [W/(m^2)]
    qtot_MC = qnconv_MC + qrad_MC + qnmass_MC;  % total heat flux
in the MC layer [W/(m^2)]
else
    qcond_MC = C1;                      % conduction heat flux in
the MC layer [W/(m^2)]
    qmass_MC = delta_H*C2;              % mass diffusion heat
flux in the MC [W/(m^2)]
    qtot_MC = qcond_MC + qrad_MC + qmass_MC;    % total heat flux
in the MC layer [W/(m^2)]
end

% in the fabric layer
qcond_F = C3;                           % conduction heat flux in the
fabric layer [W/(m^2)]
qmass_F = delta_H*C4;                   % mass diffusion heat flux in
the fabric [W/(m^2)]
qtot_F = qcond_F + qmass_F;             % total heat flux in the
fabric layer [W/(m^2)]

% in the ambient layer
qconv_E = hf_E*(T2-Te);                 % convection heat flux in
the environment [W/(m^2)]
qrad_E = epsF*sigma*(T2^4 -Te^4);       % radiation heat flux in the
environment [W/(m^2)]
qmass_E = delta_H*Kf_E*(rou2-rouE);     % mass convection heat flux
in the environment [W/(m^2)]
qtot_E = qconv_E+qrad_E+qmass_E;        % total heat flux in the
environment [W/(m^2)]
```

```matlab
%% total evaporative resistance Ret
Ret = (Psat(Ts) - phi*Psat(Te))/(qtot_MC-(Ts-Te)/Rct)

%% bare plate evaporative resistance
rouS = rouvap(Ts,1);                      % saturated water
concentration at skin surface [kg/m^3]
rouE = rouvap(Te,phi);                     % saturated water
concentration in ambient air [kg/m^3]
Tave = (Ts + Te)/2;                        % film temperature in the
ambient [K]
qmass_bp = delta_H*funKw(Tave, L, v)*(rouS-rouE);
Ret0 = (Psat(Ts) - phi*Psat(Te))/qmass_bp

%% thermal resistance of fabric system
Ref = Ret - Ret0

%% plot temperature distribution
figure(1);
plot([x1,x2]*1e3, [T_1,T_2]-273.15);
title(['MC = ',num2str(l1*1e3),'mm,', ' Te = ', num2str(Te -
273.15) '^oC'],'fontsize',14);
xlabel('Position, mm','fontsize',14);
ylabel('Temperature, ^oC','fontsize',14);
grid on;

%% plot water vapor concentration distribution
figure(2);
plot([x1,x2]*1e3, [rou_1,rou_2]);
title(['MC = ',num2str(l1*1e3),'mm,', ' Te = ', num2str(Te -
273.15) '^oC,', ' RH = ', num2str(phi*100) '%,', ' V = ',
num2str(v) 'm^2/s'],'fontsize',14);
xlabel('Position, mm','fontsize',14);
ylabel('Water vapor concentration, kg/m^3','fontsize',14);
grid on;
hold on;

%% plot flux distribution
figure(3);
qrad = [qrad_MC, 0, qrad_E]';
if RaL_MC > 1708
    qcond = [0, qcond_F, 0]';
    qconv = [qnconv_MC, 0, qconv_E]';
    qmass = [qnmass_MC, qmass_F, qmass_E]';
else
    qcond = [qcond_MC, qcond_F, 0]';
    qconv = [0, 0, qconv_E]';
    qmass = [qmass_MC, qmass_F, qmass_E]';
end

barh([qcond, qconv, qrad, qmass],'stack');hold on;
title(['MC = ',num2str(l1*1e3),'mm,', ' Te = ', num2str(Te -
273.15) '^oC'],'fontsize',14);
legend('q_{cond}','q_{conv}','q_{rad}','q_{mass}');
xlabel('Heat flux distribuion[W/m^2]','fontsize',14);
ylabel('1-MC, 2-fabric, 3-environment','fontsize',14);
```

2. other functions

The following functions are called by the above codes and are required for the calculation.

```
function y = funf0(z, para, nc)
%% 4 functions to solve for dry condition

%% 4 variables
T1 = z(1);              % temperature at x = l1 [K]
T2 = z(2);              % temperature at x = l2 [K]
C1 = z(3);              % integration constant [W/(m^2)]
C3 = z(4);              % integration constant [W/(m^2)]

%% parameters
sigma = para(1);     % Stefan-Boltzmann constant [W/(m^2*K^4)]--DD,
Sept.1,2009
l1 = para(2);        % thickness of MC [m]
l2 = para(3);        % thickness of MC + Fabric [m]
L = para(4);         % characteristic length [m]
kfiber = para(5);    % thermal conductivity of fiber [W/(m*K)]
p = para(6);         % porosity [dimensionless]
tau = para(7);       % tortuosity [dimensionless]
epsF = para(8);      % emissivity of fabric [dimensionless]
epsS = para(9);      % emissivity of skin [dimensionless]
Ts = para(10);       % skin temperature [K]
Te = para(11);       % ambient temperature [K]
v = para(12);        % air speed of the forced convection [m/s]

%% calculated quantities
eps12 = (1/epsF + 1/epsS - 1)^(-1);     % emissivity in MC
[dimensionless]
Tf = (T2 + Te)/2;                       % film (average)
temperature [K]; see Cengel P380
h = funh(Tf, L, v);                     % heat transfer
coefficient for forced convection above fabric [W/(m^2*K)]
[RaL_MC, hn_MC] = funhn_MC(Ts, T1, l1); % heat transfer
coefficient for natural convection in MC [W/(m^2*K)]

%% evaluate the vector function f
if nc == 0
    y(1) = C1*l1 + quadl(@funkMC, Ts, T1);
    y(2) = C3*(l2-l1) + quadl(@(x)funkF(x,p,kfiber), T1, T2);
    y(3) = C1 - C3 + eps12*sigma*(Ts^4 - T1^4);
    y(4) = C3 - h*(T2-Te) - epsF*sigma*(T2^4-Te^4);
else
    y(1) = 0;
    y(2) = C3*(l2-l1) + quadl(@(x)funkF(x,p,kfiber), T1, T2);
    y(3) = hn_MC*(Ts-T1) - C3 + eps12*sigma*(Ts^4 - T1^4);
    y(4) = C3 - h.*(T2-Te) - epsF*sigma*(T2^4-Te^4);
end
```

```matlab
function y = funf(z, para, nc)
%% 8 functions to solve for wet condition

%% 4 variables
T1 = z(1);          % temperature at x = l1 [K]
T2 = z(2);          % temperature at x = l2 [K]
rou1 = z(3);        % water vapor concentration at x = l1 [kg/m^3]
rou2 = z(4);        % water vapor concentration at x = l2 [kg/m^3]
C1 = z(5);          % integration constant [W/(m^2)]
C2 = z(6);          % integration constant [kg/(m^2*s)]
C3 = z(7);          % integration constant [W/(m^2)]
C4 = z(8);          % integration constant [kg/(m^2*s)]
%% parameters
sigma = para(1);    % Stefan-Boltzmann constant [W/(m^2*K^4)]
l1 = para(2);       % thickness of MC [m]
l2 = para(3);       % thickness of MC + Fabric [m]
L = para(4);        % characteristic length [m]
kfiber = para(5);   % thermal conductivity of fiber [W/(m*K)]
p = para(6);        % porosity [dimensionless]
tau = para(7);      % tortuosity [dimensionless]
epsF = para(8);     % emissivity of fabric [dimensionless]
epsS = para(9);     % emissivity of skin [dimensionless]
Ts = para(10);      % skin temperature [K]
Te = para(11);      % ambient temperature [K]
v = para(12);       % air speed of the forced convection [m/s]
phi = para(13);     % ambient relative humidity [dimensionless]
KDsur = para(14);   % surface diffusivity [m^2/s]


%% calculated quantities
eps12 = (1/epsF + 1/epsS - 1)^(-1);     % emissivity in MC
[dimensionless]
Tf = (T2 + Te)/2;                       % film (average)
temperature [K]; see Cengel P380
hf_E = funh(Tf, L, v);                  % heat transfer
coefficient for forced convection above fabric [W/(m^2*K)]
Kf_E = funKw(Tf, L, v);                 % mass transfer
coefficient of forced convection above fabric[m/s]
[RaL_MC, hn_MC] = funhn_MC(Ts, T1, l1); % heat transfer
coefficient for natural convection in MC [W/(m^2*K)]
Kn_MC = funKn_MC(Ts, T1, l1);           % mass transfer
coefficient for natrual convection in MC [m/s]
rouS = rouvap(Ts,1);                    % water vapor
concentration at the skin [kg/m^3]
rouE = rouvap(Te,phi);                  % water vapor
concentration in the ambient air [kg/m^3]

%% evaluate the vector function f
if nc == 0
    y(1) = C1*l1 + quadl(@funkMC, Ts, T1);
    y(2) = C1*(rou1-rouS) -C2*quadl(@(x)funkMC_Dvap(x), Ts, T1);
    y(3) = C3*(l2-l1) + quadl(@(x)funkF(x,p,kfiber), T1, T2);
    y(4) = C3*(rou2-rou1) -
C4*quadl(@(x)funkF_Deff(x,p,tau,kfiber,KDsur), T1, T2);
    y(5) = C1 - C3 + eps12*sigma*(Ts^4 - T1^4);
    y(6) = C3 - hf_E*(T2-Te) - epsF*sigma*(T2^4-Te^4);
    y(7) = C2 - C4;
```

```matlab
        y(8) = C4 - Kf_E*(rou2 - rouE);
    else
        y(1) = 0;
        y(2) = 0;
        y(3) = C3*(l2-l1) + quadl(@(x)funkF(x,p,kfiber), T1, T2);
        y(4) = C3*(rou2-rou1) -
C4*quadl(@(x)funkF_Deff(x,p,tau,kfiber,KDsur), T1, T2);
        y(5) = hn_MC*(Ts - T1) - C3 + eps12*sigma*(Ts^4 - T1^4);
        y(6) = C3 - hf_E*(T2-Te) - epsF*sigma*(T2^4-Te^4);
        y(7) = Kn_MC*(rouS - rou1) - C4;
        y(8) = C4 - Kf_E*(rou2 - rouE);
    end




function y = funDvap(x)
% vapor diffusivity in air [m^2/s]
% empirical equation, see Cengel P782


y = (1.87e-10)*(x.^2.072)./1;
end




function y = funh(T, L, v)
%% heat transfer coeffient for forced convection [W/(m^2*K)]
%% see Cengel P401-402

%% variable
x = T - 273.15;           % temperature; convert [K] to [C];

%% parameters
% specific heat capacity of air [J/(kg*K)]
cf_Cp = [-2.819063295939859e-008, 1.229769247192924e-005, -
0.001145656571296, 0.045111452693711, 1.006278477211970e+003]';
Cpair = cf_Cp(1)*x.^4 + cf_Cp(2)*x.^3 + cf_Cp(3)*x.^2 +
cf_Cp(4)*x + cf_Cp(5);

% thermal conductivity of air [W/(m*K)]
cf_k =[2.983587953212578e-015, 5.187633949064653e-012, -
2.541413234856413e-008, 7.563046250822273e-005,
0.023635130999766]';
kair = cf_k(1)*x.^4 + cf_k(2)*x.^3 + cf_k(3)*x.^2 + cf_k(4)*x +
cf_k(5);

% density of air [kg/(m^3)]
cf_rou = [8.643426984886860e-011, -5.426243605430176e-008,
1.753407849782240e-005, -0.004756383529224, 1.292074479209531]';
rouair = cf_rou(1)*x.^4 + cf_rou(2)*x.^3 + cf_rou(3)*x.^2 +
cf_rou(4)*x + cf_rou(5);

% Prandtl number (= mu*Cp/k) of air [dimensionless]
cf_Pr = [-2.656659140186304e-011, 1.138463336671207e-008, -
9.747406815409024e-007, -2.428044806926525e-004,
0.736189471493745]';
```

```matlab
Prair = cf_Pr(1)*x.^4 + cf_Pr(2)*x.^3 + cf_Pr(3)*x.^2 + ...
cf_Pr(4)*x + cf_Pr(5);

% dynamic viscosity of air [kg/(m*s)]
muair = Prair.*kair./Cpair;

%% heat transfer coeffient for forced convection [W/(m^2*K)]
ReL = v*rouair.*L./muair;     % Reynolds number over the flat
plate [dimensionless]

if ReL <5e5
    Nu = 0.664*(ReL).^0.5.*Prair.^(1/3);
elseif 5e5 < ReL <1e7
    Nu = (0.037*ReL.^0.8 - 871).*Prair.^(1/3);
else
    disp('Reynolds number runs out of acceptable range');return;
end

y = Nu*kair/L;
end



function [RaL_MC, hn_MC] = funhn_MC(Ts, T1, l1)
%% heat transfer coefficient for natural convection in MC
[W/(m^2*K)]
%% see Cengel P522-523

%% variable
x = (Ts + T1)/2 - 273.15;    % average temperature; convert [K]
to [C];

%% parameters
% specific heat capacity of air [J/(kg*K)]
cf_Cp = [-2.819063295939859e-008, 1.229769247192924e-005, -...
0.001145656571296, 0.045111452693711, 1.006278477211970e+003]';
Cpair = cf_Cp(1)*x.^4 + cf_Cp(2)*x.^3 + cf_Cp(3)*x.^2 + ...
cf_Cp(4)*x + cf_Cp(5);

% thermal conductivity of air [W/(m*K)]
cf_k =[2.983587953212578e-015, 5.187633949064653e-012, -...
2.541413234856413e-008, 7.563046250822273e-005, ...
0.023635130999766]';
kair = cf_k(1)*x.^4 + cf_k(2)*x.^3 + cf_k(3)*x.^2 + cf_k(4)*x + ...
cf_k(5);

% density of air [kg/(m^3)]
cf_rou = [8.643426984886860e-011, -5.426243605430176e-008, ...
1.753407849782240e-005, -0.004756383529224, 1.292074479209531]';
rouair = cf_rou(1)*x.^4 + cf_rou(2)*x.^3 + cf_rou(3)*x.^2 + ...
cf_rou(4)*x + cf_rou(5);

% Prandtl number (= mu*Cp/k) of air [dimensionless]
```

```matlab
cf_Pr = [-2.656659140186304e-011, 1.138463336671207e-008, -
9.747406815409024e-007, -2.428044806926525e-004,
0.736189471493745]';
Prair = cf_Pr(1)*x.^4 + cf_Pr(2)*x.^3 + cf_Pr(3)*x.^2 +
cf_Pr(4)*x + cf_Pr(5);

% dynamic viscosity of air [kg/(m*s)]
muair = Prair.*kair./Cpair;

% kinematic viscosity of air [m^2/s]
nuair = muair./rouair;

%% characteristic length in the MC [m]
Lc = l1;

% Rayleigh number in natural convection
RaL = 9.81*(1./(x+273.15)).*(Ts - T1).*Lc.^3.*Prair./nuair.^2;

temp1 = max(0, 1-1708./RaL);
temp2 = max(0, RaL.^(1/3)/18-1);
Nu = 1 + 1.44*temp1 + temp2;

hn_MC = kair.*Nu./Lc;
end




function y = funkF(T, p, kfiber)
%% effective thermal conductivity of the fabric layer [W/(m*K)]

%% thermal conductivity of air [W/(m*K)]
kair = funkMC(T);

y = (1-p)*kfiber + p*kair;
end




function y=funkF_Deff(x ,p, tau, kfiber, KDsur)
% effective thermal conductivity of fabric divided by effective
binary
% diffusion (mass diffusivity) in fabric layer [W/(m*K)]/[m^2/s]

% effective thermal conductivity of fabric
kF = funkF(x, p, kfiber);

% kF/Deff
% y = kF./((1.87e-10)*(x.^2.072)*p/tau + 0*KDsur);   % from
Gibson's
y = kF./((1.87e-10)*(x.^2.072)*p/tau + KDsur);   %  KD = 1e-6 ~
1e-4[m^2/s] from Min et al.'s
end
```

```matlab
function y = funkMC(T)
% thermal conductivity of the air in MC as a function of
temperature [W/(m*K)]

%% variable
x = T - 273.15;          % temperature; convert [K] to [C];

%% Coefficient of the fitted polynomial
cf = [2.983587953212578e-015, 5.187633949064653e-012, -
2.541413234856413e-008, 7.563046250822273e-005,
0.023635130999766]';

y = cf(1)*x.^4 + cf(2)*x.^3 + cf(3)*x.^2 + cf(4)*x + cf(5);
end




function y=funkMC_Dvap(x)
% thermal conductivity of air divided by binary diffusion
coefficient(diffusivity) of water vapor in MC
layer[W/(m*K)]/[m^2/s]

% thermal conductivity of air in MC [W/(m*K)]
kMC = funkMC(x);

% kMC/Dvap
y = kMC./((1.87e-10)*(x.^2.072)./1);
end




function y=funKn_MC(Ts, T1, l1)
% mass transfer coefficient as a function of heat transfer
coefficient in MC[m/s]
% h=rou_air*cp*(al/Dvap)^(2/3)*Kw;  % using Chilton-Colburn
analogy in <Cengel 14-90 p.815>

% heat transfer coefficient in MC [W/(m^2*K)]
[RaL_MC, hn_MC] = funhn_MC(Ts, T1, l1);

% thermal conductivity of air in MC [W/(m*K)]
kMC = funkMC((Ts + T1)/2);

% variable
x = (Ts + T1)/2 - 273.15;    % average temperature; convert [K]
to [C];

% parameters
% density of air [kg/(m^3)]
cf_rou = [8.643426984886860e-011, -5.426243605430176e-008,
1.753407849782240e-005, -0.004756383529224, 1.292074479209531]';
rouair = cf_rou(1)*x.^4 + cf_rou(2)*x.^3 + cf_rou(3)*x.^2 +
cf_rou(4)*x + cf_rou(5);

% specific heat capacity of air [J/(kg*K)]
```

```matlab
cf_Cp = [-2.819063295939859e-008, 1.229769247192924e-005, -
0.001145656571296, 0.045111452693711, 1.006278477211970e+003]';
Cpair = cf_Cp(1)*x.^4 + cf_Cp(2)*x.^3 + cf_Cp(3)*x.^2 +
cf_Cp(4)*x + cf_Cp(5);

% themeral diffusivity [m^2/s]
al = kMC./(rouair.*Cpair);

% mass diffusivity of vapor in air [m^2/s]
Dvap = (1.87e-10)*((x+273.15).^2.072)./1;

y = hn_MC./(rouair.*Cpair.*(al./Dvap).^(2/3));
end


function y=funKw(T, L, v)
% mass transfer coefficient as a function of heat transfer
coefficient [m/s]
% h=rou_air*cp*Kw;  % using empirical equation in <Cengel 14-90
p.815>

% heat transfer coefficient
h = funh(T, L, v);

% thermal conductivity of air in MC [W/(m*K)]
kMC = funkMC(T);

% variable
x = T - 273.15;          % temperature; convert [K] to [C];

% parameters
% density of air [kg/(m^3)]
cf_rou = [8.643426984886860e-011, -5.426243605430176e-008,
1.753407849782240e-005, -0.004756383529224, 1.292074479209531]';
rouair = cf_rou(1)*x.^4 + cf_rou(2)*x.^3 + cf_rou(3)*x.^2 +
cf_rou(4)*x + cf_rou(5);

% specific heat capacity of air [J/(kg*K)]
cf_Cp = [-2.819063295939859e-008, 1.229769247192924e-005, -
0.001145656571296, 0.045111452693711, 1.006278477211970e+003]';
Cpair = cf_Cp(1)*x.^4 + cf_Cp(2)*x.^3 + cf_Cp(3)*x.^2 +
cf_Cp(4)*x + cf_Cp(5);

% themeral diffusivity [m^2/s]
al = kMC./(rouair.*Cpair);

% mass diffusivity of vapor in air [m^2/s]
Dvap = (1.87e-10)*((x+273.15).^2.072)./1;

y = h./(rouair.*Cpair.*(al./Dvap).^(2/3));
end
```

```matlab
function y = Psat(T)
% saturation water vapore pressure as a function of temperature
% Psat is in [Pa]
% T is in [K]
% empirical equation, see Tetens, O., 1930

%% variable
x = T - 273.15;         % temperature; convert [K] to [C];

y = 610.78*exp(17.2694*x./(x + 238.3 ));
end




function y = rouvap(x, phi)
% water vapor concentration[kg/m^3] as a function of temperature
and RH
% temperature [K]
% RH [100%]

Rv = 461.5305;    % [J/(kg*K)]gas constant for water vapor

%% saturated vapor pressure[Pa]
p_sat0 = Psat(x);

%% partial pressure [Pa]
p_vapor = phi*p_sat0;

y =  p_vapor./(Rv*x);
end
```